Band 70

Schriftenreihe des Lehrstuhls für
Wasserchemie und Wassertechnologie
und der DVGW-Forschungsstelle am Engler-Bunte-Institut
des Karlsruher Instituts für Technologie (KIT)

Disinfection by-products and the application potential of nanofiltration in swimming pool water treatment

Di Peng

Herausgeber
Harald Horn

Karlsruhe 2016

Di Peng
Disinfection by-products and the application potential of nanofiltration in swimming pool water treatment

Herausgeber: Harald Horn
Band 70
Schriftenreihe des Lehrstuhls für Wasserchemie und Wassertechnologie und der DVGW-Forschungsstelle am Engler-Bunte-Institut des Karlsruher Instituts für Technologie (KIT)
Karlsruhe 2016

ISSN: 2195-2973
Lehrstuhl für Wasserchemie und Wassertechnologie und DVGW-Forschungsstelle
am Engler-Bunte-Institut des Karlsruher Instituts für Technologie (KIT)
Engler-Bunte-Ring 9
D-76131 Karlsruhe
Tel.: +49-(0)721-608-42581
Fax: +49-(0)721-608-46497
E-mail: ebi-sekretariat-wasserchemie@kit.edu
http://wasserchemie.ebi.kit.edu/

Titelbild: Public swimming pool (left) and the full-scale nanofiltration plant (right)

Disinfection by-products and the application potential of nanofiltration in swimming pool water treatment

zur Erlangung des akademischen Grades eines
DOKTORS DER INGENIEURWISSENSCHAFTEN (Dr.-Ing.)

der Fakultät für Chemieingenieurwesen und Verfahrenstechnik des
Karlsruher Institut für Technologie (KIT)

genehmigte
DISSERTATION

von
M. Sc. Di Peng
aus Shenzhen, China

Referent: Prof. Dr. rer. nat. Harald Horn
Korreferent: Prof. Dr.-Ing. Mathias Ernst
Tag der mündlichen Prüfung: 28.11.2016

Acknowledgments

First I would like to express my sincere thanks to Prof. Dr. Harald Horn for the chance of my PhD-study, for the supervision with his immense scientific literacy and for setting an example by his motivation for research. He always provides us PhD students the best conditions and tries to fulfill our needs as possible, which is such an encouragement and is very much appreciated. Thanks to Prof. Dr. Matthias Ernst for his willingness to take over the second referee. I am especially thankful to Dr. Florencia Saravia, the driving force behind membrane research at our institute, for the recommendation for the PhD position, for the enormous support and encouragement, for being a good supervisor and a good friend and for everything else.

I am deeply grateful to Dr. Gudrun Abbt-Braun for the correction of the manuscripts, thoughtful and kind support, assistance in administrative and many other different issues. I thank Dr. Marius Majewsky for the help with the manuscript revision, always giving valuable suggestions and many nice conversations that I will remember. I want to thank Dr. Michael Wagner for the great help with CLSM, always providing an idea and those discussions we had.

I am indebted to our technicians Axel Heidt, Elly Karle, Rafael Peschke, Ulrich Reichert, Reinhard Sembritzki and Matthias Weber for so many measurements and the reliable results. Additionally, my sincere thanks go to Axel for being so warm hearted that always willing to help and being reliable for all the safety issues at our institute, to Matthias for many times being willing to wait till late for my urgent samples, different discussions and help as well as the good cooperation in the Praktikum every year. And thank Antje Decker for the support in laboratory work relating microbiology. Many thanks go to Dunja Haak for the thorough technical support regarding IT.

I am very appreciative of many timely and smooth administrative help from Ursula Schäfer and Sylvia Heck and the nice and welcoming atmosphere around them. Thank Sylvia for being such a good friend and so much help that I will keep in my heart. I thank Dr. Birgit Gordalla for helping to apply for the conference travel scholarship. I also want to thank Dr. Markus Delay for the kind information about pool water sampling at the beginning of my PhD, thank Steffi West for the orders and support in solving related problems, and thank Dr. Andrea Hille-Reichel for those always nice talks and the workshop documents. Thank Alfred Herbst and the whole team as well as Stefan Herbel and Matthias Kieslich for the help with different experimental set-ups. I would sincerely thank Joachim Lang for helping me to transport the huge experiment set-up back from the swimming pool as well as the patience and kindness to me all the time.

Sharing the PhD life with other fellow PhD students is full of joy. My deep thanks go to Maria Pia Herrling for all kinds of help, the enormous encouragement and the sincere friendship. I am grateful to

my Chinese girls Chunyan Li, Jueying Qian and Meijie Ren for discussions about work, life and everything, all kinds of help as well as sharing many important moments with me, and to Shelesh Agrawal, Florian Blauert, Dominic Breitkopf, Fabian Brunner, Laure Cuny, Elham Fatoorehchi, Eva Gilbert, Norman Hack, Oliver Jung, Alexander Kondrakov, Isa Remdt, Alexander Timm, Marc Tuczinski, Samuel Welker, Felicitas Arndt (MVM) and Jan Benecke (TUHH) for questions, help and countless discussions and great time together.

All in all, the colleagues at the EBI − Water Chemistry and Water Technology throughout this period of my PhD study, thank you for giving me such a nice time and the spirit of dedication to work. I am very appreciative than I have met great people here. These past four years at the institute remains unforgettable in my life.

I would like to thank all the students who did their bachelor theses or internship with me: Daniel West, Manuel Hohm, Guillermo Cuesta, Marcel Pelikan, Kristina Bock, Jonas Schuster, Carolin Salathe, Adelmo Filho and Marcos Klimunda. They not only helped my work but I also learned how to lead. And I thank my good Hiwis: Dominik Reith, Patrick Endres, Marius Meier, Magdalena Stieß, and Verena Hilgenfeldt, with whom those countless trips to the swimming pools became easier – not only because of the help for sampling.

I thank the German Federal Environmental Foundation (Deutsche Bundesstiftung für Umwelt, DBU) for the financial support (Az: 28707), the project partner W.E.T. GmbH for the collaboration, especially Werner Sauerschell for the help with the NF-Plants and the nice handling all the time. I'd like to thank the kindest co-workers in the studied swimming pools for the generous help with the sampling. I thank Dr. Johannes Luetzenkirchen (INE, Campus Nord) for helping me with the zeta potential measurement, Dr. Jennifer Kübel (ITCP) for the ATR-FTIR measurement, and Johannes Knoll (MVM) for the LSM measurement.

Last but not least I'd like to thank my husband Zihan Yuan for giving me constructive advices on the subject, for taking good care of me all the time and countless encouragement during the hard time, and thank my family especially my mom Xiaojuan Zhou for the motivation and all kinds of help. Without her support it would not be possible for me to come to Germany to fulfill my goal. I am really thankful.

Di Peng

Abstract

Swimming pools have a great recreational value. To guarantee the health of swimming pool visitors, pool water is recirculated and treated. In this context, chlorine is a necessary disinfectant due to its residual effects which provides a certain level of active free chlorine for a continuous control of the pathogenic microorganisms in swimming pool water. However, chlorine reacts also with the organic matter in pool water and produce undesirable and potentially harmful disinfection by-products (DBP). Trihalomethanes (THM) are the most typical DBP found in chlorinated water and most regulated DBP. An inadequate pool water treatment can adversely affect water quality as the contaminants which cannot be removed by the treatment will accumulate. Nanofiltration (NF) is an attractive alternative to conventional pool water treatment based on the effective elimination of dissolved organic substances and thus DBP and the precursors. An efficient pool water treatment saves fresh water and heating energy consumption.

The primary objective of this dissertation is to investigate the DBP behavior in swimming pool water and to evaluate the application potential of nanofiltration (NF) in swimming pool water treatment regarding elimination of DBP. This work was addressed in four parts: DBP formation, THM rejection by NF, minimization of DBP by NF and fouling behavior of NF membranes in swimming pool water.

First of all, an appropriate treatment requires a better understanding of the DBP formation. The irregular input of various substances related to pool visitor behavior and long contact time with disinfectant due to water recirculation make the forecast of THM in pool water a challenge. Water quality in a public indoor swimming pool was intensively studied for 3 months with focus on the occurrence of THM. Daily sampling of pool water for 26 days showed a positive correlation between DOC and THM with a time delay of about two days, while THM and DOC didn’t directly correlate with the number of visitors. Based on the results and mass-balance in the pool water, a simple simulation model for estimating THM concentration in indoor swimming pool water was established. Formation of THM from DOC, volatilization into air and elimination by pool water treatment were included in the simulation. Formation ratio of THM gained from laboratory analysis using native pool water and information from field study in an indoor swimming pool reduced the uncertainty of the simulation. The simulation was validated by measurements in the swimming pool for 50 days. The simulated results were in good compliance with measured results. This work provides a useful and simple method for predicting THM concentration and its accumulation trend for long term in indoor swimming pool water.

Literature referred to the THM rejection by NF has been contradictory (from little to 95%). For a systematic study in THM rejection mechanisms by NF, the rejection of four THM by three commercial NF membranes of different materials was investigated in carefully designed laboratory

experiments, considering the effect of adsorption and organic fouling on rejection performance. Results indicated that NF has actually limited rejection of THM, even when the molecular weight of the THM molecules was larger than the molecular weight cut-off of the membrane. The tightest investigated membrane NF90 showed a THM rejection of max. 30–50%, while the other two membranes presented no THM rejection at steady-state. Adsorption has significant influence on rejection, facilitating the mass transport of THM through NF membrane. Membrane material plays a substantial role in the intrinsic adsorption capacity and consequently has the impact on rejection. The cellulose acetate membrane (SB90) showed little adsorption capacity of THM and therefore THM could pass cellulose acetate very quickly. It can be assumed that the occupation extent of the available adsorption capacity in the membrane plays a significant role in how the adsorption facilitates the transport of molecules through the membrane and thus decreases membrane rejection. Natural organic matter in feed solution and organic fouling layer had little effects on THM rejection. Organic fouling lowered the adsorption of less adsorptive THM due to blocking of the membrane surface.

Despite the low rejection of THM, the successful simulation supported the observed positive correlation between DOC and THM with a time delay of 2 days, which indicated a possible minimization of DBP by quick removal of the precursors using NF. For the first time NF was integrated in a real swimming pool water system in a pilot-plant for the backwash wastewater treatment and in a full-scale plant as a branch current for the mainstream treatment. Chlorine-resistant NF membrane of cellulose acetate (SB90) fulfilled sufficient rejection performance for 17 months under pool water condition with 0.2 mg/L free chlorine present in feed water. By quenching chlorine in advance the polyamide NF90 membrane endured excellent rejection performance in 8 months operation. Compared to the original treatment process, integration of a branch current NF treatment for 1.3% of the mainstream could reduce the general level of DBP and the precursors as well as the DBP reactivity in swimming pool water. Long-term onsite experiments at a real swimming pool demonstrated the feasibility of NF in pool water treatment, which provided a better pool water quality compared to the original treatment.

Finally, for an effective fouling control regarding the realistic application, fouling of the NF membrane in swimming pool treatment was thoroughly investigated onsite through bench-scale experiments in different pool water qualities and autopsy studies of the two plants mentioned above after realistic long-term operation. Fouled membranes were characterized using scanning microscopy coupled with energy dispersive spectroscopy, Fourier transform infrared spectroscopy with attenuated total reflection, confocal laser scanning microscopy, zeta potential measurement and contact angle measurement. Fouling deposits were analyzed by mass measurement after heating at 110 °C and 550 °C, elemental analysis, organic carbon and inductively coupled plasma optical emission spectroscopy. Results were associated with feed water properties to evaluate the major foulants. Autopsy studies showed that the decline of membrane permeability was mainly due to accumulation of

organics and biofilms on the membrane. The foulants identified were mainly biopolymers including protein- and polysaccharide-like substances. A concentration of 0.2 mg/L chlorine in feed water could not avoid biofouling but might influence the biofilm morphology and composition. Antiscalant with polyacrylates and polyphosphonates seems to enhance biofouling. Among the little inorganic foulants, Aluminium was found the most accumulated, probably from the flocculation pretreatment. Results indicated that in swimming pool water treatment NF membrane was dominated by biofouling in combination of organic fouling, while scaling could be well suppressed by antiscalant. The results fulfilled the information vacancies about fouling in such water properties and enabled to choose the appropriate cleaning method/pre-treatment for minimizing fouling formation under swimming pool water condition.

NF showed a promising application potential in swimming pool water treatment regarding efficient elimination of DBP. The firsthand experiences provided the unique information for the fundamental understanding of the DBP formation and the performance of NF membranes in swimming pool water.

Keywords: Nanofiltration, Swimming pool water treatment, Disinfection by-products, Trihalomethanes, Membrane fouling

Zusammenfassung

Schwimmbäder sind beliebte Freizeiteinrichtungen. Um die hygienische Sicherheit der Badegäste zu gewährleisten, wird das Schwimmbeckenwasser typischerweise kontinuierlich aufbereitet und nach der Aufbereitung in das Becken zurückgeführt. In diesem Zusammenhang ist Chlor ein verbreitetes Desinfektionsmittel. Aufgrund seiner „Depotwirkung“ besteht eine kontinuierliche Reduzierung der Pathogene im Schwimmbadwasser, da immer ein Restgehalt an aktivem freiem Chlor zur Verfügung steht. Reaktionen des Chlors mit im Wasser befindlichen gelösten Substanzen können jedoch zu einer unerwünschten Chlorzehrung sowie zur Bildung unerwünschter potenziell reizender oder gesundheitlich bedenklich Desinfektionsnebenprodukte (DNP) führen. Trihalogenmethane (THM) sind die bekanntesten organischen DNP in gechlortem Wasser. Eine ungenügende Schwimmbeckenwasseraufbereitung kann sich auf die Wasserqualität negativ auswirken, da die Verunreinigungen, die nicht durch die Aufbereitung entfernt werden können, akkumulieren. Die Nanofiltration (NF) ist aufgrund der effektiven Elimination der gelösten organischen Substanzen und teilweise der DNP und deren Präkursoren eine attraktive Alternative zur konventionellen Schwimmbeckenwasseraufbereitung. Eine effiziente Schwimmbeckenwasseraufbereitung reduziert den Frischwasser- und Energieverbrauch.

Das Ziel dieser Dissertation ist die Untersuchung des Verhaltens der DNP im Schwimmbeckenwasser und die Ermittlung des Anwendungspotentials der NF in der Schwimmbeckenwasseraufbereitung bezüglich der Elimination von DNP. Die vorliegende Arbeit wurde in vier Abschnitte unterteilt: die DNP-Bildung, Rückhalt von THM durch NF, Minimierung der DNP durch NF und das Foulingverhalten der NF-Membranen durch Schwimmbeckenwasser.

Für die Optimierung der Aufbereitung bedarf es eines besseren Verständnisses der DNP-Bildung. Der unregelmäßige Eintrag verschiedener Präkursoren bezüglich des Besucherverhaltens und die lange Kontaktzeit mit Desinfektionsmittel aufgrund der Wasserumwälzung machen die Prognose von THM im Schwimmbeckenwasser zu einer Herausforderung. Die Wasserqualität in einem öffentlichen Hallenbad wurde über einen Zeitraum von 3 Monaten mit Fokus auf das Vorkommen von THM intensiv untersucht. Die tägliche Probenahme des Beckenwassers über 26 Tage zeigte eine positive Korrelation zwischen DOC und THM mit einer Zeitverzögerung von etwa zwei Tagen. Im Vergleich dazu korrelierten THM und DOC nicht direkt mit der Besucherzahl. Basierend auf diesen Ergebnissen und einer Massenbilanz im Beckenwasser wurde ein einfaches Simulationsmodell zur Abschätzung der THM-Konzentration im Hallenbadbeckenwasser entwickelt. Die Bildung von THM aus DOC, die Verflüchtigung der THM in die Luft und die Elimination durch die Beckenwasseraufbereitung wurden in der Simulation berücksichtigt. Die Simulation wurde durch die Messungen im Schwimmbad für weitere 50 Tage validiert und war in guter Übereinstimmung mit den gemessenen Ergebnissen. Diese

Arbeit stellt eine nützliche und einfache Methode zur Vorhersage der THM-Konzentration und des THM-Entwicklungstrends im Hallenbadbeckenwasser dar.

Die Literatur zum THM-Rückhalt durch NF ist widersprüchlich. Für eine systematische Untersuchung der Mechanismen des THM-Rückhalts durch NF wurde der Rückhalt von vier THM‘s durch drei kommerziellen NF-Membranen aus verschiedenen Materialien durch sorgfältig gestaltete Laborexperimente durchgeführt. Der Einfluss der Adsorption und des organischen Foulings auf den Rückhalt wurde berücksichtigt. Die Ergebnisse zeigten, dass die NF tatsächlich einen begrenzten THM-Rückhalt verursacht, selbst wenn das Molekulargewicht der THM-Moleküle größer als die Trenngrenze der Membran war. Die dichteste untersuchte Membran NF90 zeigte einen THM-Rückhalt von max. 30–50 %, während die anderen beiden Membranen keinen THM-Rückhalt im stationären Zustand aufwiesen. Die Adsorption von THM an der Membran hat einen signifikanten Einfluss auf den THM-Rückhalt, der den Massentransport der THM durch NF-Membranen erleichtert. Das Membranmaterial spielt eine wesentliche Rolle bei der intrinsischen Adsorptionskapazität und hat folglich einen Einfluss auf den Rückhalt. Die Membran SB90 aus Celluloseacetat zeigte wenig Adsorptionskapazität für THM. Es kann angenommen werden, dass das Ausmaß der Adsorption in der Membran eine wichtige Rolle für den Transport der Moleküle durch die Membran spielt, d.h. diesen erleichtert. Natürliche organische Stoffe in der Feed-Lösung und die organische Foulingschicht hatten wenig Auswirkung auf den THM-Rückhalt. Organisches Fouling verringert die Adsorption von weniger adsorptiven THM aufgrund der Blockade der Membranoberfläche.

Trotz des geringen THM-Rückhalts ergab die bestätigte zeitliche Verzögerung zwischen DOC und THM von zwei Tagen eine mögliche Minimierung der DNP durch eine schnelle Entfernung der Präkursoren durch NF. Zum ersten Mal wurde die NF bei einem realen Schwimmbad in einer Pilotanlage für die Rückspülwasseraufbereitung und in einer großtechnischen Anlage als Teilstrom für die Schwimmbeckenwasseraufbereitung integriert. Die chlorbeständige NF Membran aus Celluloseacetat (SB90) erfüllte eine ausreichende Rückhaltleistung für 17 Monate bei der Konzentration von 0,2 mg/L freiem Chlor im Feed. Wenn das Chlor im Voraus gequencht war, behielt die Membran NF90 aus Polyamid eine ausgezeichnete Rückhaltleistung für 8 Monate bei. Im Vergleich zu dem ursprünglichen Aufbereitungsverfahren konnte die Aufbereitung eines Teilstroms von 1,3 % mit NF das gesamte Niveau der DNP und deren Präkursoren sowie die DNP-Reaktivität im Schwimmbeckenwasser reduzieren. Die langfristigen Experimente vor Ort bei einem realen Schwimmbad demonstrierten die Realisierbarkeit der NF bei der Schwimmbeckenwasseraufbereitung, die eine bessere Wasserqualität im Vergleich zu der ursprüngliche Aufbereitung zur Verfügung stellt.

Abschließend wurde das Fouling der NF-Membranen bei der Schwimmbeckenwasseraufbereitung durch Experimente im Labormaßstab bei zwei Beckenwasserqualitäten und zwei Autopsiestudien der beiden oben erwähnten Anlagen nach langfristigen Betrieb untersucht. Gefoulte Membranen wurden mit verschiedenen Methoden wie z.B. Rasterelektronenmikroskopie gekoppelte mit

Energieverteilungsspektroskopie, konfokale Laser-Scanning-Mikroskopie, Fourier-Transformations-Infrarot-Spektroskopie, Zetapotentialmessung und Kontaktwinkelmessung charakterisiert. Die Fouling-Ablagerungen wurden auch durch Elementaranalyse, Messung des organischen Kohlenstoffs und mittels optischer Emissionsspektroskopie mit induktiv gekoppeltem Plasma analysiert. Die Ergebnisse wurden mit der Eigenschaft des Feeds verglichen, um die wichtigsten Foulingstoffe zu bewerten. Autopsiestudien zeigten, dass die Senkung der Permeabilität hauptsächlich auf die Akkumulation von organischen Stoffen und Biofilmen auf der Membran zurückzuführen ist. Die identifizierten Foulingstoffe waren im Wesentlichen Biopolymere einschließlich Protein- und Polysaccharid-artiger Substanzen. Eine Konzentration von 0,2 mg/L Chlor im Feed konnte Biofouling nicht vermeiden, kann aber mit Einschränkungen die Morphologie und Zusammensetzung des Biofilms beeinflussen. Unter den weinigen anorganischen Foulingstoffen wurde Aluminium am stärksten akkumuliert, wahrscheinlich eingetragen aus der Vorbehandlung mit Flockungsmittel. Die Ergebnisse verdeutlichten, dass bei der Schwimmbeckenwasseraufbereitung die NF-Membranen hauptsächlich Biofouling in Kombination mit organischem Fouling aufwiesen, während das Scaling durch Antiscalant unterdrückt werden konnte. Die Ergebnisse dieser Experimente schließen die Lücke über Informationen bei Membranfouling durch Schwimmbeckenwasser und ermöglichen es, ein optimales Reinigungs- bzw. Vorbehandlungsverfahren zu wählen.

Die NF zeigte ein vielversprechendes Anwendungspotential bei der Schwimmbeckenwasser-aufbereitung bezüglich der effizienten Elimination der DNP. Diese Arbeit liefert somit eine wertvolle Hilfe für das grundlegende Verständnis der DNP-Bildung und der Performance von NF-Membranen bei der Schwimmbeckenwasseraufbereitung.

Contents

1 Introduction

1.1 Motivation

Swimming pools have a great recreational value all over the world. In Germany the people who go swimming often in their leisure time increased in 2012–2015 and accounted about 6.5 million in 2015 (IfD-Allensbach, 2016). In U.S. swimming is the third most popular sport or exercise activity (Bureau, 2009). To guarantee the health of swimming pool visitors, pool water is practically treated and recirculated over large periods of time. Disinfection is a necessary step in order to control the pathogenic microorganisms. Chlorine, the most common disinfectant in swimming pools, reacts with the organic matter in swimming pool water and produce undesirable and potentially harmful disinfection by-products (DBP). DBP in swimming pool water have been linked to human health effects such as bladder cancer (Villanueva et al., 2007).

The organic matters in swimming pools comprise natural organic matter (NOM) from filling tap water, contaminants brought by the swimmers and from the pool water maintenance. Understanding the behavior of DBP-formation in pool water is complex due to the irregular new input of contaminants and the recirculation of swimming pool water over long periods of time (Chowdhury et al., 2014). Trihalomethanes (THM) as the most typical organic DBP in chlorinated water have been widely studied. However the occurrence of THM in swimming pool water is difficult to predict due to the fact that the bather and contaminant load, chlorine dosage, DBP concentration and fresh filling water can vary considerably both over short and longer time scales. Such studies in the field of swimming pool water are still missing. Effects of such recirculation system of pool water on DBP formation are not well-understood to date.

An inadequate pool water treatment can adversely affect water quality as the contaminants which cannot be removed by the treatment will accumulate (Müller and Uhl, 2011, Zwiener et al., 2007). Nanofiltration (NF) is an attractive alternative to conventional pool water treatment based on the effective elimination of dissolved organic substances and thus DBP and the precursors. Literature concerning the rejection behavior of THM by NF has been a matter of contradictions, ranging from little to 95% in rejection (Agenson et al., 2003, Doederer et al., 2014, Klüpfel et al., 2011b, Levine et al., 1999, Uyak et al., 2008, Waniek et al., 2002), which indicates a crucial need of a systematic study in the rejection performance and mechanisms. Although many studies in drinking water treatment showed that removal of precursors by NF before the disinfection procedure could largely reduce the disinfection by-product formation potential (DBPFP), the produced water returns back to swimming pool and stay for a much longer contact time with chlorine. The fate of the remaining dissolved organic matters (DOM) in NF permeate and the effect of DOC-rejection in a recirculated system is yet unknown.

Fouling is an overall problem in membrane filtration, which could negatively influence the membrane performance. A good identification and characterization of foulants and fouling mechanisms after realistic operation is essential for effective fouling control. Membrane fouling in pool water treatment was little investigated. Swimming pool water features high temperature, low bicarbonate, chlorine, NOM and anthropogenic input as well as their products with chlorine, which is different from the most studied waters such as surface water or wastewater. Information of fouling in swimming pool water treatment is essential considering the application of NF.

The introduction of a new application commonly encompasses start-up problems or unexpected results. The work to be presented here addresses the application potential of NF for swimming pool water treatment concerning the formation of DBP, the minimization of DBP by NF and the fouling behavior of NF membranes from a firsthand experience. Since swimming pool water cannot easily be simulated in the laboratory, most experiments were carried out on-site at public swimming pool.

1.2 Objective and structure of the work

The objective of this work is to gain a deeper understanding of the formation of DBP in swimming pool water and the application potential of nanofiltration in swimming pool water treatment. The thesis is divided into four parts:

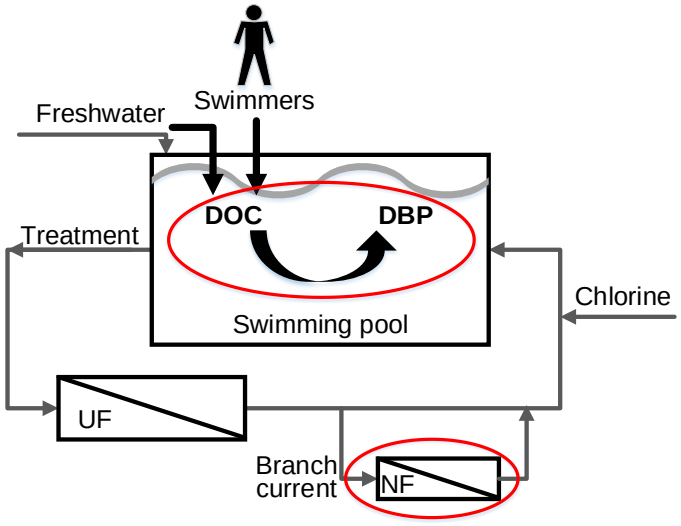

Figure 1.1: Key positions for this study in a swimming pool water system

1) Investigation of **the occurrence of THM in indoor swimming pool water** in correlation with: a) dissolved organic carbon (DOC) concentration, b) the number of visitors and c) water treatment process, in order to develop **a DOC-based predictive model for THM formation**. Data were acquired through on-site investigations as well as lab-controlled chlorination experiments of native swimming pool water. The results can be used to quantitatively evaluate the THM-formation in swimming pool water. **(Chapter 4)**

2) Evaluation of **the THM rejection by NF and the effect of adsorption and organic fouling on the rejection performance**. Considering the volatility of THM, filtration experiments were carried out in a closed set-up using pressure vessels and stirred cells. Three NF membranes with similar or smaller MWCO than the molecular weight of THM were investigated. Additionally, fouling experiments were performed to study the effects of NOM in feed and the fouling layer on rejection performance. The THM-adsorption on membranes was calculated by mass balance. Membranes material functional groups, surface morphology and hydrophobicity were characterized. **(Chapter 5)**
3) Investigation of **the elimination of DBP and the precursors by NF in swimming pool water treatment**. Long-term experiments were carried out with a chlorine-resistant NF membrane (cellulose acetate) in a pilot plant and a polyamide NF membrane in a full-scale plant. The **rejection performance and the influence on the pool water quality** were accordingly studied. The results were compared to the situation without NF treatment. **(Chapter 6)**
4) Analysis of **the fouling characteristics of NF membranes in swimming pool water treatment**. Fouling of two chlorine-resistant NF membranes (NTR-7470pHT and SB90) was studied with bench-scale cross-flow set-up onsite at two swimming pools with different pool water matrices. Autopsy studies of fouled spiral wound modules from the two NF plants after long-term operation (in Chapter 6) were carried out. Results were associated with feed water properties to evaluate the major foulants in order to give the first valuable insight into the fouling behavior of NF membranes for pool water treatment. **(Chapter 7)**

2 Background

2.1 DBP in swimming pool water

To guarantee the health of swimming pool visitors, pool water is practically treated and recirculated over large periods of time. Disinfection is a necessary step in order to control the pathogenic microorganisms. To date chlorine-based chemicals are still the most common and practiced disinfectants, including chlorine gas, sodium/calcium hypochlorite, or sodium hypochlorite produced through electrolytic generation (Black and Veatch, 2010). Although other disinfectants such as chloramine have been increasingly applied in recent years, a residual level of active free chlorine in public swimming pool water is usually required to continuously maintain the disinfection effect, which makes chlorine-based disinfectants necessary. Different hydrogen peroxide-based products were also compared to sodium hypochlorite (NaOCl) in killing microorganisms in simulated swimming pool water condition, which indicated that NaOCl was more effective (Borgmann-Strahsen, 2003). Pool water chlorination regulation and guidelines vary from country to country. The term "free chlorine" is practically defined as the sum of available HOCl, OCl^-, and Cl_2 (aq). HOCl has the most potent disinfection power. The World Health Organization suggests that free chlorine residual should be maintained at 1–3 mg/L in the pool water when only chlorine products are used (WHO, 2006). The New South Wales Ministry of Health, Australia recommends a free chlorine concentration ≤ 2 mg/L for indoor swimming pool water (pH-value < 7.6) (NSW, 2013). The province of British Columbia, Canada, mentioned that the free chlorine level must be equal or lower than 0.5 mg/L (temperature ≤ 30 °C) or lower than 1.5 mg/L (temperature > 30 °C) (BC Reg 296/2010, 2010). In Germany according to the German Pool Water Standard DIN-Norm 19643-1 (DIN, 2012a) the free chlorine in swimming pool water generally should be maintained at 0.3–0.6 mg/L and for hot whirlpool at 0.7–1.0 mg/L to achieve a sufficient disinfection capacity. A maximum concentration at 1.2 mg/L is allowed for certain operation conditions.

Chlorine reacts with inorganic and organic matters in pool water and produce undesirable and potentially harmful disinfection by-products (DBP). The negative health effects such as bladder cancer which have been associated with DBP have driven much attention in recent years (Richardson et al., 2007, Villanueva et al., 2007). DBP in drinking water have been widely investigated in recent decades. Natural organic matter (NOM) from humic origin is generally accepted as precursors for DBPs in drinking water (Barrett et al., 2000, Krasner et al., 2006, Rook, 1974). NOM is a major reactant in and a product from biogeochemical processes. The amount and composition of NOM depend on the water source. Humic substances are the major fraction of NOM in surface water such as lake or river. They are refractory anionic compounds which range from low to moderate molecular weight to macromolecules (Leenheer and Croué, 2003). After drinking water treatment a fraction of NOM still remain in tap water, which is brought into swimming pool with the filling water and composes the

basic matrix of organics in the pool water when the pool is filled with tap water. Additionally pool water receives the exogenic precursors such as hair, saliva, urine, personal care products, etc. from visitors, which are more reactive than the NOM from filling water (Kanan and Karanfil, 2011). Other inputs can also come from the pool water maintenance. Trihalomethanes (THM) are the most typical organic DBP in chlorinated waters such as drinking and swimming pool water. Haloacetic acids (HAA) are the second DBP group which receives major attention. Nitrogenous compounds such as urea, amino acids and creatinine form chloramines, which are responsible for the typical odor of a swimming pool and are measured as bound chlorine. By far, more than 100 species of DBPs have been identified in the swimming pool waters (Richardson et al., 2010). But the majority of total DBPs are still unidentified. A sum parameter, absorbable organically bound halogens adsorbable on activated carbon (AOX), has been used to give the general level of DBP in chlorinated water.

DBP levels in swimming pool water are higher than in drinking water (Kanan and Karanfil, 2011) and induced more genomic DNA damage than the source tap water (Liviac et al., 2010), mainly associated with chlorination at higher water temperature (25–35 °C) (Simard et al., 2013). The conventional treatment process of swimming pool water, which comprises mainly flocculation and sand filtration, cannot effectively remove the dissolved organic matters (DOC) to keep the pool water hygiene and security, especially when increased levels of contaminants are brought by swimmers during intensive visits. Therefore the problem is particularly more evident in swimming pool water, where the treated water is almost entirely recirculated. Here, the substances which cannot be removed by the treatment will accumulate (Barbot and Moulin, 2008, Müller and Uhl, 2011, Simard et al., 2013). Understanding the behavior of DBP-formation in pool water is complex due to the irregular new input of contaminants and the recirculation of swimming pool water over long periods of time (Chowdhury et al., 2014). However it's essential to develop the appropriate treatment strategy.

2.1.1 THM in swimming pool water

Trihalomethanes (THM) are the most typical organic DBP in chlorinated water. The four mostly studied THM are chloroform ($CHCl_3$), bromodichloromethane ($CHCl_2Br$), dibromochloromethane ($CHClBr_2$) and bromoform ($CHBr_3$). Usually chloroform is the predominant THM formed, contributing an average of more than 95% by weight to the total THM (Bessonneau et al., 2011, Simard et al., 2013). Other THM compounds are normally found in much lower concentrations than chloroform. Bromide containing THM are produced when there is Br- in water (Erdinger and Kühn, 2004). Volatile DBPs like THM can be taken up via inhalation, dermal adsorption and ingestion. Compared to intake of tap water, gastrointestinal exposure in pool water and skin exposure during showering, skin exposure while swimming is the main intake route of THM contributing cancer risk (Panyakapo et al., 2008).

Practically the total THM concentration is the sum of different THM calculated and given as chloroform. The European Communities (Drinking Water) (No. 2) Regulations implemented the limit

for total THM at 100 µg/L from December 2008 (Communities, 2007). In Germany the limit of THM in drinking water regulation is 50 µg/L (TrinkwV, 2016). The U.S. Environmental Protection Agency (EPA) issued the "Stage 1 Disinfectants/Disinfection By-Products Rule (D/DBP)" in 1998 giving the maximum allowable annual average level for total THM at 80 µg/L (EPA, 2002). In swimming pool water the regulatory limit is even stricter. According to the German Pool Water Standard (DIN, 2012a) the recommended concentration for THM in swimming pool water is 20 µg/L.

Various studies have reported a wide variation of THM occurrence in swimming pool water. However, THM concentration can vary significantly in pool water over one day, weeks and months (Kristensen et al., 2010). Intermittent sampling can be insufficient for investigation of the formation mechanism in the whole swimming pool water system. Comprehensive understanding of THM formation, occurrences and their variability is essential for DBP study in swimming pool water. THM formation is affected by the disinfectants, disinfection conditions and character of water sources. To date no meaningful relationships between certain compound physiochemical properties and THM formation has been found (Bond et al., 2012). Most studies use sum parameter such as total organic carbon (TOC), dissolved organic carbon (DOC), UV_{254} and/or specific UV absorbance (SUVA) to represent organic precursors. TOC has been proved being able to represent the release of the anthropogenic pollutants (Keuten et al., 2012). In a study of 2 outdoor swimming pools with 81 samples it was estimated that on average 1.09 g DOC per person is brought into swimming pool water (Glauner, 2007). DBP-FP (formation potential) experiments by dosing a certain amount of chlorine are usually applied to elucidate reactive precursors, kinetic behavior and formation mechanisms. Several studies applied body fluid analog (BFA) or materials of human origin to investigate the THM formation yield (Borgmann-Strahsen, 2003, Hansen et al., 2012, Judd and Bullock, 2003). But the BFA might result in a lower THM formation potential due to the fact that the presence of NOM brought by the filling tap water contributes to an additional DBP formation (Kanan and Karanfil, 2011). In another study urine was added to model solutions containing humic material. The overall THM formation was reduced, which was attributed to the depletion of active free chlorine by forming chloramines (Judd and Jeffrey, 1995). Chlorination experiments of more various materials from human origin mixed within ground water or surface water indicated a significant correlation between TOC and DBP formation but the composition of DBPs can be considerably different due to different water sources (Kim et al., 2002). Experiments with native water rather than only model compounds are needed to have results which are comparable to real situation in the swimming pool.

2.1.2 Modeling of THM

Many modeling attempts have been made to predict the occurrence of THM in the past three decades but primarily in the field of drinking water. Most of them are function models based on empirical and mechanistic relationships of water quality and operational parameters (Chowdhury et al., 2009). Additionally regression or statistical methods were extensively used (Golfinopoulos and Arhonditsis,

2002). The research of THM modeling has been established in principle by linking THM with water quality parameters including TOC or DOC, type of organic precursors, pH, temperature, reaction time, UV absorbance, chlorine and bromide (Br^-) concentration, etc. (Abdullah and Hussona, 2013, Sadiq and Rodriguez, 2004). Although the connection of specific model compounds to DBP formation remains uncertain (Hua et al., 2014), generally the increase of chlorine concentration, pH, temperature and reaction time leads to higher formation of THM (Abdullah and Hussona, 2013, Zhang et al., 2013). Some studies tried to establish a proportional relationship between the DBP formation and chlorine consumption. But chlorine consumption may actually largely result from chlorine decomposition or reaction with other reductive substances so that leads to an overestimation (Bond et al., 2012). Moreover, typically the THM loss due to adsorption or volatilization was not considered in these studies on drinking water.

Compared to drinking water, modeling of DBP in swimming pool water attracted much less attention, although that swimming pool has a great recreational value. A possible reason can be the increased complexity of swimming pool water in comparison to the typical drinking water systems due to unpredictable input from visitors, variability and interactions of different precursors and much longer contact time with disinfectant (Chowdhury et al., 2014, Zwiener et al., 2007). Water temperature is typically adapted to the specific requirements with respect to energy or economic aspects and is often set to be certain value in swimming pool. The pH-value is usually kept relatively stable for sufficient chlorination efficiency. However, due to the fact that the bather and contaminant load, chlorine dosage, DBP concentration and fresh filling water can vary considerably both over short and longer time scales, different pool water scenarios are not easily comparable. Preparation of model swimming pool water in the laboratory is even more difficult. For the less reactive moieties, reactions with chlorine can be too slow to be observed during the drinking water disinfection. Glauner et al. (2004) observed in an outdoor swimming pool that a THM peak appeared two days after DOC increased. Additionally, effects of such recirculation rates of pool water system on DBPs are not well-understood to date. A few models for THM in indoor swimming pool air have been developed for exposure to THM for visitors (Chen et al., 2011, Hsu et al., 2009). To our knowledge, no simulation to predict THM in swimming pool water was to date established.

In summary:

- Precursors of DBPs in swimming pool water include NOM from tap water and anthropogenic input from visitors.
- THM are the most typical DPBs, while the majority of total DBPs remain unidentified.
- THM formation is affected by disinfectant, disinfection condition and character of water.
- No meaningful relationship between certain compound physiochemical properties and THM formation was found yet.
- To date there has been no information about THM modeling in swimming pool water.

2.2 Nanofiltration for eliminating DBP

2.2.1 Nanofiltration for eliminating DBP precursors

Regarding drinking water treatment, different methods were studied to eliminate DBP precursors. Activated carbon adsorption is one of the common treatments for controlling DBP especially THM (Potwora, 2006, Uhl et al., 2005). But the capacity is limited and new activated carbon has to be replaced regularly. Ozone can convert the hydrophobic fractions of DOC into hydrophilic ones and results in the reduction of THMFP, of which the combination with coagulation leads to a further reduction (Sadrnourmohamadi and Gorczyca, 2015). Combination of coagulation, MIEX® anion exchange resin and NF was also studied for reduction of DBP precursors (Bond et al., 2010).

Membrane filtration has experienced a significant development and represents one of the major technologies for water treatment. Nanofiltration (NF) has gained in importance for varies applications in the last decade and has become an interesting alternative for elimination of DBP precursors in water. Most commercial NF membranes have a molecular weight cut-off (MWCO) of about 200–2000 Da. NF will remove most of the dissolved salinity solids especially multivalent ions, a large percentage of the dissolved organic matter (DOC), parasites and essentially all of the bacteria and viruses (Agenson et al., 2003, Patterson et al., 2012). Hence NF treated water is also disinfected. Rejection properties of NF has been used commercially since more than 20 years, often used to treat the through microfiltration (MF) or ultrafiltration (UF) pretreated water for indirect potable water reuse or water softening. First large-scale application of NF in water filtration plant was in France, which aimed at the removal of hardness, organic matters and trace contaminants, which showed satisfactory experience for two years (Cyna et al., 2002). NF can provide moderate to good recovery at pressure 5–20 bar (Mulder, 1996). However, most of the membranes such as thin-film composite membranes can end in rapid degradation by strong oxidizers as chlorine, which limits the application (Do et al., 2012, Kang et al., 2007). Emerging NF membranes made of chlorine-resistant materials such as polyethersulfone are possible to be applied in harsh alkaline conditions or under conditions with chlorine (Schlesinger et al., 2006), which can be interesting for treatment of pre-chlorinated water.

Removal of DBP precursors in drinking water by NF was extensively studied, often applying chlorination tests to determine the formation potential (FP) of DBP. DBPFP of feed water and permeate were compared to calculate the removal by NF. Model compounds or natural water samples were investigated. Despite that rejection of NF depended to a great extent on the water composition and the ionic strength of the raw water (Saravia et al., 2013), many studies showed that removal of precursors by NF before the disinfection procedure could largely reduce the DBPFP. Over 75% of the THMFP in natural water was eliminated using a NF membrane with the MWCO of 450 Da (Sentana et al., 2011). Increases in el. conductivity of feed from 786 to 1100 μS/cm didn't affect the reduction of HAAs or THMs formation potential in surface water (Sentana et al., 2010). Above 90% of DOC, THMFP and HAAFP in surface water could be removed by a few NF membranes (Siddiqui et al.,

2000). In a pilot plant study with NF (200 Da) for groundwater treatment in Germany, the rejection of NOM, AOXFP and THMFP was > 95% (Gorenflo et al., 2002). (Lee et al., 2005) presented that THMFP removal was proportional to the NOM removal.

Based on the experience in drinking water treatment, to quickly remove precursors brought by visitors before further reaction with disinfectants could be a potentially effective approach of controlling DBP in swimming pool water. Commonly when the DBP concentration breaks the regulatory limit, extra fresh water is filled into swimming pool to make a dilution effect and meet the limit. So a more efficient treatment will not only improve the water quality but also saving water and energy for heating the newly filled water. NF became attractive alternative regarding a more efficient treatment minimizing DBP and DBP precursors. However, water temperature in swimming pool is much higher (approximately 30 °C) than in drinking water treatment. Doederer et al. (2014) determined the rejection of 29 DBP by NF, and found that in general rejection decreased when temperature increased and permeate flux decreased. The performance of NF in swimming pool water treatment cannot be straight related to NF performance in drinking or waste water treatment and therefore needs to be investigated. A few studies intended to investigate the application of NF in swimming pool water treatment. A combination of advanced oxidation processes (AOP) and NF was shown to remove up to 80% DBP/DBP-FP, including the reduction of AOX, AOXFP and THMFP at 61–67% by NF membrane NF200B-400 (DOW) (Glauner et al., 2005a). Klüpfel (2012) investigated NF in bench-scale for swimming pool water treatment. Results showed that DOC and AOX could be rejected up to 70–80% by NF, which implied the concentration of DBP and DBP precursors could be largely reduced in pool water, when an appropriate portion of mainstream is treated using NF. By calculating DOC mass balance the possibility to integrate NF into pool water treatment as an effective alternative to conventional treatment was proposed. Further benefits such as saving fresh water consumption were also announced. Additionally, the combination of treatment process with ultrafiltration (UF) was added into the German Pool Water Treatment Standard DIN 19643-4 (DIN, 2012b). This serves as a suitable pretreatment step for NF which makes the integration of NF in pool water treatment even more feasible.

Nevertheless, a high rejection of DOC and UVA_{254} may not always necessarily mean that the DBP levels produced afterwards will be low. Studies showed that DOC rejection was higher than the DBPFP reduction, which means the organic matter that forms DBP was still present in the NF permeate (de la Rubia et al., 2008, Sentana et al., 2011). Ates et al. (2009) showed although NF membranes (100–300 Da) reduced the formation potential of THM and HAA above 90%, DOC and UVA_{254} rejections could not be directly linked to DBP formation reductions by the tested membranes. Because low molecular weight organic fractions which are less effectively rejected by NF membranes may form other unregulated and/or unknown DBP, which can be measured by AOX. The precursors of HAA and THM were determined to be associated primarily with the hydrophobic fraction, although

the hydrophilic fraction is important as well (Roccaro et al., 2014). Diverse results regarding different fractions which were more effectively removed by NF were reported. In a study of surface treatment by NF, UVA_{254} rejection was higher than DOC rejection, which indicates that aromatic/hydrophobic compounds of the NOM can be preferentially removed (de la Rubia et al., 2008). Cortés-Francisco et al. (2014) used a combination of ultrahigh resolution Fourier transform ion cyclotron mass spectroscopy (FT-ICR MS) and nuclear magnetic resonance (NMR) spectroscopy to characterize molecular change of dissolved organic matter (DOM) in surface water after NF pilot plant. Results revealed that NF preferentially removed compounds with higher oxygen and nitrogen content (more hydrophilic compounds), whereas molecules with longer pure aliphatic chains and less content of oxygen were capable of passing through the membranes. By fractionation of swimming pool water Glauner et al. (2005b) found that compounds with a molecular weight (MW) of 200–1000 g/mol accounted for a major part of the AOXFP. Highest formation of THMs was from the low-MW fraction (< 200 g/mol). The genotoxicity was found to be strongest also in the low-MW fraction. Therefore DBP removal by NF with MWCO down to 200 g/mol was recommended. Moreover, different from drinking water treatment, the produced water returns back to swimming pool and stay for a much longer contact time with chlorine. The fate of the remaining DOC in NF permeate and the effect of DOC-rejection in a recirculated system is yet unknown.

2.2.2 Nanofiltration for THM rejection

For systems with previously chlorinated water, NF is an attractive option to directly reject THM. However, literature concerning the rejection behavior of THM by NF has been a matter of contradictions, ranging from little to 95% in rejection (Agenson et al., 2003, Doederer et al., 2014, Klüpfel et al., 2011b, Levine et al., 1999, Uyak et al., 2008, Waniek et al., 2002). Details of selected studies are listed in Table 2.1.

Table 2.1: Selected studies about THM rejection by NF membranes.

Feed	Membrane	Filtration time	THM Concentration	Pressure (bar)	THM rejection	Source
Water designed in laboratotry	NF200	4 h	40 µg/L	25	65–95%	(Uyak et al., 2008)
	DS5		40 µg/L	10	80–85%	
Water designed in laboratotry	NF90	6 days	50 µg/L	2.2	5%	(Doederer et al., 2014)
Water designed in laboratory	UTC60	3 h	1250 µg/L	3	5–7%	(Agenson et al., 2003)
	NTR729HF				24–55%	
Swimming pool water	SB90, XN45, NP030	22 d	Pool water	10	little	(Klüpfel et al., 2011a)

Most of the studies were short term experiments. The variety of experimental conditions is also limited, mostly in deionized water prepared in the laboratory which didn't consider the interactions between THM and the different water constituents (e.g. ions, natural organic matter) and the THM-properties

(e.g. volatilization). Some studies often had unrealistic high concentration of THM in the model solution, which would have huge impact on the diffusion process through membrane. Moreover, the volatility of THM makes the actual aqueous concentration during experiments difficult to control. However, only one work (Doederer et al., 2014) mentioned special experimental set-up to avoid the volatilization.

THM belong to micropollutants and are relatively small organic molecules with the molecular weight of 119 to 253 g/mol. Some work has been done to study the rejection of micropollutants such as pharmaceuticals, pesticides, personal care products or DBP by NF (Hajibabania et al., 2011, Kimura et al., 2003b, Xu et al., 2005). Previous studies showed that most organic micropollutants could be effectively rejected by NF (Wang et al., 2015). In general neutral and small molecules are often associated with low rejection. To date no accepted method is known to predict the rejection of organic solute by polymeric membranes (Verliefde et al., 2009a).

2.2.3 Rejection mechanisms

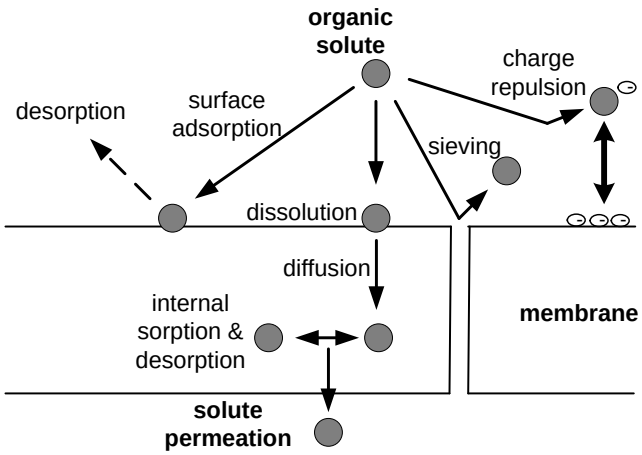

Figure 2.1: Adopted schematic of hypothesized rejection and transport paths for organic substances through NF membranes after (Steinle-Darling et al., 2010). The main transport mechanism for organic solutes, which are too large to pass through the pores, is solution-diffusion through the bulk membrane material. A fraction of those organic solutes may be adsorbed in the process of passing through the membrane.

Rejection of organic pollutants by NF membranes is dominated by different mechanisms. The well accepted major rejection mechanism in NF is physical sieving or also called steric exclusion of solutes which are larger than the membrane MWCO (Bellona et al., 2004). It's also recognized as the primary mechanism in the rejection of organic micropollutants by NF (Wang et al., 2015). NF membranes are intermediate between ultrafiltration membranes and reverse osmosis (RO) membranes. So both convection through pores (defects) and solution-diffusion are involved for mass transport of solutes. Nghiem et al. (Nghiem et al., 2004) found out that the application of pore transport model lead to an overestimation of the rejection of natural hormones, probably because the hormones could pass the membrane both through convection and adsorption-dissolving-partitioning. Another study illustrated that the assumption of steric exclusion as exclusively rejection mechanism lead to an overestimation of

rejection for solutes which have strong affinity to membrane material (Verliefde et al., 2009a). Hypothesized rejection mechanisms and transport paths for organic substances through NF membranes are illustrated in a schematic Figure 2.1 adopted after (Steinle-Darling et al., 2010).

Solute-membrane interactions such as electrostatic effects and "solute-membrane affinity" play also a significant role in NF-rejection. NF are able to effectively remove natural organic matter (NOM) through a combination of size exclusion and physical-chemical interactions such as charge repulsion (Teixeira and Rosa, 2006). For negatively charged membranes, electrostatic repulsion can increase the rejection of negatively charged solutes and electrostatic attraction can decrease the rejection of positively charged solutes (Verliefde et al., 2008). It was even discovered that negatively charged solutes do not engage in hydrophobic interactions since they cannot approach the membrane surface. THM present in water are neutral so the electrostatic effects shouldn't play a role in rejection. Solute-membrane affinity has been a term which includes many different factors other than the widely studied electrostatic effects, such as the size, charge, hydrophobicity, hydrogen bonding and dipole moment, which may affect the solute-membrane interactions. This has been broadly investigated but hasn't been not well understood. The influences of these factors become especially more important for low molecular weight organic compounds (Boussu et al., 2008, Wang et al., 2015).

2.2.4 Effects of adsorption and organic fouling

Adsorption of solutes to the membrane is an important solute-membrane interaction. Neutral micropollutants which have high n-octanol/water partition coefficient (log K_{ow}) or hydrogen bonding capacity usually can adsorb to the membrane (Kimura et al., 2003a). Adsorption can affect the mass transport of the solutes so as to the rejection. First, high initial rejection due to adsorption followed by decrease of rejection over time has been already observed for different organic micropollutants (Kimura et al., 2003a, Steinle-Darling et al., 2010, Xu et al., 2006). An accurate evaluation of the rejection of hydrophobic compound should be done only after the adsorption reaches the steady-state or the "saturation". Once the sorption capacity of the membrane is exhausted, rejection is supposed to be dominated by the mechanisms regarding diffusion through the membrane. Adsorption might also have indirect effects on the steady-state rejection, because adsorption of solutes in the membrane separating layer may significantly affect the properties of the membrane with respect to its rejection performance. Absorption of organic molecules to the membrane seemed to facilitate the diffusion transport of solutes through membrane and hence decreases the rejection (Arsuaga et al., 2010, Steinle-Darling et al., 2010).

Rejection mechanisms of micropollutants by NF membranes in real water matrices (i.e. in the presence of organic macromolecules) are very complex. The reported overall rejection value and effects of different feed water matrices vary significantly. Moreover, the presence of high content of organics in water often leads to organic fouling, which is a common problem in membrane filtration. Fouling could change the membrane surface properties and alter the interactions between solutes and

membrane. The influence of water matrices and fouling on NF membrane performance is not completely understood. Different effects of fouling on the rejection were reported. Generally, increase in rejection after membrane fouling was attributed to the formation of a denser layer which serves as an additional filtration layer (Mahlangu et al., 2014, Verliefde et al., 2009b) or pore blocking which narrows the pores (Nghiem et al., 2008). NOM rejection by NF could be affected also by fouling of calcium-organic precipitate (Schäfer et al., 2000). One study showed that fouling by filtrated secondary effluent increased rejection of hydrophobic non-ionic organic solutes but facilitated organic transport through cellulose triacetate membranes (Xu et al., 2006). Agenson and Urase (2007) determined the change in membrane performance after organic fouling by sludge and landfill leachate using 36 neutral trace organic matters filtrated with aromatic polyamide NF and RO membranes. A lowered rejection of higher molecular weight solutes was observed. The given explanation was that the attachment of foulants on membrane polymer and subsequent diffusion of the large solute molecules through the membrane facilitated the transport.

In summary:

- Studies in drinking water showed that removal of DBP precursors by NF before disinfection could largely reduce the DBPFP.
- A high DOC rejection may not always lead to low DBP production in subsequent disinfection.
- Literature concerning the rejection of THM by NF has been contradictory, ranging from little to 95% in rejection.
- Major rejection mechanisms of organic substances by NF membranes include sieving and charge repulsion, while the interactions of solute and membrane such as adsorption play an important role, which hasn't been well understood.

2.3 Fouling of NF membranes in swimming pool water treatment

Despite the promising perspectives for NF, fouling is an overall problem in membrane filtration, which could decrease the permeability, change the rejection performance, increase the energy consumption and maintenance cost, and reduce the life of membrane. Remaining constituents from the pre-treatment can adsorb, accumulate or precipitate within or on the membrane polymer matrix leading to fouling.

2.3.1 Fouling type and mechanisms

Membrane fouling may be defined as the deposition of suspended or dissolved substances such as retained particles, colloids, emulsion, suspensions, macromolecules, salts etc. on or in the membrane (Koros et al., 1996, Mulder, 1996). Commonly fouling has been classified to colloidal/particle fouling, scaling, organic fouling and biofouling. Colloidal/particle fouling refers to accumulation of fine particles with the rough size range of 1−1000 nm, which has been largely studied and the understanding has been advanced (Tang et al., 2011). A proper pretreatment such as ultrafiltration (UF)

can provide effective prevention. Scaling refers to inorganic precipitates such as metal hydroxides and sparingly soluble salts when the dissolved ions in feed at the membrane surface become supersaturated. Precipitated deposits grow from nucleation gradually to form a scaling layer, which can considerably reduce the membrane permeability. The mechanisms of scaling have been widely investigated (Al-Amoudi, 2010). Adjusting pH and appropriate antiscalants are possible means to control scaling (Shirazi et al., 2010). Organic foulants including macromolecules or biological substances may cause organic fouling and promote biofouling. Organic fouling is commonly due to NOM such as humic substances and their derivatives, protein and carbon hydrate. While NOM fouling on UF membranes has been reported in many studies using UF to remove NOM from surface water, the studies on NOM fouling on RO and NF membranes have increased lately (Braghetta and DiGiano, 1998, Hong and Elimelech, 1997, Lee and Elimelech, 2006, Seidel and Elimelech, 2002). In many cases, model foulants such as humic acid, fulvic acid and NOM standards from the International Humic Substance Society (IHSS) have been used (Lee and Elimelech, 2006, Tang et al., 2007). Nutrients from feed or from deposits on membrane can supply microbial growth. Biofouling is a dynamic process of microbial colonization and growth, which results in the formation of microbial biofilms. Biofouling is prevailing within membrane systems (Vrouwenvelder and van der Kooij, 2001). Biofouling causes severe damage in membrane because biofilm is very difficult to remove, yet many systems operate satisfactorily even with a biofilm (Baker and Dudley, 1998). As summarized by Schäfer et al. (2004), typically particulate/colloidal and rapid biofouling occur in the early stage of membrane modules due to higher permeate drag force. In the long run biofouling slowly spreads to latter stages with time. Organic fouling is yet not completely understood, which can occur in the beginning or end stages, depending on the foulant properties. Scaling and silica fouling usually happen in the latter membrane stages when the increased concentration exceeds the solubility limit.

It's usually accepted that main mechanisms of fouling include adsorption, pore blocking, precipitation, cake layer formation and gel formation (typically for protein containing solutions) (Al-Amoudi and Lovitt, 2007, Schäfer et al., 2004). Concentration polarization tends to assist in the fouling mechanisms such as adsorption, cake layer formation and gel formation (Sablani et al., 2001). Braeken et al. (2005a) stated that adsorption of dissolved organic compounds on polymeric NF membranes is comparable to that on activated carbon. Mechanism involved in biofouling is microbial attachment followed by biological growth for biofouling. Biofilm formation always precedes biofouling, which becomes an issue only when biofilms reach thickness and surface coverage that may cause problems (Al-Amoudi and Lovitt, 2007). Production of extracellular polymeric substances (EPS) is responsible for the biofilm. Fouling mechanisms have been studied but it remains difficult to describe theoretically and to predict and distinguish which mechanism participates in the operation (Mohammad et al., 2015).

Because fouling is a complex process, in which different interactions between feed and membrane properties as well as operating conditions play a part (Al-Amoudi, 2010), which will be described

respectively in the next paragraphs. The most studied factors affecting fouling are briefly summarized in Table 2.2.

Table 2.2: Summary of the most studied factors affecting fouling.

Factors affecting fouling		Manifestation
Feed water properties	pH	• more severe NOM fouling at low pH
	ionic strength	• more severe organic fouling at higher ionic strength
	divalent cation	• interaction with carboxyl functional groups of humic substances and formation of complex enhance NOM fouling • stronger effect than monovalent cation, most notably Ca^{2+}
	composition of constituents	• more adsorption of hydrophobic fraction than hydrophilic fraction on membrane • more interaction of high MW than low MW fractions with divalent ions for fouling
	concentration	• commonly more severe fouling at higher concentration in feed
Membrane properties	surface roughness	• more severe fouling for rougher surface
	surface charge	• higher fouling tendency for uncharged membranes
	surface hydrophobicity	• less fouling tendency for less hydrophobic interactions between solute and membrane
Operation conditions	(initial) permeate flux	• more rapid flux decline at higher initial flux
	pressure	• increased compaction of biofilm at higher pressure

Feed water properties including foulant concentration, temperature, pH, ionic strength, ionic composition and specific interactions between solutes (hydrogen bonding, dipole-dipole interactions) have influences on fouling formation. Generally, low pH, high ionic strength enhances organic fouling, which was principally attributed to the reduced electrostatic repulsion (Hong and Elimelech, 1997, Seidel and Elimelech, 2002, Tang et al., 2007). Divalent ion (Ca^{2+} and Mg^{2+}) enhances organic fouling by forming complexes with NOM (Li and Elimelech, 2006). Seidel and Elimelech (2002) found that the deposited mass of humic acid in fouling cake layer was greatly increased when 1 mM Ca^{2+} was present in the feed solution. Furthermore, hydrophobicity, polarity and molecular charge (Braeken et al., 2005b, Van der Bruggen et al., 2002b, Wang and Tang, 2011) may affect fouling.

Membrane properties play a key role in flux decline, the accumulation of fouling material and the composition of constituents on the membrane (Saravia et al., 2013). Hydrophilic and smooth membrane surface typically show the best resistance to fouling. Increasing hydrophobicity commonly leads to more organic fouling and increasing roughness increase colloidal fouling (Boussu et al., 2008,

Elimelech et al., 1997). However humic acid fouling was found largely independent of virgin membrane properties (Tang et al., 2007). Fouling of charged compounds also strongly depends on the charge of membrane but no consistent conclusions were drawn, depending on the foulant properties. Some stated that membrane with high zeta potential encounters less fouling (Boussu et al., 2008) while some claimed that uncharged or less charged membrane had lower amount of organic fouling (Saravia et al., 2013). Supposedly, membrane surface properties play an important role the initial phase of fouling, which determines the interactions between foulants and membrane. But with time fouling can modify the membrane surface properties which lead to the interaction between fouling layer and foulants in feed. After fouling with similar foulant the hydrophobicity of two different membranes became close (Xu et al., 2006). Humic acid may increase the hydrophobicity and negative charge of membrane (Mänttäri et al., 2000). Furthermore, the ratio of molecular size to membrane pore size is important for fouling (pass through or not). Organic fouling was found to be more severe for membranes with larger pore size (Nghiem and Hawkes, 2007, 2009). Saravia et al. (2013) reported that the concentration of ions in the membrane "pores" correlated directly with the MWCO of the membranes.

Operation such as hydrodynamic condition will also affect fouling propensity. Flux performance depends on hydrodynamic conditions and solution composition. High initial permeate flux causes severe fouling by humic acid due to higher permeation drag which overcomes charge repulsion resulting in rapid deposition (Tang et al., 2007). Higher pressure also leads to more compaction of fouling layer resulting in higher resistance (Wang and Tang, 2011). Hydrodynamic condition seems to strongly affect biofouling regarding bacteria adhesion. The first step of biofilm formation on membrane is conditioning film formation and initial bacteria adhesion, which is affected by deferent factors such as feed composition, bacteria species, cross-flow and permeation hydrodynamics and membrane surface properties (Habimana et al., 2014, Semião et al., 2014). Increased permeate flux leads to increased initial bacterial adhesion. Membrane surface properties and bacterial growth phases have little impact on initial bacterial adhesion to NF and RO membranes (Semião et al., 2014). Heffernan et al. (2014) reported that bacteria penetrate the organic fouling layer and adhere directly to the membrane surface. And fouling served as an obstacle to hinder the initial bacteria adhesion, which means a previously formed organic fouling layer will reduce the initial bacteria adhesion. Furthermore, due to pressure drop along the channel affected by fouling layer, more bacteria can penetrate the fouling layer with higher permeate drag force and adhere to the membrane in the inlet region than in the rear region. In this case probably inlet region is favored for biofouling in short term, while in long term biofouling usually spread out to the whole module. Convective flux to the membrane overcomes the influences of the membrane surface properties such as roughness (Heffernan et al., 2014). Higher pressure also results in increasing compaction of biofilm and resistance (Dreszer et al., 2014).

In most real cases different fouling types occur together. Al-Amoudi and Farooque (2005) stated that a typical SEM micrograph of fouled NF membrane showed a combination of organic and inorganic matters and biofouling, as well as their corresponding electron dispersion X-rays (EDX) spectra. For example, carbon, phosphorous, diatoms as well as iron were observed on the membrane surface. Different foulants can promote or suppress each other. Synergistic effects of combined fouling were investigated using model substances such as silica/latex colloids, humic acid and alginate. Specific interactions between chemical functional groups on membrane surface and of organic foulants was observed (Li and Elimelech, 2006, Mahlangu et al., 2015). Furthermore, most membranes experienced higher fouling in the NF of polysaccharide mixtures using model foulants humic acid, vanillin and high MW polysaccharides than in the single polysaccharides (Mänttäri et al., 2000). Similarly, flux decline in the presence of oppositely charged macromolecules (lysozyme and alginate) was much more severe than with single foulants (Wang and Tang, 2011). Lee et al. (2009) observed that the presence of dissolved organic matter reduced $CaSO_4$ scaling. Such studies predominantly used model solutions. Whether the results can be transferred to realistic application requires more research because complex mechanisms are needed. For example, adsorption of organic foulant to the clean membrane surface was found only impacting the very beginning fouling stage and doesn't have a lasting effect on the overall flux decline behavior (Contreras et al., 2009). In practice membrane fouling often causes continuous flux decline.

2.3.2 Methods for characterizing fouling

Traditionally fouling potential is determined by using silt density index (SDI) and modified fouling index (MFI) for prediction of particulate/colloidal fouling. There are also indexes for measuring the potential of scaling such as Langelier Saturation Index (LSI). Yet there is no suitable method for organic and biological fouling prediction. Feed pretreatment, membrane modification and membrane remediation by chemical cleaning to restore membrane fluxes have been studies and often employed to fight against fouling. If permeate flux decline reaches 10−15% a chemical cleaning is suggested (Arnal et al., 2011). But frequent cleaning may also deteriorate membrane performance. A good identification and characterization of foulants and fouling mechanisms is essential for effective fouling control.

Autopsy study of membrane modules after realistic operation is a diagnostic tool which provides convincing insights for the practical application and comprehensive information such as the dominant type of fouling, distribution of foulants and impact of feed water chemistry (Pontié et al., 2007). It's however a destructive method, normally considered when the membrane is damaged or the performance cannot be restored. The amount of autopsy studies has been increased in recent years (Beyer et al., 2014, Touffet et al., 2015, Tran et al., 2007). Diverse techniques were applied to the autopsied membrane sample for fouling characterization.

Fouling deposits can be scrapped off the membrane. Wet and dry mass of deposit can be measured. Organic/inorganic content can be determined after thermal treatment at 550 °C. With elemental analysis through combustion the mass proportion of C, H, N, O and S can be determined. Thermogravimetric analyzer (TGA) was used to measure the weight loss along the "temperature curve" (Tay et al., 2003). However it's not a common method and has many limitations such as the material of polymer membrane.

Fouling deposits can be washed off and dissolved by cleaning agent such as acid or base and measured using liquid analytic methods such as DOC, IC and ICP-OES (Saravia et al., 2013). SEC-OCD has been applied to investigate the MW distribution of foulants (Jarusutthirak and Amy, 2007). There was also studies which used salt solution such as sodium sulfate at high ionic strength for extraction (Her et al., 2007). Such analytical methods provide quantitative analysis of foulants. However, many such studies miss the comparison with feed water properties for the significance of foulant accumulation. Magnetic resonance spectroscopy may determine the chemical structure of substances. The ^{13}C NMR-spectra of NOM give the quantitative information of structure (Kimura et al., 2008, Saravia et al., 2003). The 3-dimensional fluorescence excitation-emission matrix has also been used (Chon and Cho, 2016).

Foulants can also be determined by methods which directly compare the clean and fouled membranes. The commonly used surface characterization methods such as zeta potential, AFM and contact angle can show a possible change after fouling formation. Optical and scanning electron microscopy (SEM) can visualize the morphology and structure of fouling deposits, especially in the case of scaling. SEM coupled with energy dispersive X-ray spectroscopy (EDX), semi-qualitative analysis of chemical elements composition in fouling layer can be obtained. However, purely organic fouling and biofouling cannot be well defined by this method. Fourier transform infrared spectroscopy with Attenuated Total Reflection (ATR-FTIR) is used for measuring functional groups, which is useful to predict the structure of the compounds and yet difficult to identify the exact organic compounds.

For biofouling more methods have been applied. Adenosine Triphosphate (ATP) was used (Vrouwenvelder and van der Kooij, 2001), which is considered an essential indicator of living bacteria and gives a measure of the amount of active biomass over the membrane surface. Many studies tried out extraction of EPS using centrifugation, ultrasonication, cation exchange resin, heating, alkaline reagents such as NaOH. Low effectiveness, artifacts from extraction process, hydrolysis of high MW compounds have been shown (Mondamert et al., 2009). Most of the studies focused on the overall parameters such as COD, total quantification of polysaccharides, proteins, carbohydrates, phospholipids, sugar content, biopolymers and size distribution, but couldn't identify even the majority of these compounds (Kunacheva and Stuckey, 2014).

New trends are to develop non-destructive and visual on-line observation methods to study biofouling. Imaging has been lately an intuitive tool to study the biofilm on membrane in-situ using optical coherence tomography (OCT) (Dreszer et al., 2014, West et al., 2016) or confocal laser scanning microscopy (CLSM) (Herzberg et al., 2009, West et al., 2014). The advantage is the thickness and morphology can be observed non-destructively and even in real-time using designed membrane fouling simulators (MFS) with viewing area ― commonly a transparent window (Huang et al., 2010, Vrouwenvelder et al., 2006). Magnetic resonance imaging (MRI) has been recently applied to study biofouling in RO membranes (Creber et al., 2010, Graf von der Schulenburg et al., 2008).

2.3.3 Major foulants of NF Fouling and potential foulants in swimming pool water treatment

Characterization and quantification for the identity and localization of major foulants is of great concern. Lab-scale studies focusing on identifying the foulants usually just investigated fouling after a few filtration cycles in a bench-scale system. But organics accumulation on the membrane is a long-term process. Lab experiments may not represent the real situation. A few researches have conducted autopsy studies and investigated membrane foulants in various feed waters. Autopsy studies have been mainly in drinking water production especially in desalination.

The analysis of a first stage of RO membrane in a seawater desalination plant after two years operation presented biofilm of manganese and iron-oxidizing bacteria with their metabolites, where chemical cleaning was not successful (Schaule et al., 2009). Foulants on RO membrane after two years operation in brackish water treatment showed besides particles mainly Si-Al-Fe colloids, hydrophobic organics (phthalic acid esters) and microorganisms (Luo and Wang, 2001). Another autopsy study of brackish water treatment after one year experienced initial thin amorphous fouling layer which comprised organic-Al-P complexes with embedded aluminium silicates and further accumulation of EPS (Tran et al., 2007).

NF has been applied in surface water treatment, where NOM was considered as major foulants. Earlier Cho et al. already reported that non-charged NOM fractions such as polysaccharides-like substances were important foulants in both types of source waters containing relatively hydrophilic and hydrophobic NOM (Cho et al., 1998). Polysaccharides and proteins were found as major foulants on NF membranes in natural surface water treatment for drinking water production (Her et al., 2007, Saravia et al., 2013, Sari and Chellam, 2013).

As NF and RO has been increasing applied in wastewater reclamation, recently there have been more autopsy studies in this field with the secondary effluent as feed water. In a UF-RO system after 2 months operation, organic fouling was found as the major problem of the RO membrane, which largely composed microbial-derived and humic-like organic matters, with hydrophobic acids and hydrophilic neutrals as the two largest fractions after resin fractionation of dissolved organic matter (Tang et al., 2014). In another study hydrophilic fractions were found as major constituents of the

desorbed NF membrane foulants (Chon et al., 2013). Dominant biofouling in combination with organic, colloidal fouling and scaling was found in NF and RO modules fouled by MF pretreated secondary effluent after 54 d operation. Polysaccharides-like substances were revealed by ATR-FTIR measurement and 1−10 μm precipitates were identified as calcium phosphate (Xu et al., 2010).

The greatest scaling potential species in NF membrane are $CaCO_3$, $CaSO_4$ and silica, while the other potential scaling species are $BaSO_4$, $SrSO_4$, $Ca_3(PO_4)_2$, ferric and aluminium hydroxides (Schäfer et al., 2004). An autopsy study of a pilot plant for anoxic groundwater treatment found inorganically bound Ca and organically bound Si as the major foulants, with Fe as main contributor to irreversible fouling (Gwon et al., 2003).

Fundamental understanding of dominant fouling type and involved fouling mechanisms in the practical applications remains incomplete. Membrane fouling in pool water treatment was little investigated. Swimming pool water has a different water quality in comparison with the typical feed water in desalination or surface water treatment. The concentration of bicarbonate is low due to the addition of acid and the water recirculation for long time periods. Depending on the local filling water and the pool water treatment, generally in pool water the organic matters are higher than in the filling water. Filling water is normally tap water, which contains mainly humic substances as potential organic foulants. Additionally, swimmers can bring solid contaminants such as hairs, skin debris/dead skin or fiber pieces into the pool water and also dissolved organic matter such as sweat, saliva, urine or personal care products. So the basic matrix of DOC in pool water includes mainly low to moderate molecular weight organic compounds. Furthermore, although most NOM are refractory to rapid biodegradation, chlorine may break organic substances down to be more biodegradable compounds and select the more persistent bacteria, which might facilitate the biofouling (Baker and Dudley, 1998). (Hambsch et al., 1993) reported higher biodegradability of humic substances after chlorination. Most commercial NF membranes are not chlorine resistant so the chlorine will be quenched in the feed before entering membrane modules. In drinking water treatment biofouling problems with dechlorination of feed water are quite common, not to mention the high temperature at approximately 30°C and an enhanced nutrient offering all benefit biofouling. It can be conclude that with suitable pretreatment scaling should be minimized in swimming pool water treatment but organic and biological fouling can be a concerns. Moreover, the contribution of anthropogenic input by visitors is unclear. The effects of continuous water disinfection in swimming pool water on organic input with specific regard to biofouling have not been discussed in the literature. Furthermore, swimming pool water is almost entirely recirculated. Therefore the problem of comparability is particularly acute, because different filling water and treatment processes can lead to significantly diverse water properties.

In summary:

- Fouling can be mainly classified to colloidal/particle fouling, scaling, organic fouling and biofouling, while in most real cases different types occur together.
- Organic fouling is not well understood, which is largely due to macromolecules such as humic substances and their derivatives, protein and polysaccharides.
- The properties of feed water, membrane and operation have influences on fouling formation.
- Autopsy study of membrane modules after operation provides comprehensive information of fouling, which has increased in recent years.
- Dominant fouling type and involved mechanism in different practical applications remain incomplete.
- Little information is known about membrane fouling in swimming pool water treatment or similar conditions.

3 Materials and methods

Experiments at different locations and with different set-ups were carried out. To investigate the occurrence of THM and its possible correlation with visitor numbers and other parameters, water samples, operational data such as visitor numbers and fresh water consumption were collected at the public indoor swimming pool A. To determine the rejection of THM by NF membranes, dead-end filtration experiments were conducted in the laboratory at the Engler-Bunte-Institut (EBI). To study the NF membrane performance in two different pool water matrices, bench-scale cross-flow filtration experiments were carried out onsite at two swimming pools A and B. Finally, upscale NF experiments using a pilot plant and a full-scale plant were operated again at the swimming pool A. An overview of the main parameters of the two pools, related chapters, set-ups and membranes can be found in Table 3.1.

Table 3.1: Overview of the main parameters of the swimming pool A and B, related chapters, set-ups and membranes used.

	Pool A	**Pool B**	**Lab (EBI)**
Volume	817 m^3	1100 m^3	–
Recirculation flow	135 m^3/h	120 m^3/h	–
Turnover rate	6 h	9 h	–
Occurrence and simulation of trihalomethanes in swimming pool water	Chapter 4	–	–
THM rejection by nanofiltration membranes and the effects of adsorption and NOM fouling	–	–	Chapter 5 Stirred cell (SB90, NTR-7470pHT, NF90)
Minimization of DBP in swimming pool water by NF	Chapter 6.1 Pilot plant (SB90)	–	–
	Chapter 6.2 Full-scale plant (NF90)	–	–
Fouling of NF membrane in swimming pool water treatment	Chapter 7.1 Bench-scale cross-flow set-up (NTR-7470pHT, SB90)		–
	Chapter 7.2 Pilot plant (SB90)	–	–
	Chapter 7.3 Full-scale plant (NF90)	–	–

DOC was taken as indicator of organic load from filling tap water and visitors in swimming pool water. THM and AOX were taken as indicator parameters of DBP and precursors, representing the load of DBP in pool water. As the regulated parameter and most typical DBP, THM was extensively investigated. The sum parameter AOX was measured in addition to THM to capture most of the other DBP.

3.1 Description of swimming pool A and sampling strategy

Public indoor swimming pool A consists of a standard-sized multipurpose pool (volume 741 m^3, surface area 312 m^2, recirculation flow 95 m^3/h) and a smaller wading pool (volume 76 m^3, surface area 100 m^2, recirculation flow 40 m^3/h). Both pools are continuously recirculated and treated in parallel by the same water treatment facility with a volumetric flow of 135 m^3/h (turnover rate approx. 6 h). The treated water returns to the pool through 4 horizontal line-shape supply devices evenly distributed on the pool bottom (25 m along the length of the pool, distance between each 2.34 m).

During the study in Chapter 4 the original treatment process at the swimming pool was in operation. It consisted of an inline flocculation using aluminium hydroxide based flocculant, powdered activated carbon (PAC) dosage and ultrafiltration (UF), which corresponds to the German Pool Water Treatment Standard DIN 19643-4 (DIN, 2012b) describing combination of treatment processes with UF. The UF is supposed to remove any particulate substances between 0.02–200 µm in water. Dosage of PAC was approx. 1 g/m^3, which was 0.135 kg for one treatment passage. A simplified schematic of the pool water system and treatment is shown in Figure 4.2. Disinfection is performed using chlorine gas after UF before water is returned into the pool. The pH-value is controlled by addition of sulfuric acid. The UF modules are shortly backwashed a few times a day. During the backwash the mainstream treatment is stopped. The backwash wastewater is treated by a combination of UF-NF and recirculated to the main stream, contributing approx. to 1% of total treatment flow.

The study site is a typical public swimming pool subjected to a moderate usage mainly by the local residents, averaging around 200 visitors per day including school pupils' classes in the morning on weekdays for approximately 1.5–3 h. Intensive visits from a swimming club of around 100 people came every Friday night.

Swimming pool water samples were collected regularly in short time intervals. Most samples for month-profile were sampled between 17 and 18 o'clock in the afternoon. Sampling consists of collecting water in the same place in both pools approximately 50 cm from the pool edge and 20 cm under the water surface. Water quality was almost the same at different sampling places. This has been proved by sampling at the four corners, middle and two edges of the pool. Free chlorine, total chlorine, pH-value and temperature were measured daily onsite. Additionally samples were taken in different corresponding glass bottles and transported to the laboratory for the following physical-chemical

analysis: DOC, THM, electrical conductivity and ions such as chloride and bromide. Samples were stored at T = 4 °C before measurement and were measured latest within a week.

3.2 Swimming pool B

University swimming pool B has only one pool (water volume 875 m^3). In the whole recirculation system including treatment is about 1100 m^3 of water. The continuous recirculation flow of 120 m^3/h (turnover rate approx. 9 h). The treatment facility includes flocculation using aluminium chlorohydrate, multi-layer filtration and chlorination using sodium hypochlorite solution (NaClO, 15–16%). The two multi-layer filters running parallel (each 60 m^3/h) consist of activated carbon, sand and gravel, which are backwashed for about 7 min once a week. Backwash wastewater is discharged to the sewer.

The pool opens only on working days. Visitors are primarily adult swimmers which consist of students, employees or a swimming club. The local filling tap water contains a markedly lower DOC than the filling water at swimming pool A.

3.3 Nanofiltration experiments

In total, three commercial NF membranes (described in Chapter 3.3.1) were used in different parts of the studies, as indicated in the next chapters for procedure description of each experiment (Chapter 3.3.2–3.3.5).

3.3.1 NF membranes

Table 3.2: Properties of used nanofiltration membranes.

	Manufacturer	Membrane type	NaCl rejection[1]	MWCO[2] (Da)	Chlorine-resistance (ppm)	Zeta potential[3] (mV)
NF90	DOW/Filmtec	Polyamide thin film composite	90%	100	< 0.1	-47.5
NTR-7470pHT	Hydranautics/Nitto-Denko	Sulfonated polyethersulfone	50%	500	10	-36.8
SB90	TriSep	Cellulose acetate blend	80%	200	1	-10.7

Test conditions: [1]2000 mg/L NaCl in demineralized water, ambient temperature, dead-end filtration at 6 bar. [2]25°C, cross-flow filtration at 8 bar, $V_{crossflow}$ = 0.22 m/s, neutral organic compounds such as sugars and polyethylene glycols in demineralized water. [3]10 mM KCl, pH = 7.

Table 3.2 summarizes the most relevant characteristics provided by the manufacturers or measured in the laboratory. NF90 is a high-flux thin-film composite (TFC) membrane with an aromatic polyamide separating layer and a supporting layer made of polysulfone on polyester. NTR-7470pHT and SB90 are made of sulfonated polyethersulfone (PES) and cellulose acetated blend respectively. MWCO of the membranes was determined using 9 neutral organic compounds (ethanol, ethylene glycol, glycerin,

glucose, maltose, raffinose and polyethylene glycols in different molecular weight). Rejection curves for MWCO determination can be found in Appendix A1. Zeta potential measurement at different pH values can be found in Appendix A2.

3.3.2 THM rejection by nanofiltration and the effects of adsorption and NOM fouling (Chapter 5)

Laboratory-scale filtration experiments were carried out by dead-end filtration (Figure 3.1) using two stirred cells Amicon M2000 (Millipore), with an effective membrane area of 0.017 m^2 and a volume of approx. 2.5 L. Nitrogen gas and stainless steel pressure vessels (Amicon) were used to provide the feed pressure. Permeate flow was calculated by measuring the mass of liquid permeating each membrane in 1 min by a balance (Sartorius). Three commercial NF membranes made of different materials were used (Table 3.2).

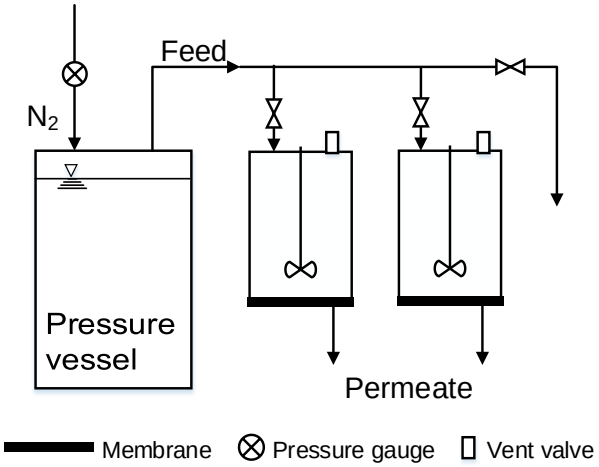

Figure 3.1: Schematic diagram of the experimental set-up for dead-end filtration: pressure vessel and two stirred cells.

Table 3.3: Properties of used trihalomethanes.

	M (g/mol)	Molecular width[1] (nm)	Molecular length[1] (nm)	Dipole moment[2] (D)	log K_{ow}[3]
$CHCl_3$	119.38	0.176	0.450	1.16	1.97
$CHCl_2Br$	163.83	0.180	0.473	1.07	2.10
$CHClBr_2$	208.28	0.185	0.495	0.99	2.24
$CHBr_3$	252.73	0.191	0.495	0.91	2.38

[1](Agenson et al., 2003); [2](de Ridder, 2012); [3](Mackay et al., 2006).

Feed solutions were made with demineralized water (electrical conductivity = 8.9 µS/cm). Chloroform and bromoform (Merck, Ph. Eur.), bromodichloromethane (≥ 97%) and dibromochloromethane (≥ 98%) (Sigma-Aldrich) were used as target compounds. The relevant properties of the four used THM for filtration experiments are summarized in Table 3.3 (Agenson et al., 2003, de Ridder, 2012, Mackay et al., 2006). To investigate the THM rejection and the potential effect of adsorption on rejection,

separate filtration experiments either with 100 µg/L chloroform or with four THM mix ($CHCl_3$, $CHCl_2Br$, $CHClBr_2$ and $CHBr_3$, each 100 µg/L) in the feed solution were carried out for each membrane. Filtration experiments were carried out at approx. 6 bar and over 6 days.

Additionally, NOM fouling experiments were performed to study the fouling effect on THM rejection and adsorption. The feed solution was prepared using the NOM rich water (brown water lake Hohloh, Germany, 0.45 µm filtrated using PES membrane, β(DOC) = 22 mg/L) as solvent which has low ion content (electrical conductivity = 33 µS/cm) instead of demineralized water. All the other parameters remained the same. The effect of NOM fouling on THM rejection was investigated during the fouling layer formation and compared to the results in demineralized water tests.

For all the experiments, 3 mM sodium chloride (NaCl) was dosed for an electrical conductivity of around 360–400 µS/cm as background electrolyte. Hydrochloric acid (HCl) and sodium hydroxide (NaOH) from company VWR, both of p.a. quality, were used to adjust the pH-value to 7.

Samples of feed and permeate were taken intermittently. Feed samples were taken directly out of stirred cells through the valve to measure the actual feed THM concentration. To reduce volatilization of THM a closed set-up was essential in these experiments: (1) closed pressure vessels for feed solution was filled full to the brim; (2) by means of the air valve the stirred cells were always filled to the top without air bubbles; (3) feed solution in the pressure vessel was replaced every day.

Rejection of solutes was determined as

$$Rejection = 1 - \frac{c_p}{c_f} \tag{3.1}$$

where c_f and c_p are the solute concentration in the feed and the permeate samples. THM samples were taken in duplicates in 40-mL glass vials which were capped with polytetrafluoroethylene (PTFE)-faced silica septum. Besides THM rejection, permeability decline, salt and organic matter rejection and membrane hydrophobicity (contact angle measurement) were used to analyze the membrane performance.

The amount of adsorbed THM to membranes was determined by mass balance.

$$m_{adsorbed} = m_{feed} - m_{rejected} - m_{permeate} \tag{3.2}$$

The mass of feed and permeate was calculated through integration from the filtrated volume and concentration measured intermittently. The rejected mass was calculated from the volume and concentration measured in the remaining retentate in the stirred cells when the experiments finished.

Furthermore, static adsorption experiments were carried out parallel to the filtration experiments to confirm the adsorption of THM to the membrane. A membrane with the same active area as in the filtration experiments was submerged in the same feed solution with four THM mix in demineralized

water as in the filtration experiments in 1-L brown glass bottles. The adsorbed amount was determined by the difference between the concentration of THM in the solution before and after 6 days contact time.

Table 3.4: Overview of experiments for each membrane

Number	THM in feed	THM concentration (µg/L)	Solvent	Experiment
1	$CHCl_3$	100	demineralized water	filtration
2	4 THM mix	100 each	demineralized water	filtration
3	$CHCl_3$	100	Hohloh lake water	filtration
4	4 THM mix	100 each	Hohloh lake water	filtration
5	$CHCl_3$	100	demineralized water	static adsorption
6	4 THM mix	100 each	demineralized water	static adsorption

Table 3.4 shows an overview of the experiments for each membrane. Each test was carried out with new membrane samples in duplicates, parallel. Prior to the tests all membranes were cleaned with demineralized water for 24 h, under operating conditions at 6 bar. All the experiments were performed at T = 22 ± 1 °C.

3.3.3 NF membrane fouling in two different pool water matrices (Chapter 7.1)

To investigate the performance of chlorine-resistant NF membranes in two different pool water matrices, bench-scale cross-flow filtration experiments were carried out onsite at two swimming pools A and B. Only the two chlorine-resistant NF membranes (NTR-7470pHT and SB90) were used due to the present free chlorine in swimming pool water. The set-up completely made of stainless-steel has six flat-sheet modules parallel which allow experiments with different membranes under the same condition. Each module enables an active membrane area of 0.008 m^2 (4 cm × 20 cm). The feed tank permits a maximum volume of 200 L. During the experiments the pretreated swimming pool water was continuously supplied into the feed tank through a magnetic valve controlled by a float switch, which maintained the water volume at about 150 L in the tank. A high pressure pump (Grundfos) supplied the operating pressure. The pressure on the permeate side was at atmospheric pressure. Feed flow was maintained at 25 L/h for each module. The mass of liquid permeating each module in 1 min was measured by a balance (Kern) during the experiments, which was recorded every minute together with pressure, temperature and flow using LabVIEW-based software. Permeate flow was thus calculated. All filtration experiments were conducted with a cross-flow velocity (V_{CF}) of 0.22 m/s and the applied feed pressure was 8 bar. Permeate samples were taken directly from each module through hand valves and feed samples were taken directly from the feed tank.

At swimming pool A the feed was pool water treated through the combination of flocculation, adsorption on PAC and UF (Chapter 3.1). The two membranes were tested in triplicates parallel for 640 h. At the end all membrane samples were taken out for fouling layer characterization. At

swimming pool B the feed was pool water treated through flocculation and multi-layer filtration (Chapter 3.2). The two membranes were tested separately in two experiments with the same membrane in six modules parallel. In order to follow the fouling layer development, membrane samples were taken out for characterization after about 70 h, 230 h, and 405 h (duplicates).

Table 3.5: Feed water properties in two experiments with NF treating swimming pool water

Parameter	Unit	Swimming pool A[1] (*n* = 13)	Swimming pool B[2] (*n* = 12)
		Mean ± SD	Mean ± SD
Temperature	°C	28.9 ± 0.4	29.4 ± 0.9
pH		7.3 ± 0.1	7.3 ± 0.2
el. Conductivity	µS/cm	700 ± 13	3387 ± 57
Free chlorine	mg/L	0.25 ± 0.06	0.06 ± 0.03
DOC	mg/L	3.3 ± 0.2	1.4 ± 0.2
Al^{3+}	mg/L	0.034 ± 0.002	0.008 ± 0.003
Ba^{2+}	mg/L	0.101 ± 0.004	0.059 ± 0.001
Ca^{2+}	mg/L	112 ± 3	206 ± 53
Fe^{n+}	mg/L	< 0.01	< 0.01
K^{+}	mg/L	3.8 ± 0.4	8.3 ± 1.0
Mg^{2+}	mg/L	12.0 ± 0.4	26.2 ± 4.7
Na^{+}	mg/L	21 ± 1	546 ± 73
Si	mg/L	5.9 ± 0.3	8.1 ± 0.3
Cl^{-}	mg/L	114 ± 13	613 ± 161
ClO_3^{-}	mg/L	< 0.1	49 ± 13
NO_3^{-}	mg/L	3.8 ± 0.8	9.3 ± 2.7
PO_4^{3-}	mg/L	< 0.1	< 0.1
SO_4^{2-}	mg/L	190 ± 21	649 ± 161
HCO_3^{2-}	mg/L	43.0 ± 11.9	42.9 ± 4.2

[1] pool water treated through the combination of flocculation, adsorption on PAC and UF. [2] pool water treated through flocculation and multi-layer filtration.

The different filling water matrices and treatment process between pool A and B offered two types of water for fouling research. The treated swimming pool waters were used for feed as they were and no further chemicals were added. Water properties are listed in Table 3.5. Pool A offered a high organic content while pool B had only half of its DOC but much higher ionic strength. There was no quenching of chlorine in the feed. Free chlorine in feed was on average 0.25 mg/L and 0.06 mg/L respectively during the experiments. They were lower than in the swimming pool (0.3–0.6 mg/L) water due to the treatment process and retention in the feed tank. No antiscalant was used.

3.3.4 Pilot plant at swimming pool A

UF in swimming pool A is backwashed using the permeate from UF. The backwash wastewater of UF is treated by a combination of UF-NF. The NF treatment was used as a pilot plant set-up for experiments in Chapter 6.1 and 7.2. Three 4-inch spiral wound modules of membrane SB90 (Trisep) were serially connected. Diamond shaped feed spacer 0.787 mm (31 mil) was used. Feed pressure was at 11 bar with a permeate flow of 450 L/h, a recirculation flow of 350 L/h and a concentrate flow of 150 L/h, which gave a total recovery at 75% and the average permeability at 1.9 L/(h·m^2·bar) at the beginning phase. The plant ran intermittently depending on the backwash frequency and the amount of backwash wastewater. Permeate was transported back to the mainstream and to the swimming pool. Water quality in feed and permeate was measured weekly during the experiment.

To avoid scaling formation the antiscalant Genesys RC was used during the pilot-plant experiments. According to manufacturer's information it's a synergistic blend of neutralized carboxylic and phosphonic acids which is effective at preventing inorganic scale formation such as common scales calcium carbonate/sulfate, barium/strontium sulfate, calcium phosphate and metal hydroxides. The operation time of these membrane modules was in total 17 months (approx. 2 years with two 4-month summer pauses). During summer pauses the modules were conserved with sodium bisulfite. The modules were only once cleaned with sulfuric acid at pH 2 for 1.5 h. After the experiment the front module of the three was dissembled for autopsy study.

3.3.5 Full-scale plant at swimming pool A

Finally, for upgrade experiments in the realistic full-scale situation (Chapter 6.2–6.3 and 7.3), a full-scale NF plant was built by the company W.E.T and integrated in the original treatment process at the swimming pool A (Chapter 3.1). A branch current of the mainstream out of UF was treated by NF while the PAC dosage was turned off (Figure 1.1). The permeate returns to the mainstream going to the pool. The plant has two stages, which consist of six modules in three pressure vessels in the first stage and four modules in two pressure vessels in the second stage (Figure 3.2).

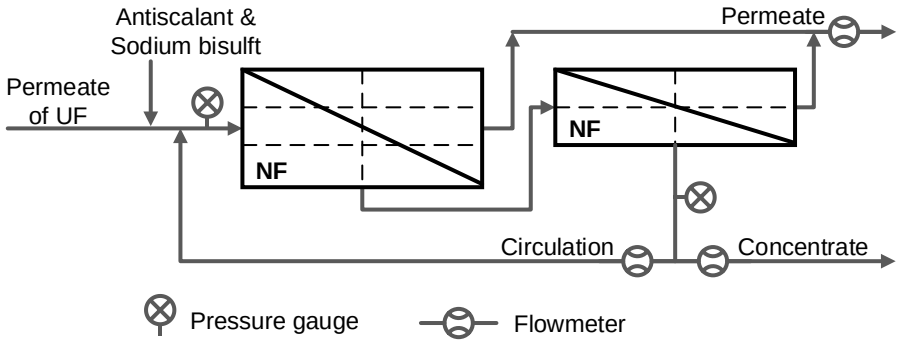

Figure 3.2: Schematic of the full-scale nanofiltration plant at the public swimming pool A. It has two stages, which consist of six modules in three pressure vessels in the first stage and four modules in two pressure vessels in the second stage.

Membrane modules NF90-4040 (DOW) were mounted in the full-scale plant based on its high permeability. Feed spacer 0.8636 mm (34 mil) was used. The plant was configured with the permeate flow of 2.5 m^3/h, the recirculation flow of 2.5 m^3/h and the concentrate flow of 0.625 m^3/h, which corresponded to a recovery at 80%. A continuous operation of the plant covers 1.85% of the mainstream. At the beginning the feed pressure started at 5 bar which gave the average permeability of 6.6 L/(h·m^2·bar). An intermittent operation with different time intervals was applied aiming at the intensive load brought by the swimmers in rush hours.

Free chlorine was quenched in feed using sodium bisulfite. Antiscalant ROPUR RPI 3000A was dosed, which is a stabilized solution of organic phosphonates and polyacrylates. According to the manufacture's information it's specially designed to inhibit the scaling in RO with polyamide, CA and polyether membranes with anionically charged surface, which can inhibit calcium sulfate/carbonate and stabilize barium/strontium sulfate as well as iron. Sodium bicarbonate was added in the permeate flow before entering the mainstream. Operating parameters such as pressure, flow and temperature were read manually once a day. Feed and permeate were sampled at least once a week. Not only the performance of the NF plant but also correlation between the NF treatment and water quality in swimming pool was also monitored. Water samples from the swimming pool were taken every day during operation time. Different parameters such as DOC, THM, AOX, free and bound chlorine, pH-value, electrical conductivity, UV and ions were measured in different intervals.

During the operation time for 8 months (236 d) chemical cleaning using alkaline surfactants was carried out once after 6 months. After 8 months operation a front membrane module from the first stage and a second one from a rear position were dissembled for autopsy study.

3.4 Characterization of fouling layer

3.4.1 Fouling layer analysis of bench-scale flat-sheet membranes

After experiments at swimming pool, membrane samples from the bench-scale flat-sheet set-up were taken out and brought back to the laboratory immediately. The 4 cm × 20 cm active area of membrane sample was cut into four times of 4 cm × 5 cm parts, from which two were dissolved in 0.01 M sodium hydroxide (NaOH) for organic carbon analysis and the other two were dissolved in 0.01 M nitric acid (HNO_3) for analysis of ions (Saravia et al., 2013). The remaining fouled membrane samples of duplicates or triplicates were room temperature dried and analyzed with contact angle, scanning electron microscopy (SEM) and energy dispersive X-ray spectroscopy (EDX).

3.4.2 Autopsy procedure of fouled membrane modules

After long time operation in swimming pool A, membrane modules were taken out, carefully packed to avoid the dry out and brought back for destructive analysis (autopsy study) in the laboratory. Before the autopsy study the membrane modules were and stored at 4 °C.

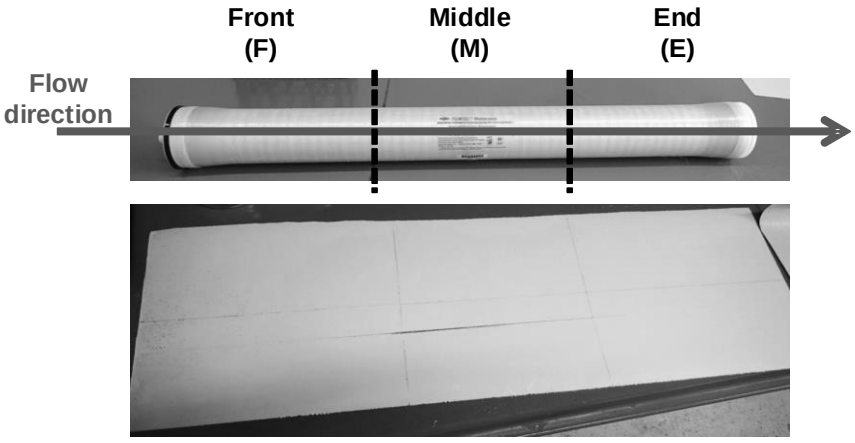

Figure 3.3: Three zones of the membrane modules separated along the flow direction

The two tight bound ends of spiral membrane modules were cut off and the hard crust was cut lengthwise using a circular saw in order to open the module without damaging the membrane and fouling layer inside. The carefully unrolled membrane and feed spacer was cut into three parts to separate different zones along the flow direction as "front", "middle" and "end" (Figure 3.3). Samples were taken where the fouling deposited was well preserved.

To characterize the surface properties, samples of fouled membrane were characterized using scanning microscopy coupled with energy dispersive spectroscopy, Fourier transform infrared spectroscopy with attenuated total reflection, confocal laser scanning microscopy, zeta potential measurement and contact angle measurement. Fouling deposits on the membrane surface were carefully scraped off using a Teflon rod scraper. With the help of clean membrane pieces of the same type, which were fixed on the sides as support, fouling layer on the membrane surface is supposed to be scrapped off without damaging the membrane and scrapping trace pieces of membrane material off (Gorenflo et al., 2001). The scrapped fouling deposit was weighed immediately and then weighed again after being heated at 110 °C overnight and at 550 °C for 4 h. Dry and organic mass of fouling deposits were thereby calculated. The fouled membrane "as it is", the scraped fouling deposit and the membrane after being scrapped were all inserted in 0.01 M HNO_3 or 0.01 M NaOH solution for further analysis of organic carbon and ions respectively, after the fouling deposit was dissolved. Solutions were prepared with ultrapure water (referred as Milli-Q water), which was produced at resistivity 18.2 MΩ/cm (Veolia Water/Purelab Flex, Ireland). Extracted deposit was calculated back based on mass balance and normalized to the membrane area. All the analysis was carried out in triplicates. Furthermore, large amount of fouling deposit were scrapped off and measured by elemental analysis to determine the proportion of C, H, N, O, and S in the fouling deposit.

3.5 Analytical methods

All the measurements were carried out in the Engler-Bunte-Institut (EBI), if not indicated specifically.

3.5.1 pH-value, electrical conductivity

Electrical conductivity and pH-value were measured using a WTW multi set 350i or a WTW multiparameter instrument MultiLab P4 with the electrodes TetraCon®325 and SenTix 41 respectively. The calibration was carried out once a week during experiments.

3.5.2 Dissolved organic carbon (DOC)

DOC was measured either using a Shimadzu Total Carbon Analyzer TOC V_{CSN} with combustion catalytic oxidation method or a Sievers TOC 820 with wet chemical oxidation method depending on the concentration of samples. The concentration range according to the available calibrations is 0.2–50 mg/L and 0.05–5 mg/L respectively.

DOC was also characterized using size exclusion chromatography with organic carbon detection (SEC-OCD). The gel-chromatographic separation of the organic substances was done through a Fractogel® TSK HW-50 S-column (Grom). The separation was primarily according to the molecular size of the molecules: the bigger the molecules, the sooner the elution through the column. Smaller molecules penetrate deep into the pores so they elute later. This separation principle will be influenced by secondary effects such as hydrophobic and electrostatic interaction (Huber and Frimmel, 1994). Phosphate eluent solution (1.5 g/L $Na_2HPO_4 \cdot 2H_2O$ and 2.5 g/L KH_2PO_4) was used as the mobile phase with a flow rate of 1 mL/min. Online detectors for organic carbon, UV absorbance at λ = 254 nm and variable fluorescence could provide the comprehensive information such as the size distribution of organic substances in the sample. The main components of organic carbon detection are the Graentzel Thin-Film Reactor where the organic carbon was exposed to UV radiation and oxidized to carbon dioxide and non-dispersive IR-Detector (NDIR).

3.5.3 Anions, cations and other elements

Anions were measured by ion chromatography (IC) using Metrohm 790 Personal IC with the analytical column Metrosep Anion Dual 3 - 100/4.0. The concentration range in calibration is 0.1–100 mg/L. Metal cations; silica, phosphor and sulfur were measured using inductively coupled plasma optical emission spectroscopy (ICP-OES) with a Vista-Pro CCD simultaneous ICP-OES spectrometer (Varian). The limit of detection is 10 µg/L for metal ions and 40 µg/L for phosphorus.

3.5.4 Chlorine

Free and total chlorine were determined using a photometric-test (Spectroquant® cell test Nr. 100597) with a photometer photoLab S12 (WTW). The method is based on a colorimetric analysis (Dipropyl-p-phenylendiamine, DPD method). A small spatula of DPD was added into 5 mL water sample in a round cuvette, which creates a pink color to be then measured by the photometer. Total chlorine can be measured afterwards by adding 2 drops of potassium chloride for a redox reaction of the bound chlorine. Applicable range was 0.03–6.00 mg/L free chlorine. Bound chlorine was determined from the difference between total chlorine and free chlorine.

3.5.5 Trihalomethane (THM)

THM samples were collected in duplicates in 40-mL glass vials and were capped with polytetrafluoroethylene (PTFE)-faced silica septum. Sodium thiosulfate was added to quench the residual free chlorine according to the German DIN-Norm 38407-30 (DIN, 2007). Sampling vials were carefully filled and sealed without air bubbles (headspace free). The determination of THM was carried out using a headspace sampling capillary gas chromatograph (Agilent HP 6890, column DB-5MS) with electron capture detection. The limit of detection were set to 0.4 µg/L for chloroform, 0.2 µg/L for bromodichloromethane, 0.5 µg/L for dibromochloromethane and 0.7 µg/L for bromoform. Each sample was measured at least twice.

3.5.6 Absorbable organically bound halogens adsorbable on activated carbon (AOX)

The concentration of AOX was determined with the TOX analyzer Euroglas ECS 1200 (Thermo Electron GmbH) according to the DIN EN ISO 9562 (DIN, 2005). Sodium thiosulfate was added to the water samples directly during sampling to quench the rest free chlorine. 100 mL water sample was mixed with 5 mL sodium nitrate solution (0.2 mol/L $NaNO_3$ and 0.02 mol/L HNO_3) in a 250 mL Erlenmeyer flask. 50 mg powdered activated carbon (PAC) was added and the closed flask was shaken horizontally for at least 3 h. The loaded PAC was filtrated out by a glass frit, washed with nitrate wash solution (0.01 mol/L) and burned at 1000 °C in the TOX analyzer. The produced hydrogen halides from organic bound halogens were detected with the micro coulometric titration method. 4-chlorphenol was used as standard. The detection range was 50–200 µg/L with a deviation of ± 10%.

3.5.7 Formation potential of THM and AOX

The rest maximum formation potential of THM (THMFP) and of AOX (AOXFP) was measured to analyze to what extent new THM and AOX can be formed from the investigated pool water. The method used in this study is according to DVGW-Worksheet standard W 295 (DVGW, 1997). Samples of swimming pool water were taken freshly in 1-liter brown reagent bottles full to the brim, which were made free of chlorine consumption before sampling. In each bottle 20 ± 0.3 mg/L free chlorine was dosed using sodium hypochlorite (12%, Roth, Germany). The same volume of water as the dosage of sodium hypochlorite was taken out before dosing to make the bottle headspace free. Each test was carried out at least in duplicates. For tap water sample the test was in triplicates. After 46 ± 2 hours at ambient temperature (21 ± 1 °C) a minimum chlorine residual of 1 mg/L was confirmed and the reaction was stopped by adding an over-stoichiometric amount (one spatula, approx. 0.3 g) of sodium thiosulfate (Merck, Germany). The THM and AOX concentrations determined in the solutions corresponded to the maximum THMFP and AOXFP. The rest maximum THMFP and AOXFP corresponds to the difference of concentration bevor and after the chlorination test.

3.5.8 Contact angle

Static contact angle between dried membranes and Milli-Q water was measured using the sessile drop method at room temperature. An optical contact angle measurement system OCA 20 (Dataphysics,

Germany) with integrated video and analysis function was used. At least 15 spots of each membrane sample were measured and averaged. The larger the contact angle is, means the more hydrophobic the membrane surface is.

3.5.9 Zeta potential

Zeta potential was measured with a SurPASS electrokinetic analyzer (Anton Paar). For the measurement an electrolyte solution out of 10 mM KCl was used. Membrane samples were cut to the dimensions of the sample holders and fixed using double-sided tape. During measurement the solution flows through an adjustable gap cell with the channel of 20 mm * 0.1 mm * 10 mm L/W/H. Tangential mode of analysis was used. The streaming potential was measured for increasing pressure from 0 to 300 mbar in both flow directions. Zeta potential was calculated from the measured streaming current using the Helmholtz-Smoluchowski equation. The pH value was adjusted using HCl and KOH solutions. The measurements were carried out at the Institute for Nuclear Waste Disposal (INE, KIT).

3.5.10 Scanning electron microscopy and energy dispersive X-ray spectroscopy

Morphology of membrane surface or membrane cross-section (breaking edge) before and after fouling was analyzed using a scanning electron microscope (SEM) (Leo Gemini 1530, Zeiss) with the software SmartSEM V05.03.01. For the cross-section view, membrane samples were submerged shortly in isopropanol, then frozen in liquid nitrogen, broken and peeled from the supporting layer with two tweezers. Before the measurement air-dried or freeze-dried membrane samples were coated with platinum in high vacuum circumstance and fixed on a metal plate with silver drops for better electron conductivity. Composition of chemical elements contained in the membrane or the fouling layer was semi-quantitatively analyzed through energy dispersive X-ray spectroscopy (EDX). The measurement was carried out at the Laboratory for Electron Microscopy (LEM, KIT).

3.5.11 Confocal laser scanning microscopy (CLSM)

Microscopic observation and imaging acquisition of the fouled membrane samples were carried out using the confocal laser scanning microscopy (CLSM) to reveal the presence of biofouling. Microorganisms and extracellular polymeric substances (EPS) of the biofilm can be visualized. A confocal microscope LSM700 (Zeiss) was used. Bacteria were stained with the SYTO60 (ThermoFisher), which is a red fluorescent nucleic acids stain. EPS glycoconjugates were marked with the Aleuria aurantia lectin (AAL) Fluorescein isothiocyanate (FITC) (LINARIS Biologische Produkte GmbH). The stock solution of SYTO60 and AAL-FITC as supplied were used at a dilution of 1:1000 and 1:10 in Milli-Q water respectively. Fresh membrane samples were cut into approximately 1 × 1 cm^2 pieces and put in a Petri dish. First samples were stained with 100 µL AAL-FITC for 20 min and excessive stain was washed off using tap water afterwards. Then samples were counterstained with SYTO60 for 5 min and rinsed again. Original feed water from the membrane plant was added to submerge the membrane samples to avoid drying out.

AAL-FITC and SYTO60 were excited by laser at 488 nm and 639 nm respectively. At least five spots randomly chosen were measured for each membrane sample. Images were acquired using a water immersible objective lens (W Plan-Apochromat 40×/1.0 DIC M27) with the field of view at 266 × 266 μm^2. Image was obtained and analyzed using software ZEN (Zeiss). Image processing was carried out using software Fiji and ImageJ. Average coverage was calculated by counting the pixels and compared to the field dimension. Biofilm thickness was calculated from the wet biomass in the image stacks.

3.5.12 ATR-Infrared-Fourier-Spectroscopy (ATR-FTIR)

The functional group characteristics of membranes were measured using a Vertex 70 Fourier transform infrared (FTIR) spectrometer (Bruker) with an Attenuated Total Reflection (ATR) element of diamond crystal and a deuterated triglycine sulfate (DTGS) detector. The spectra were recorded by a single reflection method with 128 scans collected from 600 to 4000 cm^{-1} at a wave number resolution of 4 cm^{-1}. A blank measurement was taken to justify the differences in instrument response and the atmospheric environment and subtracted from the measurement. Membrane active layer was pressed firmly against the diamond crystal plate. Each sample was measured at least three times. No further baseline corrections were applied. The measurement was carried out at the Institute for Technical Chemistry and Polymer Chemistry (ITCP, KIT), Division Polymeric Materials.

4 Occurrence and simulation of trihalomethanes in swimming pool water*

*This chapter has been published in Water Research (2016), volume 88: 634–642 in collaboration with F. Saravia, G. Abbt-Braun and H. Horn.

4.1 Occurrence and correlation of DOC and THM in swimming pool water

To investigate the occurrence of THM and its possible correlation with visitor numbers and other parameters, water quality including DOC, THM and other physical-chemical parameters in an indoor swimming pool were investigated for 26 days. DOC was assumed as precursor to link organic matter and THM formation. The DOC concentration was linked to the number of visitors and THM (Figure 4.1). The profiles started on Friday, on which the numbers of daily visitors usually exceeded 330 due to the activity of a swimming club. The DOC concentration in swimming pool water was on average at 3.3 mg/L. On day 12 and day 19 the DOC concentration increased to 3.7 and 4.2 mg/L respectively. The THM concentration varied from 13–47 µg/L with an average value of 25 µg/L. Alike DOC, we observed two huge peaks of THM at nearly twice of the average concentration, but both came two days after the DOC peaks (day 14 and day 21). The subsequent increases of THM after DOC indicate a clear positive correlation between DOC and THM with a time delay about 2 days. Although this swimming pool has a typical turnover rate of 6 h, increase of DOC showed that the pool water treatment was limited in removing DOC from water. Similar result was reported by Glauner et al. (2004) in an outdoor swimming pool (turnover rate about 4 h). In a weekly profile the maximum concentration of THM followed the increase of DOC after 1–2 day. This kind of phenomenon is mainly due to the recirculation of pool water, which provides the long reaction time and is not observed in drinking water system. It's likely to conclude that the major THM formation from DOC occurred in the first 48 h during reaction with chlorine. In a chlorination experiment of outdoor swimming pool water Glauner (2007) also pointed out that after 48 h no further increase of THM was observed (chlorine concentration above 2.3 mg/L). Therefore we can speculate that in a conventional swimming pool water treatment the major part of DOC accumulated in pool water and cannot be eliminated by the treatment. Besides, the major part of THM formation in a swimming pool with conventional water treatment takes about 2 days. The time delay should depend on the properties of DOC in water and the treatment, which can be different in the swimming pools with advanced treatment process. Zwiener et al. (2007) also pointed out that this kind of time delay is linked with the treatment cycles needed for efficient chlorination.

We noticed that peaks of THM decreased quickly on the next day when the numbers of visitors were high. A reasonable explanation is the enhanced loss of THM into air due to vigorous activities of the swimmers. Kristensen et al. (2010) has also observed by online monitoring that THMs increased during the closing hours and decrease during opening hours. This implies that the elimination of THMs from pool water correlates strongly with activity in the water, which assists the transfer of THMs from the water into the air by splashing.

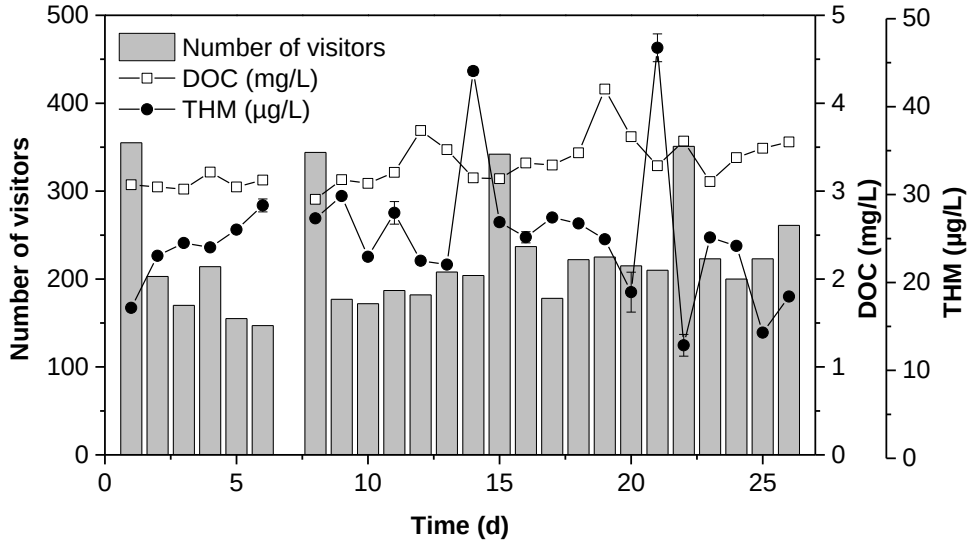

Figure 4.1: Profile of the number of visitors, DOC- and THM-concentration obtained from daily sampling for a period of 26 days in the indoor swimming pool water (total water volume 817 m3, water recirculation flow 135 m3/h). Treatment process consists of an inline flocculation, PAC dosage and UF; no PAC was dosed within the first sampling period 16 d.

Interestingly, the much more intensive visits on Friday didn't have significant effects on DOC value. No direct correlation was observed between DOC and the number of visitors, which is unlike some previous research (Chu and Nieuwenhuijsen, 2002, Glauner et al., 2004). A possible explanation is that the type and amount of input from visitors into swimming pool water depends significantly on their behavior, which might be characterized by different groups (e.g. children or adults, athletes or recreational swimmer, disciplined or incorrect hygienic behavior, etc.). An anonymous questionnaire in Italy showed different hygiene-related behaviors: Only 70.9% of visitors take a shower before entering the swimming pool and 13.5% of visitors have urinated at least once in a swimming pool (Pasquarella et al., 2014). Large variation of input from visitors into swimming pool water due to unhygienic behavior was also reported by Keuten et al. (2014). Compared to outdoor swimming pools this variation is greater in indoor swimming pools which receive more diverse visitor behaviors. We can conclude from our results that introduction of anthropogenic pollutants into swimming pool water and consequent DBP formation cannot be predicted simply from the number of visitors. To estimate the actual DBP formation the content of organic matter should be determined through analytic methods.

4.2 Development of THM simulation from DOC in indoor swimming pool water

A simple mathematical model for predicting the THM concentration in indoor swimming pool water was proposed based on mass balance. The whole recirculation system of swimming pool water and its treatment process were considered. Water in the swimming pool was assumed to be completely mixed so that THM should be evenly distributed in the pool. The parameters for the simulation are integrated in the schematic of the pool water system presented in Figure 4.2.

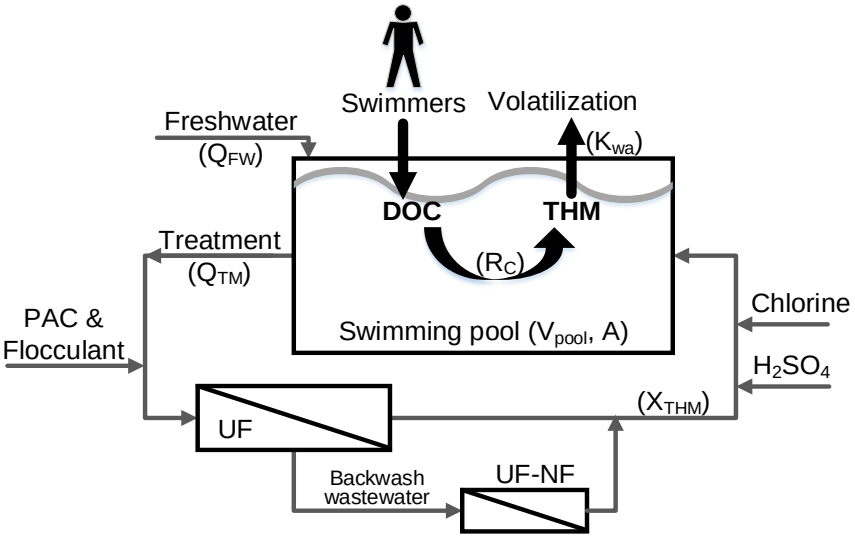

Figure 4.2: Simplified schematic of the swimming pool and the treatment process. Q_{FW} is the filling water inflow. Q_{TM} is the volumetric flow rate of pool water treatment (135 m^3/h). R_C is the specific ratio representing the production of THM from certain amount of DOC through chlorination. K_{wa} is the overall mass transfer coefficient of THM from water into air. V_{Pool} is the total water volume in the swimming pool (817 m^3). A is the water surface area of swimming pool (412 m^2). X_{THM} is the THM removal ratio in percentage during one passage of the pool water treatment process.

4.2.1 Formation and removal of THM

The change of THM concentration with time ($d\rho_{THM}/dt$) is driven by THM formation and removal. DOC was taken as a surrogate for precursors of DBP. THM formation was considered exclusively from the reaction of DOC with chlorine as a first order reaction and assumed to be stoichiometrically proportional to DOC reacted with chlorine. The specific ratio R_C (µg THM/mg C) was introduced, representing the specific production of THM from certain amount of DOC through chlorination:

$$m_{THM} = R_C \cdot m_{DOC} \tag{4.1}$$

whereas m_{THM} is the mass of THM in µg and m_{DOC} is the mass of DOC in mg. Removal of THM from swimming pool water can occur in various ways. For the THM simulation 3 different removal paths were considered: a) volatilization into air, b) exchange of fresh filling water, and c) removal by pool water treatment.

4.2.2 Volatilization

THM are volatile and have a relatively high Henry's law constant ($CHCl_3$: $3.67 \cdot 10^{-3}$ atm·m^3/mol; $CHBrCl_2$: $1.60 \cdot 10^{-3}$ atm·m^3/mol; $CHBr_2Cl$: $7.83 \cdot 10^{-4}$ atm·m^3/mol; $CHBr_3$: $5.35 \cdot 10^{-4}$ atm·m^3/mol). In swimming pools with traditional treatment process such as flocculation and sand filtration the removal of THM by treatment facility is rather little. The predominant THM removal is due to volatilization into air. Significant linear correlations of THM concentration in pool water and in indoor air were observed by Lourencetti et al. (2012), who indicated a continued transfer of waterborne THM into air. Hsu et al. (2009) observed a gradient of the THM concentration in the air along the height above water surface when there was no visitor in water, while there was no difference in the chloroform concentration in the air for 20–250 cm above water surface when there was any visitor in water. Ventilation is required for indoor swimming pools. Lourencetti et al. (2012) witnessed much lower concentration of THM than the value calculated through Henry's law based on equilibrium. This is probably due to ventilation system at the swimming pool. In this case mass transfer dominates the kinetic THM exchange between water and air in indoor swimming pools. The mass transfer coefficient is a diffusion rate constant to quantify the interphase mass transfer e.g. between water and air in this case. The basic mass transfer equation is:

Mass transfer rate (M/T) = K (L/T) · interfacial area (L^2) · driving force (M/L^3).

Mass transfer rate is commonly in g/s or mol/s. The driving force here is the concentration difference between two phases; units are g/L or mol/L. K is a proportionality factor called mass transfer coefficient usually in m/s or m/d. Based on two-film theory, the overall mass transfer coefficient considers phase boundary – air and water phase – and can be calculated from Henry's law constant (H_C) and mass transfer coefficient in single phases (Rousseau, 1987). The overall mass transfer coefficient in the liquid phase K_w (m/d) and air phase K_a (m/d) are expressed as:

$$\frac{1}{K_w} = \frac{1}{k_w} + \frac{1}{k_a \cdot H_C} \tag{4.2}$$

$$\frac{1}{K_a} = \frac{H_C}{k_w} + \frac{1}{k_a} \tag{4.3}$$

k_w (m/d) is the water-phase mass transfer coefficient and k_a (m/d) is the air-phase mass transfer coefficient. For low-solubility gases such as THM the Henry's constant (H_C) is high. And typically k_a is considerably higher than k_w, which makes K_w the preferred overall coefficient. Under these conditions, the resistance to interfacial mass transfer of THM is liquid-phase controlled (Rousseau, 1987, Tan, 2014). The overall water-air mass transfer coefficient K_{wa} (m/d) is considered equal to K_w in this study. The dimensionless Henry's constant (H_C) for the average water temperature 29.4 °C was calculated according to the method proposed by Sander (1999).

4.2.3 Treatment

THM removal can be achieved by advanced pool water treatment such as application of activated carbon.

4.2.4 Exchange of fresh filling water

To keep a certain water volume in swimming pool, water loss due to back-washing of filtration facility, vaporization and bather activities is reflected in the amount of fresh filling water, which should be at least 0.03 m^3 per swimmer according to DIN 19643-1 (2012a). In general tap water is used for filling the pool, where much frequently there is little THM. This exchange with fresh filling water reduces the THM concentration in pool water, which is also occasionally applied in practice to achieve a better water quality. In Germany the drinking water treatment often doesn't apply chlorine. Therefore tap water commonly doesn't contain or contain very little THM. Tap water at the studied swimming pool has THM < 0.4 µg/L. Therefore in this study the addition of filling water was considered to cause a reduction on THM concentration.

4.2.5 Mass balance

In summary, removal of THM from swimming pool water includes: volatilization into air, removal by pool water treatment and exchange with fresh filling water, which can be described by a removal coefficient k (d^{-1}):

$$k = (K_{wa} \cdot A + X_{THM} \cdot Q_{TM} + Q_{FW})/V_{Pool} \tag{4.4}$$

K_{wa} (m/d) is the overall mass transfer coefficient of THM from water into air. A (m^2) is the water surface area of swimming pool. X_{THM} describes the THM removal ratio (in percentage) during one passage of the pool water treatment process. Q_{TM} (m^3/d) is the volumetric flow rate of pool water treatment. Q_{FW} (m^3/d) is the filling water inflow. V_{Pool} (m^3) is the total water volume in the swimming pool. Based on equation (4.1) and using k from equation (4.4) a simple relation based on mass balance of THM in swimming pool water can be expressed as:

$$\frac{d\rho_{THM}(t)}{dt} = R_C \cdot \rho_{DOC} - k \cdot \rho_{THM}(t) \tag{4.5}$$

ρ_{DOC} (mg/L) and ρ_{THM} (µg/L) are the DOC and THM concentrations in pool water. The first part $Rc \cdot \rho_{DOC}$ represents the THM production and the second part $k \cdot \rho_{THM}(t)$ stands for THM removal. Temperature, chlorine concentration and pH-value were assumed to be constant to simplify the simulation as they are usually very stable in indoor swimming pool water. The values of simulation parameters were obtained by our field research and experimental results (Chapter 4.3). Simulation results were evaluated using the normalized mean bias and mean fractional bias.

4.3 Determination of parameters for the THM simulation

Parameters for the THM simulation were determined using data from field research, laboratory analysis and literature. In the studied pool water temperature was kept at 28.7–29.6 °C and pH was most of the time at 7.1 with a range of 6.9–7.5 (Table 4.1). Therefore it is realistic to assume the temperature, pH-value and chlorine concentration to be constant for simplifying the simulation. DOC concentration was measured daily.

Table 4.1: Physical and chemical parameters of swimming pool and filling water during the period of the study.

Parameter	Unit	Swimming pool water (n = 26)		Filling water (n = 14)	
		Mean ± SD	Range	Mean ± SD	Range
pH		7.1 ± 0.1	6.9–7.5	7.6 ± 0.2	7.6–7.8
Br^-	mg/L	< 0.1	< 0.1	< 0.1	< 0.3
Cl^-	mg/L	66 ± 14	40–86	31 ± 1	29–33
Free chlorine	mg/L	0.4 ± 0.1	0.3–0.6	< 0.1	< 0.1
DOC	mg/L	3.3 ± 0.3	2.9–4.2	2.7 ± 0.2	2.2–3.0
Temperature	°C	29.4 ± 0.3	28.7–29.6	n. d.	n. d.

n. d.: not determined, SD: standard deviation of the sampling distribution

THM formation was considered as a first order reaction and assumed to be stoichiometrically proportional to DOC reacting with chlorine. According to the observed time delay between DOC and THM occurrences in this study, THM formation can be assumed to be the product of the specific ratio R_C (µg THM/mg C) and DOC concentration from two days before ($\rho_{DOC,\ t\text{-}2d}$):

$$\rho_{THM}(t) = R_C \cdot \rho_{DOC,\ t\text{-}2d} \tag{4.6}$$

The rest maximum formation potential of THM (THMFP) of the native swimming pool water for a reaction time of 46 ± 2 h was determined in the laboratory. R_C was set to the ratio of THMFP/DOC, assuming a maximum THM formation from DOC in two days. THMFP test was carried out 5 times on different days to gain the mean value (23.8 ± 2.4 µg THM/mg C). Comparison with data found or calculated from literature shown in Table 4.2 indicates a good compliance despite the huge variance. In reality, water source, type of organic precursors, pre-oxidation, pre-disinfection or other treatment steps can all affect the DBP species and formation. The steady-state level depends more on the characteristics of the carbon source than on the organic carbon loading rate (Judd, 2003). R_C should be always determined using the actual water to be studied.

The mass balance of THM in swimming pool (Equation (4.5)) can be expressed as:

$$\frac{d\rho_{THM}(t)}{dt} = R_C \cdot \rho_{DOC,\ t\text{-}2d} - k \cdot \rho_{THM}(t) \tag{4.7}$$

After integration, the THM concentration in swimming pool was obtained as:

$$\rho_{THM}(t) = \left(\rho_{THM,0} - \frac{R_C \cdot \rho_{DOC,\ t\text{-}2d}}{k}\right) \cdot e^{-k \cdot t} + \frac{R_C \cdot \rho_{DOC,\ t\text{-}2d}}{k} \quad (4.8)$$

The measured THM concentration on day 1 was used as $\rho_{THM,0}$ (start value of the simulation). Variables for k (= $(K_{wa} \cdot A + X_{THM} \cdot Q_{TM} + Q_{FW})/V_{Pool}$) were determined separately.

Table 4.2: Specific THM formation ratio R_C (µg THM/mg C) found or calculated from literature.

R_C	Water source	Temperature	Initial chlorine	Reaction time	Source
µg THM/mg C		°C	mg/L	d	
33.8	Indoor swimming pool	21	20	2	This study
18.7	Body fluid analog in laboratory	ambient	20	2	(Glauner, 2007)
35.7–44.9	Tap water	ambient	20	2	
51	Outdoor swimming pool	Ambient	20	2	(Glauner et al., 2005)
68	Outdoor swimming pool	Ambient	20	2	
19	Groundwater	30	6	3	(Kim et al., 2002)
16.7	Groundwater + material of human origin	30	6	3	
31.7	Surface water	30	6	3	
14.2	Surface water + material of human origin	30	6	3	
16–38	Body fluid analog in laboratory	26	50	5	(Kanan and Karanfil, 2011)
12-307	Body fluid analog in laboratory	22	50	5	
48–106	Filling water before oxidation	26	50	5	

a) Volatilization (K_{wa})

Typically there are two air exchanges per hour at a fresh air supply of 50% for ventilation in an indoor swimming pool in Germany (Schmalz et al., 2011). In this study a uniform indoor airflow for the whole room was assumed. Frequently chloroform dominates in the total THM (Bessonneau et al., 2011, Simard et al., 2013). In our study we found exclusively chloroform and bromodichloromethane present. Chloroform accounts more than 95% by mass (Table 4.3). Therefore one general overall mass transfer coefficient K_{wa} is assumed here for the total THM. A general airflow velocity in indoor swimming pool was reported for 0.05–0.35 m/s from field survey (Hsu et al., 2009). Based on formulas provided by Guo and Roache (2003) using the airflow velocity of 0.35 m/h and the average

water current velocity of 2 m/s in swimming pool (Toussaint and Truijens, 2005), the K_{wa} of chloroform was calculated to be 0.132 m/h. Besides, a K_{wa} value of 0.378 m/h could be calculated by mass transfer coefficients for chloroform in water and air of an indoor swimming pool reported by Dyck et al. (2011). In this study, K_{wa} was set to be 0.237 m/h by fitting the simulated data to the measured THM concentrations. This value is within the range that gained from literature. The removal coefficient k depends mainly on K_{wa} due to the high volatilization rate of THM.

Table 4.3: Single species of THM in the indoor swimming pool water and filling water for the first sampling period of 26 d.

Parameter	Unit	Swimming pool water (*n* = 26)		Filling water (*n* = 14)
		Mean ± SD	Range	
$CHCl_3$	µg/L	24.2 ± 7.2	12.3–45.7	< 0.4
$CHCl_2Br$	µg/L	1.4 ± 0.3	0.8–2.1	< 0.2
$CHClBr_2$	µg/L	< 0.5	< 0.5	< 0.5
$CHBr_3$	µg/L	< 0.7	< 0.7	< 0.7

SD: standard deviation of the sampling distribution

b) Treatment (X_{THM})

PAC was dosed before UF, which should have a certain effect on removal of THM considered as removal ratio X_{THM}. The dosage of PAC was absent in the first 16 days. By sampling at the inlet and outlet of treatment process no elimination of THM was observed. After the day 17, PAC has been dosed. The elimination of THM by PAC could be distinguished as 1% during one treatment passage. This value was used for simulation as elimination efficiency of THM (X_{THM}) after the day 17. The low elimination rate can be attributed to the short contact time with PAC during the treatment passage, which is only approximately 20 s. It explains also the occurrence of high THM-concentration in the pool water which could not be removed by PAC.

c) Exchange of fresh filling water (Q_{FW})

The amount of daily filling water Q_{FW} was provided by the swimming pool staff, averaging approximately 21 m^3/d during our study. In this study exchange with filling water was assumed to have only removal effect on THM. However, for the locations with tap water containing THM it should be considered in the water exchange.

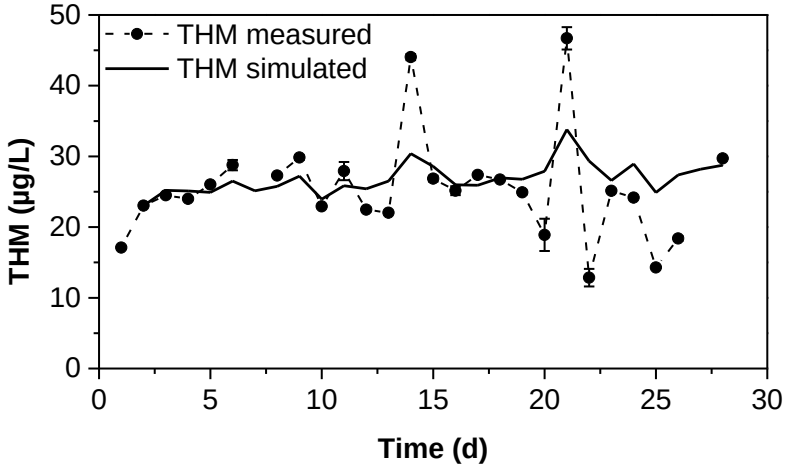

Figure 4.3: Measured and fitted THM concentrations in the indoor swimming pool water for the first sampling period.

The comparison of measured and fitted THM concentrations in pool water is shown in Figure 4.3. The general level of simulated and measured data fits with each other. The appearance of THM peaks could be predicted on the right day. However, the expressively high concentrations of THM peaks could not be predicted, which may attribute to underestimation of the reactivity of some organic matters with chlorine, probably brought into pool water by pool visitors. The simulation can be improved only if more information about the formation rate between different DOC constituents and THM is gained. Nevertheless, at the end the predicted value on day 28 fit very well with the measured value despite that there was a gap of measurement on day 27.

4.4 Validation of simulation

Validation of model requires assessing the effectiveness of the fitted equation against an independent set of data. To validate the simulation we used the data from further sampling for 50 days. Simulation started with the measured THM concentration on day 2 because of the delay between DOC concentration and THM formation. Comparison between measured and simulated THM concentration are presented in Figure 4.4. The simulated and measured THM concentrations were generally in good agreement. The simulated results represented well the tendency of THM accumulation and removal for most of the THM peaks. Slight overestimation appeared on day 27–31 and day 35–36, which may be attributed to the underestimation of the various contributions of visitors' movement to the volatilization. The movement behavior of visitors in swimming pool could strongly affect the volatilization rate of THM into air in indoor swimming pools (Hsu et al., 2009, Kristensen et al., 2010). In addition, the expressively high THM-concentration (> 40µg/L) during the first sampling period (Figure 4.3) were not observed in these 50 days (Figure 4.4). We may again speculate that the excessive THM-concentration might be a short-term value due to some reactive organic matters. In the later time after day 37 the development tendency of THM was again well approved by the actual

measurement. Normalized mean bias (NMB) and mean fractional bias (MFB) were calculated as described by Dyck et al. (2011):

$$\textit{Normalized mean bias (\%)} = \frac{\sum_{i=1}^{N}(Y_{predicted} - Y_{measured})}{\sum_{i=1}^{N} Y_{measured}} \cdot 100 \quad (4.9)$$

$$\textit{Mean fractional bias (\%)} = \frac{1}{N}\sum_{i=1}^{N} \frac{2\cdot(Y_{predicted} - Y_{measured})}{(Y_{predicted} + Y_{measured})} \cdot 100 \quad (4.10)$$

The NMB and MFB of predicted THM were 1.6% and 1.5%, which presented a close simulation. The validated simulation confirms that DOC concentration has a dominant effect on THM concentration in swimming pool water after two days. A sensitivity analysis was performed for the key parameters R_C and K_{wa} for the second period of 50 days (Appendix, Figure A3). The sensitivity analysis indicates that increase and decrease of R_C has a linear effect on the simulation. K_{wa} is more sensitive for lower values and tends to overestimate the THM concentration. When K_{wa} decreases more than -30%, the overestimation of THM increases significantly. Increase of K_{wa} has a lower impact and tends to be less sensitive when the change is higher than 30%.

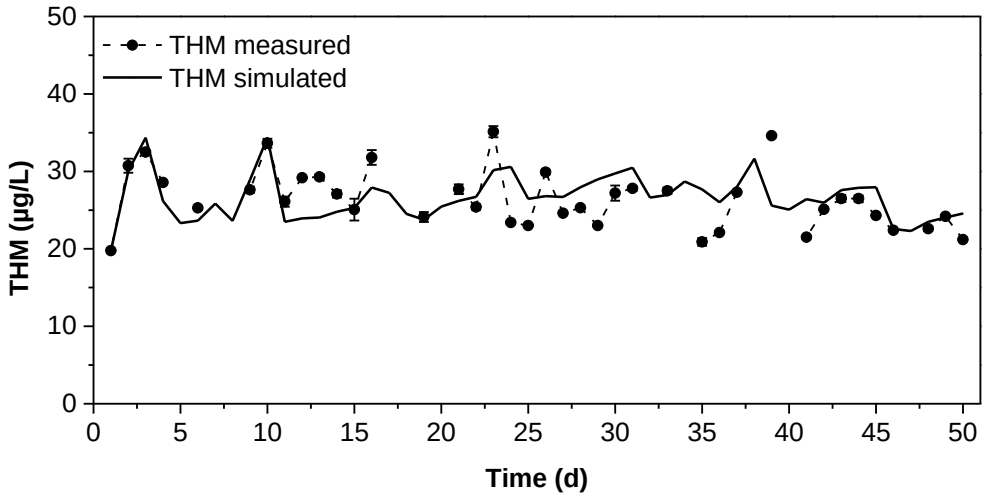

Figure 4.4: Validation for measured and simulated THM concentrations in the indoor swimming pool water for a further period of 50 d.

A simulation of THM in swimming pool water by the use of kinetic coefficient relating them to actual water quality and operational parameters was established. Formation ratio R_C of THM gained in laboratory analysis using native pool water and field sampling for relating the coefficients to operational parameters reduced the uncertainty of prediction. Establishing the formation ratio improves our understanding of the role of DOC in the THM formation which can help to manage DBP precursors in source and pool water. The unknown various activities of pool visitors and different type of organic matter are critical for THM simulation. Intensive activities contribute significantly to the volatilization of THM, which leads to an overestimation of THM concentration by the simulation model. The different reactive organic matters brought by visitors are associated with different THM

formation potential, which affects also the accuracy of simulated results. It's been indicated that fractions of DOC has various THMFP (Glauner et al., 2005b). Therefore determination of R_C should use the native pool water to obtain reliable simulation results. Moreover, recently haloacetic acids (HAA) have gained much attention. The reported HAA concentrations in swimming pool water are much higher than those for THM, possibly because the formation potential of HAA is higher and HAA are much less volatile than THM (Chowdhury et al., 2014). If the pool water treatment is not able to remove HAA and/or their precursors, an accumulation will be probably observed. Due to the much lower volatility the modeling of HAA in swimming pool water could also be feasible using a similar approach based on mass balance.

This simulation model provides a useful method for predicting THM concentration in indoor swimming pool water for a given concrete scenario. With a reduced amount of data required such as a few times of THMFP tests and determination of THM removal by the existing treatment process, formation trend of THM under indoor swimming pool water conditions can be estimated even for long term. For conventional pool water treatment process the low THM removal rate can be neglected.

4.5 Summary

The formation of THM in swimming pool water showed a clear positive correlation to DOC with a time delay in this study, which is related to the treatment process. For conventional swimming pool treatment process the major part of THM formation is within 2 days. DOC proved to be a suitable parameter for precursor to predict THM production when reaction time of 2 days is considered. Number of visitor is not reliable to estimate the organic load brought into water and to predict THM formation. For the first time we developed a simple simulation based on mass balance for predicting the THM concentration in indoor swimming pool water. The model can be used to estimate THM concentration under real indoor swimming pool water conditions with a reduced amount of data required. In the simulation, production of THM from reaction of DOC and chlorine, lose into air and elimination by pool water treatment were considered. The simulated results were generally in well agreement with measurements in reality and in good compliance with published characteristics. The unknown variance of characteristics of DOC and activities of visitors contributed to the deviation between the measurement and the simulation. Practically the model can be useful in conducting health-related risk assessment concerning exposure to DBP and in estimating infrastructure needs for upgrading treatment facilities. The production of THM from DOC is slow compared to a typical turnover rate of swimming pool water. Therefore, a quick removal of organic precursors through pool water treatment could be an effective way to minimize the THM production.

5 THM rejection by nanofiltration membranes and the effects of adsorption and NOM fouling*

*This chapter has been submitted to peer reviewed journal in collaboration with F. Saravia, K. Bock, M. Pelikan, G. Abbt-Braun and H. Horn.

Experiments were carried out in the laboratory to evaluate the THM rejection by NF and the effects of adsorption on rejection performance. Considering the volatility of THM, filtration experiments were carried out in a closed set-up using pressure vessels and stirred cells. Three NF membranes with similar or smaller MWCO than the molecular weight of THM were investigated. Additionally, fouling experiments were performed to study the effects of NOM in feed and the fouling layer on rejection performance. The THM-adsorption on membranes was calculated by mass balance. Membrane material, surface morphology and hydrophobicity were characterized.

5.1 Rejection of THM

Figure 5.1 shows the results of the THM rejection over permeate volume from the filtration experiments with THM in demineralized water for the three membranes. (a) to (c) are the experiments with $CHCl_3$ alone (experiment number 1). Membranes NF90 and NTR-7470pHT showed a high initial $CHCl_3$ rejection (> 90%), whereas SB90 presented an initial rejection of about 30%. Rejection value by all membranes decreased quickly during filtration and reached steady-state after different filtrated volume. The rejection decline was significantly more quickly for SB90 (10 h) and most slowly for NTR-7470pHT (50 h). The rapid decline of initial rejection indicates adsorption of $CHCl_3$ to membranes. At steady-state NF90 rejected 30% of $CHCl_3$ and the other two membranes had no $CHCl_3$ rejection.

Figure 5.1, (d) to (e) are the experiments with the four THM mix in the feed (experiment number 2). Similar to results of $CHCl_3$, the rejection of all four THM appeared to decrease from the beginning of filtration for all membranes. The rejection decline profiles of four THM were well separated from each other for NF90 and NTR-7470pHT. The more brominated the THM were, the later the rejection reached the steady-state and the higher adsorption capacity the membrane has. The rejection of $CHBr_3$ reached the steady-state even after 5 days for NF90 and NTR-7470pHT. Comparing the results of $CHCl_3$ alone and of CHCl3 in the THM mix, the $CHCl_3$ rejection reached the steady-state sooner when it was in the THM mix than when it was alone. This “acceleration” due to presence of other THM was most apparent for NTR-7470pHT. NF90 had the steady-state rejection of 33%, 36%, 42% and 49% for

$CHCl_3$, $CHCl_2Br$, $CHClBr_2$ and $CHBr_3$ respectively. NTR-7470pHT and SB90 showed no rejection of THM at steady-state.

During fouling experiments (experiment numbers 3 and 4) the profile of rejection decline over permeate volume was very close to those in the experiments 1 and 2 with demineralized water (data not shown). At the end of each fouling experiment the organic fouling layer on the membrane was very obvious (Appendix Figure A4). DOC from NOM rich lake water could be well rejected (> 90%) but little effect on the THM rejection during the rejection decline course or on the steady-state rejection was observed.

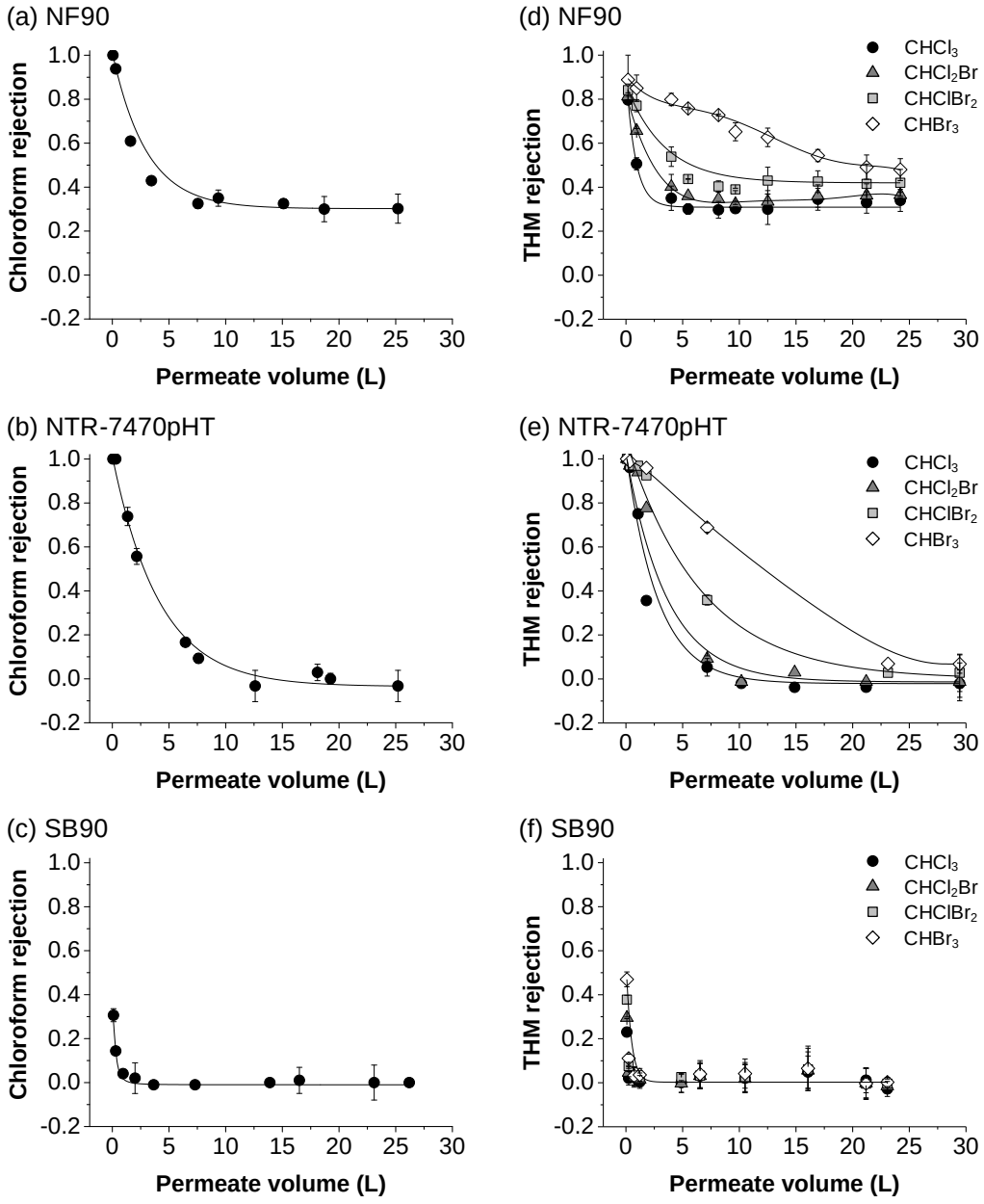

Figure 5.1: Rejection of chloroform by (a) NF90, (b) NTR-7470pHT and (c) SB90 and rejection of four THM by (d) NF90, (e) NTR-7470pHT and (f) SB90 at the same filtration condition.

5.2 Adsorption of THM

The absorbed amount of THM during filtration experiments is shown in Table 5.1. Adsorption to the filtration device (stirred cells) can be neglected considering the quick saturation of SB90. The more brominated the THM, the higher the adsorption, which confirmed the results of rejection decline profiles in which $CHBr_3$ reached the steady-state at latest. According to the molecular properties of THM (Table 3.3), molecular weight, length and width as well as log K_{ow} all exhibited a positive correlation with the adsorption. NF90 presented the highest THM adsorption capacity followed by NTR-7470pHT. The amount of THM adsorbed to SB90 was less than 10% of the amount adsorbed to NF90 and thus corresponding to the much quicker rejection decline profiles of SB90.

Table 5.1: Results of adsorbed THM during filtration experiments

Membrane	Exp. number	THM in Feed	Adsorbed mass (mg/m^2)			
			$CHCl_3$	$CHCl_2Br$	$CHClBr_2$	$CHBr_3$
NF90	1	$CHCl_3$	27 ± 3			
	2	THM mix	29 ± 2	37 ± 2	49 ± 2	83 ± 4
	3	$CHCl_3$, fouling	25 ± 3			
	4	THM mix, fouling	18 ± 2	32 ± 2	47 ± 2	86 ± 4
NTR-7470pHT	1	$CHCl_3$	24 ± 1			
	2	THM mix	15 ± 1	18 ± 1	42 ± 2	74 ± 4
	3	$CHCl_3$, fouling	25 ± 2			
	4	THM mix, fouling	13 ± 1	18 ± 1	38 ± 2	73 ± 4
SB90	1	$CHCl_3$	1.6 ± 0.1			
	2	THM mix	1.2 ± 0.1	2.5 ± 0.1	3.8 ± 0.2	5.4 ± 0.3
	3	$CHCl_3$, fouling	1.8 ± 0.2			
	4	THM mix, fouling	1.3 ± 0.1	3.1 ± 0.1	5.0 ± 0.2	4.4 ± 0.2

Comparing the results of $CHCl_3$ alone and THM mix during filtration experiments with demineralized water, the adsorbed mass of $CHCl_3$ was nearly the same for the membrane NF90. Interestingly for the membrane NTR-7470pHT, when the feed contains $CHCl_3$ alone, $CHCl_3$ adsorbed 60% more than when it was present in the THM mix. Similar phenomenon was also observed for the membrane SB90 but only to a lesser extent. A possible explanation can be that competitive adsorption between four THM molecules led to less adsorption of $CHCl_3$.

The influence of fouling on adsorption was also studied and compared to the experiments with demineralized water. When there was $CHCl_3$ alone, organic fouling didn't change the adsorbed amount obviously. In the case of THM mix, the three membranes showed different behaviors. For NF90, $CHCl_3$ and $CHCl_2Br$ adsorbed less when there was organic fouling. NTR-7470pHT didn't present a difference in adsorption with or without fouling. For SB90 the adsorption seemed to increase when there was fouling except for $CHBr_3$.

Table 5.2: Results of static adsorption experiments

Membrane	Exp. Number	THM in Feed	Adsorbed mass (mg/m^2)			
			$CHCl_3$	$CHCl_2Br$	$CHClBr_2$	$CHBr_3$
NF90	5	$CHCl_3$ alone	3.9 ± 0.1			
	6	THM mix	3.7 ± 0.1	4.6 ± 0.1	5.0 ± 0.1	5.6 ± 0.1
NTR-7470pHT	5	$CHCl_3$ alone	4.8 ± 0.6			
	6	THM mix	3.5 ± 0.1	4.0 ± 0.1	4.1 ± 0.1	4.6 ± 0.1
SB90	5	$CHCl_3$ alone	0.7 ± 0.1			
	6	THM mix	0.6 ± 0.1	0.4 ± 0.1	0.5 ± 0.2	0.8 ± 0.2

Static adsorption test was performed to quantify the adsorption of THM to the membranes only from the surface contact with membrane. The same feed solution with four THM mix in demineralized water was used. Table 5.2 presented the adsorbed amounts of $CHCl_3$ and the THM mix. Similar to the results of filtration experiments for NTR-7470pHT (Table 5.1), the adsorbed $CHCl_3$ was higher when it was alone than when it was in the THM mix. For the other two membranes this trend was minimal. Generally the adsorbed THM mass in the membrane during the static adsorption test was much lower than those in the filtration experiments, thus the competitive adsorption between the different THM and the trend with increasing bromide content is less obvious. In static adsorption experiments the molecular diffusion was the only driving force and the concentration of THM in the solution decrease with time. Therefore the driving force was lower than in the filtration experiments, in which fresh feed solution was always added to the system and the THM concentration was constant with time.

5.3 Characterization of membranes

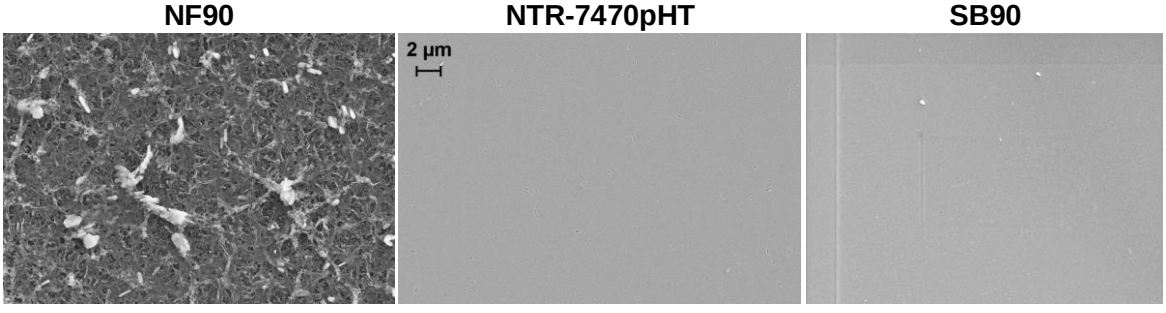

Figure 5.2: SEM measurement of the three nanofiltration membranes (virgin)

SEM images (Figure 5.2) showed the significant rougher surface of NF90 and the smooth surface of NTR-7470pHT and SB90. Roughness data of the membrane surface were found in literature (Alturki et al., 2010, Klüpfel, 2012, Nghiem et al., 2008, Xu et al., 2010) and the hydrophobicity of the surface of membranes, by measuring the contact angle, was analyzed (Table 5.3). As expected from the SEM images NF90 presented higher roughness values than SB90. Although no information for NTR-7470 was found, according to SEM pictures we can expect that the roughness should be similar as SB90. Hydrophobicity of virgin membranes was similar for all investigated membranes. After fouling all

membranes became more hydrophobic and the contact angles were still close to each other. The high deviation of contact angles for NF90 after fouling was probably due to the uneven distribution of the fouling layer. Unfortunately these surface properties couldn't be correlated to the adsorption capacity of the membranes.

Table 5.3: Characterization of three used nanofiltration membranes

	Roughness	Contact angle[1] (°)	
	(nm)	virgin membrane	after fouling experiments
NF90	63–77[2]	66 ± 3	85 ± 12
NTR-7470pHT	no data	62 ± 3	95 ± 6
SB90	9.8[3]	59 ± 4	95 ± 4

[1]Sessile drop method. [2](Alturki et al., 2010, Nghiem et al., 2008, Xu et al., 2010). [3](Klüpfel, 2012).

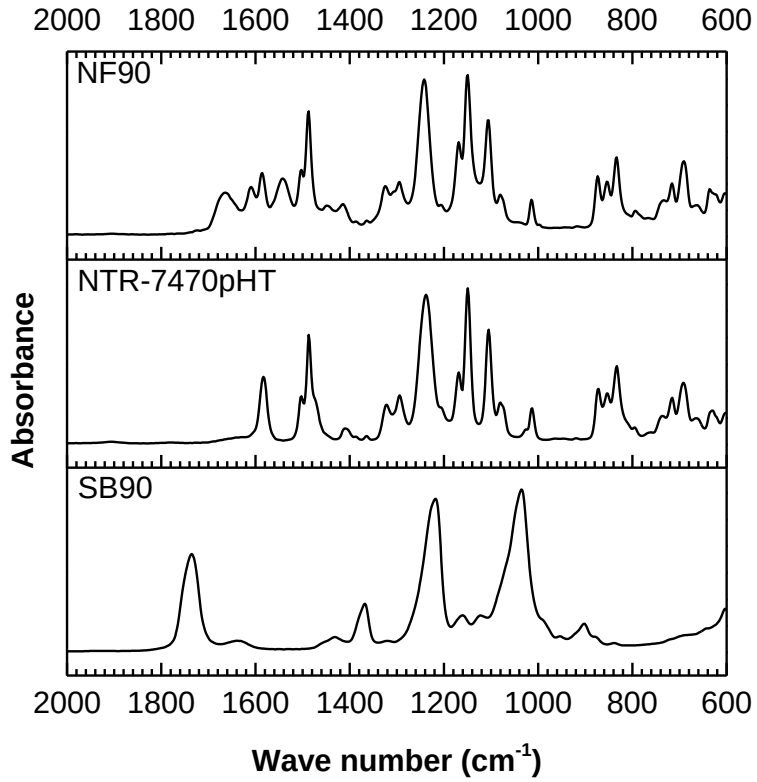

Figure 5.3: ATR-FTIR spectra of the three nanofiltration membranes (virgin) over 600–200 cm^{-1}.

Infrared spectroscopy was measured for virgin membranes and presented in Figure 5.3. The functional groups of membrane polymer were interpreted based on wave number. For NF90 amide I (C=O stretching, 1663 cm^{-1}), aromatic amide (1609 cm^{-1}) and amide II (N–H bending, 1543 cm^{-1}) peaks belong to the main features of polyamide (Koichi and John, 2003, Tang et al., 2009). Since the ATR-FTIR measurement penetrates the membrane to 6-10 µm and goes through the thin polyamide layer of NF90 to the polysulfone layer underneath, NF90 and NTR-7470pHT presented, except for the amide groups, very similar spectra. Polysulfone and polyethersulfone share common structures featuring the Ar–SO_2– and Ar–O– functional groups, which was revealed by aromatic ether band (1240 and 1107

cm^{-1}) (Klüpfel, 2012), aromatic ring (C–C stretching motion, 1585, 1487 and 1169 cm^{-1}) and symmetric O=S=O stretching (1152 cm^{-1}). And the asymmetric O=S=O vibrations at around 1325 cm^{-1} should split into three bands, 1324, 1307 and 1294 cm^{-1} for polysulfone in NF90 and 1324, 1295, 1289 cm^{-1} (shoulder, not apparent here) for polyethersulfone in NTR-7470pHT (Koichi and John, 2003). SB90 presented a completely different spectrum, which distinguished by an ester carbonyl with C=O stretching (1736 cm^{-1}), methyl groups on the acetate group (1369 cm^{-1}), a strong C–O–C stretching (1219 cm^{-1}) and pyranose ether band (1036 cm^{-1}) (Koichi and John, 2003, Murphy and de Pinho, 1995). ATR-FTIR results showed that both NF90 and NTR-7470pHT which had high adsorption THM capacity also have similar functional groups in terms of membrane/membrane support material.

5.4 Discussion

5.4.1 Effect of molecular properties on adsorption

The amount of adsorbed THM to NF90 and NTR-7470pHT, compared to similar studies found for organic compounds adsorption (Steinle-Darling et al., 2010), is relatively high. As previously mentioned, less polar and hydrophobic compounds tend to adsorb to the hydrophobic membrane polymer. All four THM have hydrophobic characteristics with log K_{ow} > 2 (Kimura et al., 2003a) and are relatively less polar, both features increased adsorption potential to the NF membranes.

$CHBr_3$ was the most preferentially adsorbed onto membrane, followed by $CHCl_2Br$, $CHClBr_2$ and then $CHCl_3$. For SB90 the steady-state was reached soon (lower adsorption capacity) therefore it could only be seen that at the beginning of the experiment higher molecular weight THM had a higher adsorption than smaller THM. The tendency showed that adsorption to membranes was preferable for THMs with higher molecular weight, higher hydrophobicity (log K_{ow}) and less polarity (dipole moment). Similar tendency was observed in THM adsorption to activated carbon, because generally the adsorption capacity of activated carbon increases with the higher molecular weight or less polarity of the compound (Lu et al., 2005, Potwora, 2006). A study showed that the extent of adsorption of phenolic compounds was promoted by hydrophobic interactions between them and the membrane structure (Arsuaga et al., 2010). Another study indicated that although the log K_{ow} was the best parameter to describe the hydrophobic adsorption, the relationship between molecular size or weight of the solute and the pore size of membrane also plays an important role (Van der Bruggen et al., 2002a).

5.4.2 Effect of membrane material on adsorption

Membranes of different materials showed highly different behaviors for THM adsorption. The different “saturation times” revealed highly different characteristics and capacity of three membranes for THM adsorption. At a realistic THM concentration range, NF90 and NTR-7470pHT could adsorb significant amounts of THM which led first to an overestimation of rejection and then to a continuous rejection decline over up to 5 days. The rejection declines of four THM were all clearly quicker for SB90 than for the other two membranes. Steady-state was reached already after 6 L permeate volume

(about 6 h). Possible reasons can be different membrane properties in material or surface which affect the interaction between membranes and THM. A static adsorption study of perfluorinated compounds and thin-film composite polyamide NF membranes also showed that the adsorption depended strongly on the material of the active membrane layer (Kwon et al., 2012).

The hydrophobicity of the three membranes shown by contact angles was similar. NF90 has significantly rough surface while the other two membranes have very smooth surface. ATR-FTIR results, in comparison, demonstrated the comparable spectra for NF90 and NTR-7470PHT and completely different spectra for SB90. The results indicated that the common structures Ar–SO_2– and Ar–O– shared by polysulfone and polyethersulfone in NF90 and NTR-7470pHT respectively can be the key for the THM adsorption. According to Kiso (1986), the dominant effect on adsorption to cellulose acetate material is the hydrophobic interaction between cellulose acetate and the solute molecule, which is mainly through the acetyl groups of cellulose acetate and the alkyl chains of the solute (Kiso, 1986). Cellulose acetate is less hydrophobic compared to polysulfone/polyethersulfone. Thus it can be assumed that cellulose acetate has less adsorption capacity for THM.

5.4.3 Effect of THM adsorption on rejection

Adsorption of THM to NTR-7470pHT and NF90 needed a considerable time period to reach a steady-state, which can result in serious overestimation of rejection in short term experiments. After the rejection reached the steady-state, NF90 could maximally reject $CHBr_3$ at 49% and NTR-7470pHT and SB90 couldn't reject THM. From both series of experiments either with $CHCl_3$ or four THM mix, the THM rejection was generally lower than what was expected based on the MWCO of the membranes (Table 3.2), especially in the case of NF90 and SB90. Since NF90 is one of the tightest commercial NF membranes, we can conclude that NF serves only as a limited barrier for THM.

One hypothesis is that the adsorbed solute in the membrane matrix facilitates the transport. According to the solution-diffusion model, solute is firstly dissolved in the membrane and then moves across the membrane by diffusion or convection. The adsorbed THM may affect this process by influencing the diffusion into membrane bulk. Previous studies also proposed that solute with a high affinity to the membrane material adsorbs to the membrane matrix more easily and thus facilitating diffusion though the membrane (Arsuaga et al., 2010, Yangali-Quintanilla et al., 2009). According to Steinle-Darling et al. (2010), steady-state rejection is lower when the adsorption is higher for the same solute. Another study also indicated higher hydrophobicity led to increase of adsorption and decrease of rejection for NF membranes, while the influence of hydrophobicity decreases when the molecular size (above the MWCO of the membrane) increases (Braeken et al., 2005b).

However, the fact that SB90 cannot reject THM at all is still interesting. Low rejection of THM by cellulose acetate membrane was observed in previous studies. The rejection of different trace organics including THM by a full-scale RO plant was studied (Reinhard et al., 1986). Smaller chlorinated

compounds could be rejected to some extent by polyamide membranes but passed through cellulose acetate membranes. It was also reported that cellulose acetate RO membrane has lower THM rejection (11–18%) than aliphatic polyamide RO membranes (40–66%) and especially aromatic polyamide RO (70–90%) (Kasai et al., 1990). Meanwhile, in this study SB90 adsorbed much less THM than the other two membranes but the rejection was the poorest considering the MWCO. So we can conclude that it's not only the high amount adsorbed in the membrane structure which leads to more permeation of the solute but probably it's the adsorption capacity of the membrane material which plays an additional role. Cellulose acetate has low THM adsorption capacity so that it's soon saturated, which has fully favored the transport of THM.

Solute-membrane affinity plays dominantly in the mechanisms for the THM rejection by NF membranes. MWCO is not always reliable for choosing membranes for specific target such as organic micropollutants even for less polar and neutral organics.

5.4.4 Competitive adsorption and effect of fouling

Compared to filtration experiments with $CHCl_3$ alone in feed, reaching the steady-state was accelerated for $CHCl_3$ in the THM mix. This acceleration due to presence of other THM was most apparent for NTR-7470pHT. Meanwhile, in both filtration and static adsorption experiments, the adsorbed $CHCl_3$ to NTR-7470pHT was higher when it was alone than in the THM mix. This could be the phenomenon of the competitive adsorption among four THM molecules which led to less adsorption $CHCl_3$. Competitive sorption was also observed for NF270, a polyamide NF membrane (Steinle-Darling et al., 2010). Solutes were rejected more in a cocktail than when it's alone.

In fouling experiments $CHCl_3$ and $CHCl_2Br$ adsorbed less when there was organic fouling for NF90. This could be attributed to 1) the competitive adsorption between THM and NOM as background organics or 2) membrane blocking by organic fouling layer which occupies the available adsorption positions and reduces THM adsorption. During fouling experiments the presence of NOM didn't affect the THM rejection profiles for the three membranes. Obviously there was no effect on a possible interaction of the hydrophobic THM with NOM, which might have influenced the adsorption of THM on the fouling layer. So the first competition from NOM should be minimal. Zhang and Minear (2006) applied the size exclusion chromatograms and pointed out that THM were not bound to Suwannee River fulvic acid. Since THM don't adsorb to NOM fouling layer, the blocking of membrane by organic fouling layer could reduce the THM adsorption by covering the membrane surface. This phenomenon was not observed in the experiments with the other two membranes, probably because the extent of membrane surface reduction due to fouling layer is much more significant on the much rougher surface of NF90 (Figure 5.2). So blocking should be the main reason here for the decrease of THM adsorption after fouling. The less adsorptive the molecule is, the more the adsorption was affected. Consequently the reduction of $CHCl_3$ and $CHCl_2Br$ was observed and $CHCl_3$ was to the largest extent.

5.5 Summary

THM rejection by three NF membranes of different materials was studied over six days. NF has actually limited rejection of THM (max. 30–50%). Large extent of THM adsorption to membrane leads to severe overestimation of rejection in short term experiments. Investigation of THM rejection by NF needs sufficient filtration volume/time. Adsorption has significant influence on rejection mechanism, facilitating the mass transport of THM through NF membrane. Membrane material plays a substantial role in adsorption and consequently has the impact on rejection. Occupation extent of the available adsorption capacity in the membrane plays a significant role in how the adsorption facilitates the transport of molecules through the membrane and thus decreases membrane rejection. Competitive adsorption among THM was observed. NOM in the feed solution and organic fouling layer had little effects on THM rejection. Organic fouling lowered the adsorption of less adsorptive THM due to blocking of the membrane surface.

6 Minimization of DBP in swimming pool water by NF

For the study on the application of NF for the minimization of DBP in swimming pool water, on-site experiments in the public swimming pool A were carried out. Free chlorine at 0.3–0.6 mg /L was present in the feed, which was pre-treated pool water by flocculation, PAC dosage and UF. Previous experiments indicated that most of the precursors can be removed by NF, which implied the possibility to minimize the DBP formation by quick removal of organic matter using NF from the pool water. In this chapter a chlorine resistant NF membrane and a polyamide NF membrane (low chlorine resistant) were investigated in a pilot plant and a full-scale plant respectively at the swimming pool A (Table 3.1). The influence on the pool water quality was accordingly studied.

6.1 Pilot plant using chlorine resistant NF membrane SB90

Based on the better permeability and rejection performance in bench-scale experiments, the membrane SB90 (chlorine resistance: 1 ppm) was selected for the experiments with a pilot plant at the swimming pool A treating the wastewater from backwash of UF membrane modules. Before entering the NF pilot plant the wastewater was pretreated by UF. The water quality (Table 6.1) was very close to that of the UF-permeate in the mainstream of swimming pool water, but with lower chlorine, DOC and AOX concentration mainly due to longer contact time with the PAC.

Table 6.1: Key parameters for feed properties of the nanofiltration pilot plant at the swimming pool A.

Parameter	**Unit**	**Feed (Backwash wastewater pretreated by UF) (*n* = 25)**	
		Mean ± SD	Range
Temperature	°C	28.0 ± 1.2	26.0–29.1
pH		7.0 ± 0.3	6.6–7.7
el. Conductivity	µS/cm	701 ± 48	610–765
Free chlorine	mg/L	0.2 ± 0.1	< 0.5
Ca^{2+}	mg/L	103 ± 9	86–113
Na^{+}	mg/L	22 ± 1	19–24
Cl^{-}	mg/L	75 ± 25	35–113
SO_4^{2-}	mg/L	202 ± 31	156–283
DOC	mg/L	2.2 ± 0.4	1.6–3.0
THM	mg/L	13.2 ± 3.4	6.3–20.6
AOX	mg/L	183 ± 57	100–269

The results of the pilot plant experiments confirmed the rejection performance of the flat-sheet-modules. As expected from the results in Chapter 5, no rejection of THM by SB90 was observed during the operation period. Figure 6.1 and Figure 6.2 presented the concentration of DOC and AOX in permeate and feed of the pilot plant, where NF showed a sufficient rejection performance (83% ± 6% for DOC and 83% ± 5% for AOX) throughout in total 17 months of operation, again indicating that most of the precursors could be removed by NF. At the beginning DOC and AOX was relatively higher due to the organic matters brought within the initial filling tap water. With time the AOX decreased considerably stabilized at 200 µg/L in the first half period. In the second half period DOC and AOX were lower compared to the first half because of the integration of full-scale NF plant, which will be described in the next sections (Chapter 6.2–6.3). A slight increase in the rejection performance with time was observed, probably because membrane fouling improved the size-exclusion effect during the filtration process.

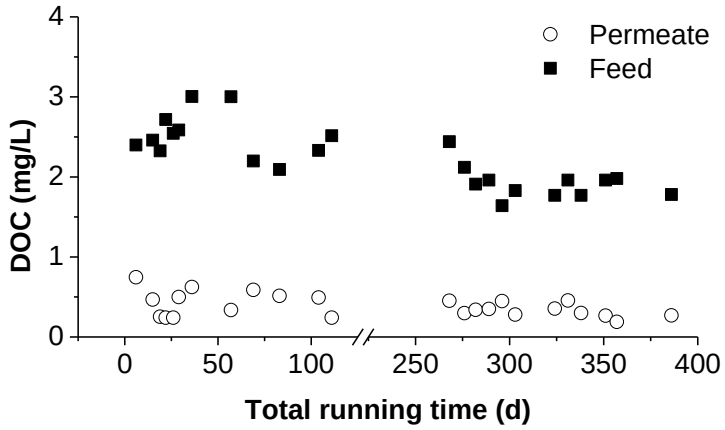

Figure 6.1: DOC in permeate and feed of the pilot plant using chlorine resistant NF membrane SB90.

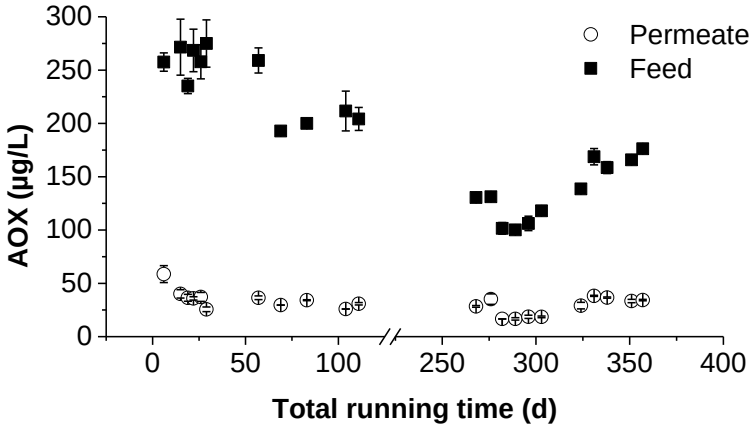

Figure 6.2: AOX in permeate and feed of the pilot plant using chlorine resistant NF membrane SB90.

The results achieved with the pilot scale NF module allowed the calculation of the possible minimization of DBP- and the precursor-formation in swimming pool water, if a branch current is treated with NF membranes.

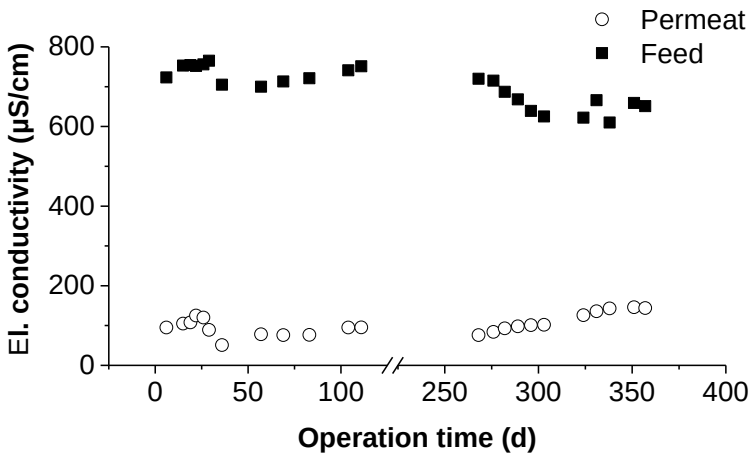

Figure 6.3: Electrical conductivity of permeate and feed of the pilot plant using chlorine resistant NF membrane SB90.

Figure 6.3 showed the electrical conductivity of permeate and feed samples. Rejection of el. conductivity was on average kept at 87% in the first half period. In later stage while the el. conductivity in feed decreased, the rejection started at 89% and decreased slightly with time. A possible reason can be hydrolysis of cellulose acetate, which gradually occurs throughout the membranes lifespan. The hydrolysis reaction breaks down cellulose acetate into cellulose and acetic acid. The pH value of feed water was 7.0 ± 0.3 on average. At pH > 7 the hydrolysis reaction occurs more rapidly particularly as temperature increases (Vos et al., 1966). In general, ion (salt) rejection will be the first and most dramatic change that is observed as the membrane degrades. Nevertheless, after 17 months operation the rejection of el. conductivity was still above 78% and rejection of organic matters was not affected. The sufficient rejection performance of DOC and AOX for long term operation demonstrated the feasibility of applying the chlorine resistant membrane for swimming pool water treatment.

6.2 Full-scale plant using polyamide NF membrane NF90

A full-scale NF plant was integrated to the existing treatment facility (flocculation + UF), accounting at maximum 1.85% of the mainstream with a continuous operation. Nevertheless an intermittent operation was applied, aiming at the intensive load brought by the swimmers in rush hours and not to make the DOC in pool water lower than the DOC in filling tap water. For the full-scale plant the membrane NF90 (chlorine resistance < 0.1 ppm) was applied due to its high permeability (approx. two times of SB90). NF90 also has a smaller MWCO (100 Da) than that of SB90 (200 Da). The feed water was UF-permeate of the mainstream of swimming pool water after chlorine was quenched and antiscalant was dosed. Key parameters for feed water properties are listed in Table 6.2. Electrical

conductivity in pool water decreased from 725 µS/cm to 622 µS/cm during operation time because NF90 has very high rejection of ions. Rejection of el. conductivity was 93−95%, by which sulfate, calcium and magnesium were nearly completely removed (> 99%). And about 50% of the sodium and chloride were removed. Sodium bicarbonate was added in the permeate to keep the buffering capacity which was reduced by the NF treatment.

Table 6.2: Key parameters for feed properties of the full-scale nanofiltration plant at the swimming pool A.

Parameter	**Unit**	**Feed (*n* = 16)**	
		Mean ± SD	Range
Temperature	°C	28.9 ± 0.4	28.0–30.8
pH		7.0 ± 0.4	6.5–7.7
el. Conductivity	µS/cm	658 ± 37	622–725
Free chlorine	mg/L	< 0.03	< 0.03
Ca^{2+}	mg/L	97 ± 12	81–112
Na^{+}	mg/L	24 ± 1	23–25
Cl^{-}	mg/L	52 ± 7	42–60
SO_4^{2-}	mg/L	207 ± 17	190–236
DOC	mg/L	2.8 ± 0.2	2.5–3.1
THM	mg/L	20.7 ± 5.4	13.1–33.0
AOX	mg/L	236 ± 34	179–280

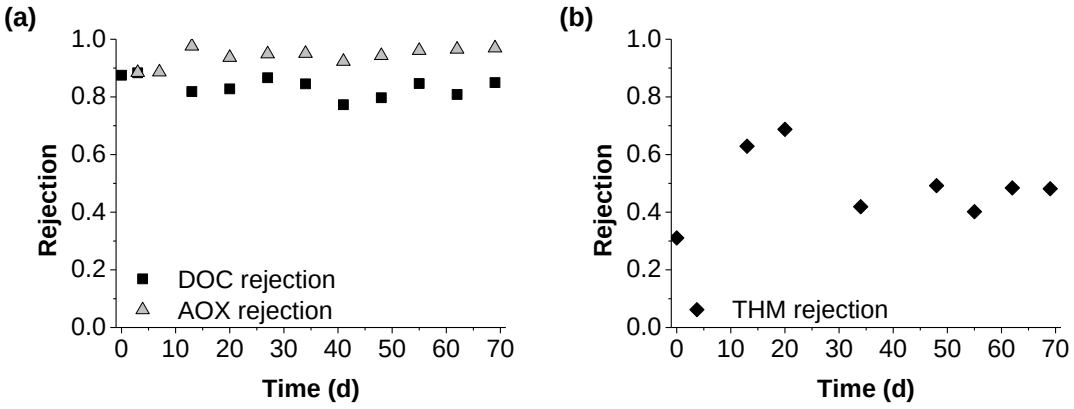

Figure 6.4: Rejection of (a) DOC and AOX (b) THM by full-scale nanofiltration plant using NF90.

Expectedly, NF90 had 80%–90% rejection of DOC and 90%–96% rejection of AOX (Figure 6.4), which indicated an even higher removal of DBP precursors than SB90 has. Furthermore, this tight membrane could reject 30%–50% of THM. From the results a substantial THM reduction in pool water could be expected. The fluctuant rejection values were due to the great fluctuation of THM in feed. NF90 showed stable rejection performance for 8 months operation. No decline of the rejection was observed.

6.3 Influence of DOC-rejection by NF on DBP in swimming pool water

Water quality with and without NF was compared with extensive measurement data. DOC, THM, AOX in swimming pool water were intensively measured (possibly daily) throughout the operation period.

Figure 6.5 shows the DOC and AOX in swimming pool water for about 80 days with the original treatment process (PAC+UF) and backwash water treatment with UF-NF (1% of mainstream). Dash line shows the DOC level in the filling tap water. DOC in pool water was all the time higher than in tap water, where the input from visitors have raised the level of organic matters is clearly seen. Results indicated that the PAC+UF treatment couldn't remove DOC effectively. Accumulation of AOX was obviously shown by increase especially from day 1−23 and day 60−75, which means the original treatment was inadequate to remove DBP precursors. On day 23 extra amount of fresh tap water was filled, which led to a decrease of AOX, while the AOX in tap water was < 10 µg/L. DOC was relative unaffected by dilution because of the high DOC in tap water (2.7−3.0 mg/L). Data of THM was already shown in Chapter 4. No accumulation of THM was observed due to their high volatility.

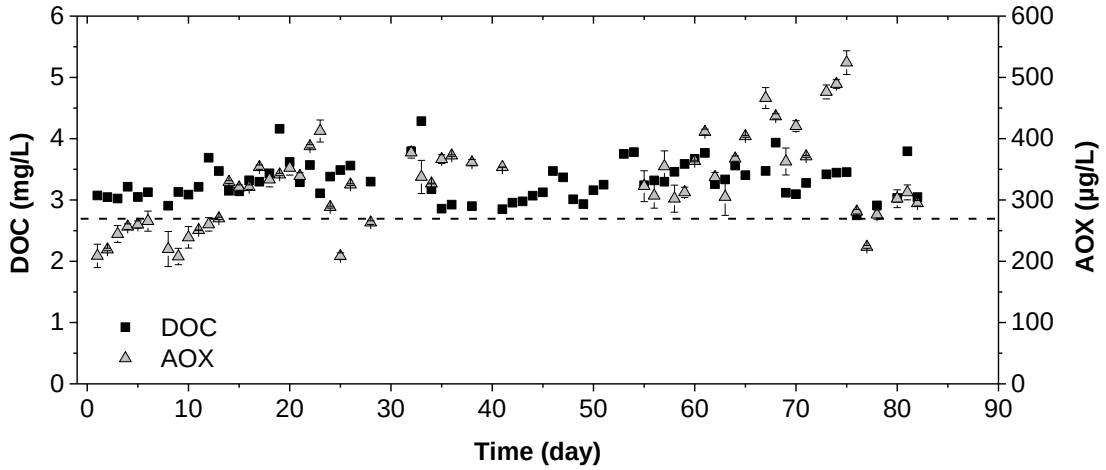

Figure 6.5: DOC and AOX in swimming pool water with the original treatment process (PAC+UF) and backwash wastewater treatment with UF-NF. Dash line shows the DOC level in the filling tap water.

The full-scale NF plant was integrated, accounting at maximum 1.85% of the mainstream with a continuous operation. Based on mass balance of DOC in swimming pool water (Klüpfel et al., 2011a), simulation of DOC representing DBP precursors with different portion of branch current NF treatment was carried out. In addition to the existing backwash wastewater treatment using NF (corresponds to approx. 1% of the mainstream) described in Chapter 6.2, the operation time of the full-scale plant was first at 4 h/d (0.3% of the mainstream) for 6 months and then at 6/h (0.45% of the mainstream) for 2 months. After 32 days the dosage of PAC was turned off.

The monitored DOC and AOX concentration in pool water for the first 70 days were plotted in Figure 6.6. In contrast to the situation with the original treatment, although at the beginning DOC was close

to that in tap water (2.8−3.0 mg/L), with the process combination PAC+UF+NF the concentration of DOC decreased to 2.3−2.5 mg/L in 15 days. Correspondingly AOX was under 200 µg/L. DOC and AOX were much lower compared to the previous levels without NF, which is marked by the dash line. Especially AOX was significantly reduced nearly 50%. After PAC was turned off DOC increased slightly and AOX increased to a larger extent, but both were still well below the previous level. Generally the profiles became flatter than before. The previously observed huge fluctuation of organic load due to intensive input from visitors was alleviated by the effective NF treatment, which means the formation of DBP could be better controlled.

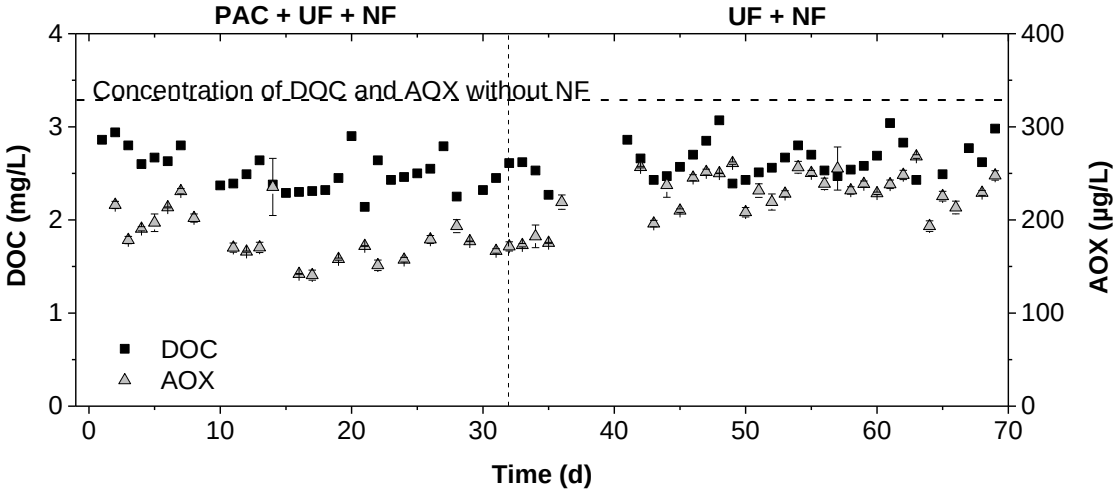

Figure 6.6: DOC and AOX in swimming pool water with full-scale nanofiltration plant integrated in treatment. Dash line shows the DOC and AOX level without NF.

Table 6.3 summarized the average statistic measurement results for different treatment processes including data of bound chlorine and freshwater consumption. Compared to the original treatment, 1.3% of NF branch current could reduce DOC and AOX markedly without increasing water consumption. When PAC was replaced by NF, DOC and AOX in pool water were reduced by 18% and 30% respectively. Bound chlorine was slightly reduced, giving the fact that it was already well under control before the integration of NF. Other regulated DBP such as chlorite and chlorate were also well under the limit with the original treatment so they are not discussed here. The operation at 4 h/d consumes itself 2.5 m^3/d of fresh water due to the discharge of concentrate. However, freshwater consumption was only marginally increased (from 22.2 to 22.7 m^3/d) after NF completely replaced PAC, probably because the improvement of water quality has reduced fresh water exchange.

Table 6.3: Comparison of average water quality in swimming pool water during different treatment processes.

Parameter	DOC in filling water	DOC	AOX	THM	Bound chlorine	Freshwater consumption
	mg/L	mg/L	µg/L	µg/L	mg/L	m^3/d
PAC+UF (*n* = 82)	2.7	3.3	328	24	0.12	22.2
PAC+UF+NF (*n* = 25)	2.8	2.5	166	32	0.11	22.2
UF+NF (*n* = 164)	3.0	2.6	216	22	0.11	22.7

The maximal formation potential of THM (THMFP) and AOX (AOXFP) in the filling tap water and in the swimming pool water with different treatment processes are compared in Table 6.4. During the time with the PAC+UF treatment, which couldn't remove DOC effectively, anthropogenic input from visitors didn't affect THMFP/DOC significantly but AOXFP/DOC was doubled compared to tap water. This indicates that in a swimming pool where the local tap water contains high DOC, the main THM precursor source is still the NOM in the filling water, while anthropogenic input can form a wide range of much other DBP. Bond et al. (2010) investigated nine NOM surrogates and their removal by coagulation, MIEX anion exchange resin and NF membranes. It was not possible to selectively remove compounds which form high amounts of DBP. Therefore although THM is the only regulated parameter for organic DBP, it is not always able to reveal the total DBP level in water.

Table 6.4: Ratio of the THM- and AOX-formation potential (THMFP and AOXFP) in the filling tap water and in the swimming pool water with different treatment processes PAC+UF and UF+NF.

	THMFP/DOC µg/mg DOC	**AOXFP/DOC** µg/mg DOC
Tap water (*n* = 6)	31 ± 4	81 ± 11
PAC+UF (*n* = 3)	34 ± 1	174 ± 48
UF+NF (*n* = 5)	22 ± 2	112 ± 2

It has to be noticed that THM concentration in swimming pool water still remained at a high level (Table 6.3), even though the THMFP/DOC of pool water was reduced after the NF was integrated. During the time with the process combination PAC + UF + NF which had the highest DOC and AOX removal THM was even higher. The kinetic of THM formation depends highly on the species of DOC input from swimmers which is difficult to know. Probably there were organic substances with high THM formation during the starting phase.

Table 6.5: Formation potential in feed and permeate of the pilot plant and the full-scale plant.

Sampling	**Sample**	**DOC (mg/L)**	**THMFP (µg/L)**	**THMFP/DOC (µg/mg)**	**AOXFP (µg/L)**	**AOXFP/DOC (µg/mg)**
1 Pilot plant (SB90)	Feed	2.5	66 ± 2	26	278 ± 22	111
	Permeate	0.2	20 ± 1	84	52 ± 7	215
2 Full-scale plant (NF90)	Feed	2.8	45 ± 2	16	290 ± 21	102
	Permeate	0.4	12 ± 0	32	17 ± 1	47

Formation potential tests of feed and permeate were carried out for the pilot plant and the full-scale plant. Results of representative samplings for each plant were presented in Table 6.5. SB90 could reject 65−70% of THMFP and 63−81% of AOXFP, while NF90 could reject 70−75% of THMFP and 91−95% of AOXFP. Except AOXFP removal by NF90, the rejection of DBPFP was lower than DOC removal. In other words, the DBP formation per unit DOC became larger after NF-treatment. de la Rubia et al. (2008) claimed the ratio of THMFP/DOC (µg/mg), which represents the DBP reactivity in

terms of THM formation, could be even greater in the NF permeate than in the raw water, which was also the case here. The ratio THMFP/DOC in permeate became more than doubled as in feed. It can be assumed that the small amounts of the low molecular weight DOC remained in permeates may be problematic due to its high THM reactivity.

To further characterize the fate of DOC during NF, feed and permeate samples were measured using SEC-OCD. Figure 6.7, (a) presented the results for SB90 and (b) for NF90. The chromatograms of the feed sample from both plants were similar, showing mainly high to moderate MW substances (retention time 42 min < t < 58 min), which was supposed to be mostly natural humic substances from the relatively high content of DOC in fresh water (≈ 3 mg/L) and was oxidative degraded by chlorine. The narrow peak at t = 55 min can be associated with low MW organic acids. After t = 60 min a small amount of low MW organic substances were present. A small peak at t = 76 was assigned to be urea by SEC-OCD with organic nitrogen detection (Appendix Figure A5). The chromatogram of the permeate samples showed very low DOC signals because DOC was mostly rejected by the applied NF.

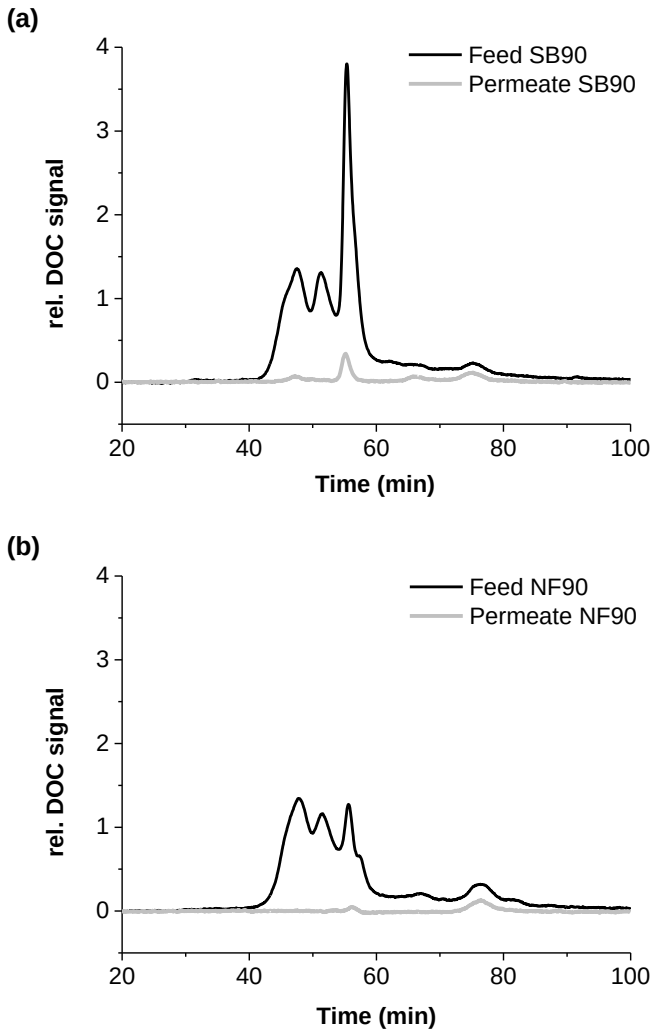

Figure 6.7: SEC-OCD chromatograms of (a) DOC in feed (2.6 mg/L) and permeate (0.2 mg/L) of the pilot NF plant using SB90; (b) DOC in feed (2.2 mg/L) and permeate (0.1 mg/L) of the full-scale NF plant using NF90.

However, the low MW fractions such as the peak at t = 55 min and t = 76 min were not completely removed by NF in both plants. The results support the hypothesis that the small DOC molecules remained in permeates may have high THM reactivity. Glauner et al. (2005b) also reported that highest formation of THMs was from the low-MW fraction (< 200 g/mol) of DOC in swimming pool water. Nevertheless, urea is not a THM precursor (De Laat et al., 2011). Results indicated that THM formation in swimming pool water with integration of NF, which will change the composition of substances in the recirculated system, may refer to a more complicated case which cannot be simply revealed by THMFP/DOC. Interestingly, AOXFP/DOC became more than doubled after filtration with SB90 but decreased after NF90. Compared to SB90, the most apparent difference was the higher rejection of the peak at t = 76 min by NF90. This suggests that this fraction has high AOX formation reactivity, which confirmed the increased AOXFP/DOC due to anthropogenic input in Table 6.4.

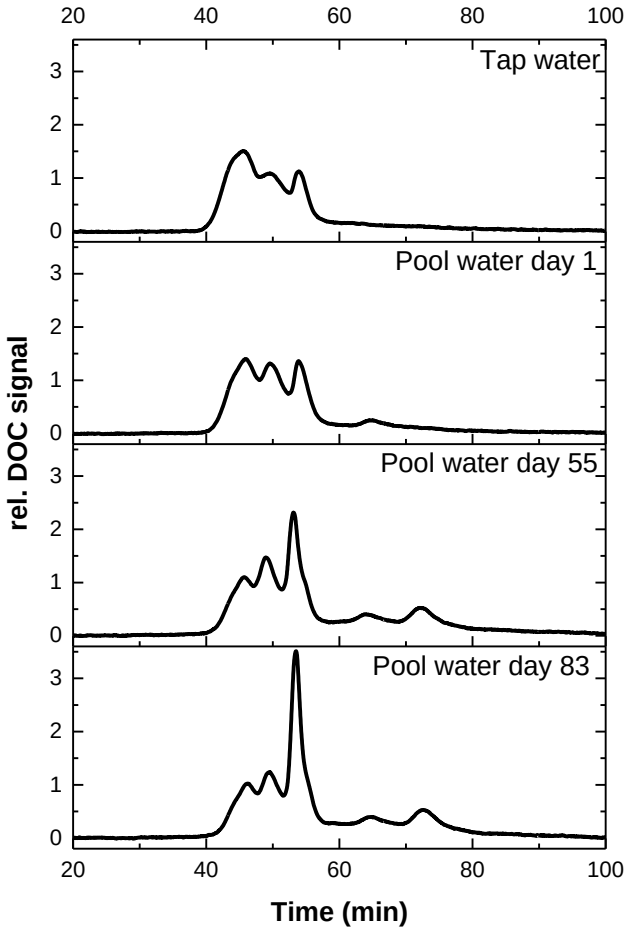

Figure 6.8: SEC-OCD chromatograms showing evolution of DOC in swimming pool water with operation time and in comparison to the filling tap water.

SEC-OCD chromatograms showing evolution of DOC in swimming pool were made and compared to the filling tap water (Figure 6.8). The swimming pool is drained, cleaned and refilled with fresh tap water every year at the beginning of the new opening period. Originally in tap water there was mainly NOM. Once the tap water was in contact with chlorine (day 1), degradation of NOM due to oxidation

begins to shift high MW substances to smaller ones. With time this shift can be seen clearly for the increasing peaks at t = 53/64 min. Besides, the peak at t = 72 min appeared. As mentioned before permeate of NF in swimming pool water contains urea as the dominant fraction besides traces of NOM. These fractions of low MW compounds resulted from the chlorine degradation of NOM and the anthropogenic input from pool visitors which couldn't be completely removed by the treatment. The remaining small molecules could be more easily oxidized by chlorine. Therefore, it can be suggested that the small compounds which come after t = 60 min reached a plateau and were not further accumulated.

6.4 Summary

Application of NF in swimming pool water treatment exhibited high rejection of DOC and AOX, indicating a high elimination of the DBP precursors. Chlorine-resistant NF membrane fulfilled sufficient rejection performance for 17 months under pool water condition with 0.2 mg/L free chlorine present in feed water. By quenching chlorine in advance the polyamide NF membrane endured excellent rejection performance in 8 months operation. Compared to the original treatment process PAC+UF, integration of a branch current NF treatment for 1.3% of the mainstream could reduce the general level of DBP and the precursors (DOC and AOX) as well as the DBP reactivity (THMFP/DOC and AOXFP/DOC) in swimming pool water. Results implied the feasibility of minimizing DBP formation by quick removal of dissolved organic matter (and thus DBP-precursors) from the pool water. Long-term onsite experiments at a real swimming pool demonstrated a realistic option of an efficient treatment, which provided a better pool water quality with only marginally increased fresh water consumption compared to the original treatment PAC+UF. By optimization of the NF-treatment a reduction of fresh water and energy consumption might be further achieved.

7 Fouling of NF membrane in swimming pool water treatment

Fouling of NF membrane during swimming pool treatment was investigated by collecting operational data and autopsy study to characterize the foulants. Fouling of two chlorine-resistant NF membranes (NTR-7470pHT and SB90) was studied with bench-scale cross-flow set-up onsite at two swimming pools A and B with different pool water matrices. Furthermore, autopsy study of fouled spiral wound modules from the two NF plants (the pilot plant equipped with SB90 and the full-scale plant with NF90) at the swimming pool A were carried out. Results were associated with feed water properties to give an insight of fouling of NF membrane during swimming pool water treatment.

7.1 Membrane fouling by two different types of pool water

The treated swimming pool waters were used for feed as they were. No further chemicals (e.g. antiscalant) were added. Pool water A offered a high organic content (3.3 mg/L DOC), while pool water B had only 1.4 mg/L DOC but almost five times higher electrical conductivity due to considerably more Na^+, Cl^- and SO_4^{2-} and two folds of Ca^{2+}, Mg^{2+} and K^+. Detailed feed properties are in Table 3.5.

7.1.1 Permeability profiles

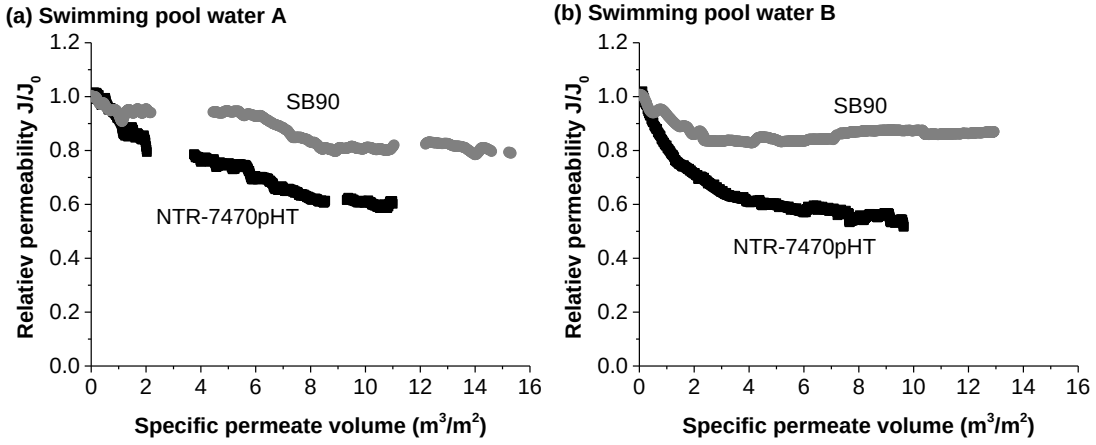

Figure 7.1: Relative permeability of two chlorine-resistant NF membranes treating swimming pool water from (a) a public swimming pool A for 640 h and (b) a university swimming pool B for 405 h.

The relative permeability of the two used membranes during treatment of pool water A and pool water B are shown in Figure 7.1, (a) and (b) respectively. Relative permeability was calculated relative to the stabilized initial permeability. For pool water A the permeability of NTR-7470pHT continued rapid decreasing and at the end stabilized at 60% of the initial permeability, while the permeability of SB90 stabilized first at 95% of the initial permeability, then suddenly decreased fast in the middle of the experiment and kept at 80% for the second half period. For pool water B the permeability of both

membranes decreased faster at the beginning and stabilized sooner. After 405 h of filtration, the relative permeability of NTR-7470pHT sank to 53%, which was lower compared to pool water A after the same produced permeate volume. In contrast, permeability of SB90 only presented the decline at the initial phase and then stabilized at 87%, which showed a better permeability compared to pool A. The rejection performance was analyzed by regular sampling during the whole experiment and the permeability decline was not due to membrane damage.

Biopolymer and humic substances are considered as important foulants for NF membrane. Organic fouling due to adsorption and pore blocking commonly contribute to the flux decline at the beginning phase of filtration process and slows down. For pool water A which contains high DOC it's prone to have organic fouling. The permeability decline could possibly be explained by organic fouling and biofilm formation due to high DOC. However, the much lower concentration of DOC at pool B didn't result in much less flux decline. In contrary, the permeability of NTR-7470pHT was worse at the end of experiment, which indicates the contribution of other foulants. Commonly high ionic strength enhances membrane fouling. Humic substances accelerate organic fouling with increasing Ca^{2+} concentration. Biofouling commonly causes continuous permeability decline, which should not be the major contribution to fouling at pool B. The Ca^{2+} concentration at pool B was approximately 5 mM. A reduction of biofouling at increased concentration 5 and 8 mM Ca^{2+} was observed (Zhao et al., 2015), probably because higher ionic strength suppresses biofouling.

7.1.2 Major constituents of fouling deposits

Fouled membrane pieces were inserted in acid or alkaline solutions to dissolve the fouling deposit for analysis of organic carbon (OC) and other elements. The results are presented as a ratio of specific mass ($m_{sp.}$) over feed concentration, with a unit of $(mg/m^2)/(mg/L)$, which corresponds to the measured mass normalized to membrane area and concentration in feed. Easily soluble constituents such as Na^+ were taken as a reference. Constituents with higher ratio than those of easily soluble constituents are considered accumulated as fouling. Such kind of comparison by associating fouling deposits with feed water properties provides a clear illustration of which element is actually accumulated, avoiding the influence of remaining constituents from dried out water which was in the membrane and fouling layer structure. The most relevant elementary constituents in fouling deposits are listed in Table 7.1.

The mass of organic carbon on NTR-7470pHT was 42 ± 8 mg/m^2 for pool water A and 13 ± 0 mg/m^2 for pool water B, which correlates with the DOC concentration in pool water A and B. According to these results, the accumulation ratio of OC was similar for both pools. The main reason for the different OC accumulation ratios can be that pool water B had the much higher ionic strength and especially the concentration of divalent ions Ca^{2+} and Mg^{2+}, which was double as high as it in pool water A. As known from literature, high ionic strength leads to more severe organic fouling (Tang et al., 2007). And divalent ions such as Ca^{2+} and Mg^{2+} enhances organic fouling by forming complexes

with NOM (Li and Elimelech, 2006). They can bind with the acidic functional groups of the NOM, elevating the degree of hydrophobicity of the NOM molecules, and developing a dense fouling layer. Teixeira and Rosa (2006) suggested that the presence of Ca^{2+} ions is more important than the type of NOM for flux decline. OC analysis for SB90's fouling deposits was unfortunately not applicable, because cellulose acetate hydrolyses in alkaline solution.

Table 7.1: Constituents in the fouling deposits of bench-scale experiments with two different types of swimming pool water A and B. The results are presented as a ratio of specific mass ($m_{sp.}$) over feed concentration, with a unit of (mg/m^2)/(mg/L), which corresponds to the measured mass normalized to membrane area and concentration in feed.

Constituents	Feed (mg/L)		$m_{sp.}$(i) over feed concentration (mg/m^2)/(mg/L)			
	Pool A (n = 13)	Pool B (n = 12)	Pool A NTR-7470pHT	Pool A SB90	Pool B NTR-7470pHT	Pool B SB90
OC	3.3*	1.4*	13 ± 3	n.a.	10 ± 0	n.a.
Al^{3+}	0.034	0.008	239 ± 17	189 ± 35	214 ± 6	650 ± 32
Ba^{2+}	0.101	0.059	42 ± 4	6 ± 1	n.d.	n.d.
Ca^{2+}	112	206	0.7 ± 0.1	0.5 ± 0.1	0.2 ± 0.0	0.2 ± 0.0
Fe^{n+}	< 0.01	< 0.01	> 405	> 261	> 561	> 2581
Na^{+}	21	546	0.6 ± 0.0	0.5 ± 0.1	0.1 ± 0.0	0.1 ± 0.0
PO_4^{3-}	< 0.1	< 0.1	> 12	> 12	> 14	> 71
SO_4^{2-}	190	649	3.4 ± 0.9	1.8 ± 0.9	0.1 ± 0.0	0.1 ± 0.0

* DOC concentration in feed. n.a.: not applicable. n.d.: not detectable.

The accumulation ratio of the constituents in the fouling deposits was compared to that of Na^+. Ca^{2+} and SO_4^{2-} were accumulated to a minor degree for pool water A and were surprisingly not accumulated particularly for pool water B, which had much higher concentration in SO_4^{2-}. Although no antiscalant was used, $CaCO_3$ or $CaSO_4$ scaling were not the major fouling constituents in filtrating swimming pool water. PO_4^{3-} and Fe^{n+} were not detectable in feed water. The minimal value of the ratio was calculated using the detection limit, which is the maximum possible concentration in feed water. Therefore the ratio was presented with ">". Compared to Na^+, Al^{3+} and Fe^{n+} were the most severely accumulated inorganic constituents in both pool waters, probably as metal hydroxides. Al^{3+} was probably from the aluminium based flocculant which was used in both swimming pools. Fe^{n+} came probably from the aged pipeline or tubing. The multi-layer filters used at the swimming pool B have also metal outer housings. PO_4^{3-} was found accumulated on all membranes, which had the similar accumulation ratio as OC, though the amount of deposits was relatively little.

7.1.3 Pore and surface fouling

Cross-section of fouled membrane samples for pool water A were analyzed using SEM (Figure 7.2). On the surface of NTR-7470pHT it was hard to distinguish the fouling layer. But organic-like structures bound to the membrane polymer were observed underneath the dense surface inside the

membrane matrix. This indicates that the major fouling mechanism of NTR-7470pHT was fouling in the membrane structure probably by adsorbed organic matters. In contrast, on the surface of the denser membrane SB90 was an apparent fouling layer (dried layer approximately 6−10 µm). Inside the membrane matrix no fouling deposit was observed. Fouling of SB90 was more likely affected by cake or gel layer formation (surface coverage). Results indicated that under the same condition pore fouling of membrane caused more severe permeability decline of NTR-7470pHT.

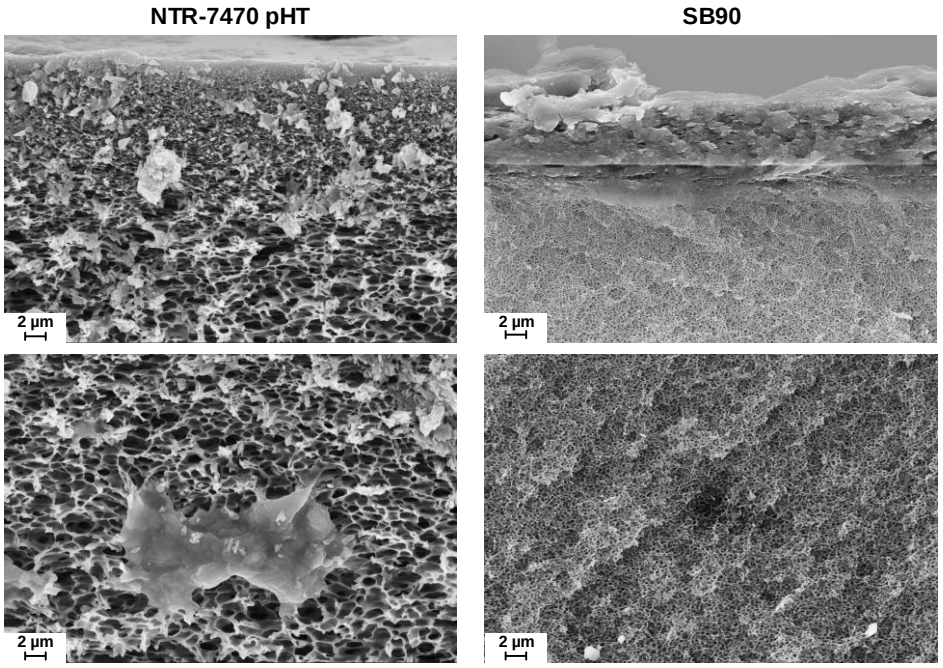

Figure 7.2: SEM images of membrane cross-section near the membrane surface (upper) and below the membrane surface (lower) after 640 h filtration of the swimming pool water A. NTR-7470pHT (left) showed mainly pore fouling and SB90 (right) showed surface fouling.

7.1.4 Surface characterization

Surface of fouled membranes was characterized using SEM and EDX. Figure 7.3, (a) and (c) showed the surface of NTR-7470pHT and SB90 fouled with the swimming pool water A. On both membranes organic-like foulant structures were observed. As discussed above, NTR-7470pHT possessed mainly pore fouling so the clear membrane surface is still visible. EDX spectrum of a representative spot on SB90 was presented in (e), which indicated that there was mainly organic fouling on the membrane.

NTR-7470pHT and SB90 fouled with the swimming pool water B were shown in (b) and (d). Compared to pool water A, Pool water B seemed to have formed mixture of organic and inorganic foulants. Especially on SB90, which has higher salt rejection, a few crystal-like structures were observed. EDX spectrum of SB90 in (f) revealed signals of Na, Cl, Ca, and S, which were probably from NaCl and $CaSO_4$ which precipitated when the pool water dried out after membrane samples were taken out, since pool water B contains high concentration of these salts. The high oxygen signal can be

possibly attributed to sulfate salts and aluminium or iron hydroxides, since Al and Fe were found significantly accumulated (Table 7.1).

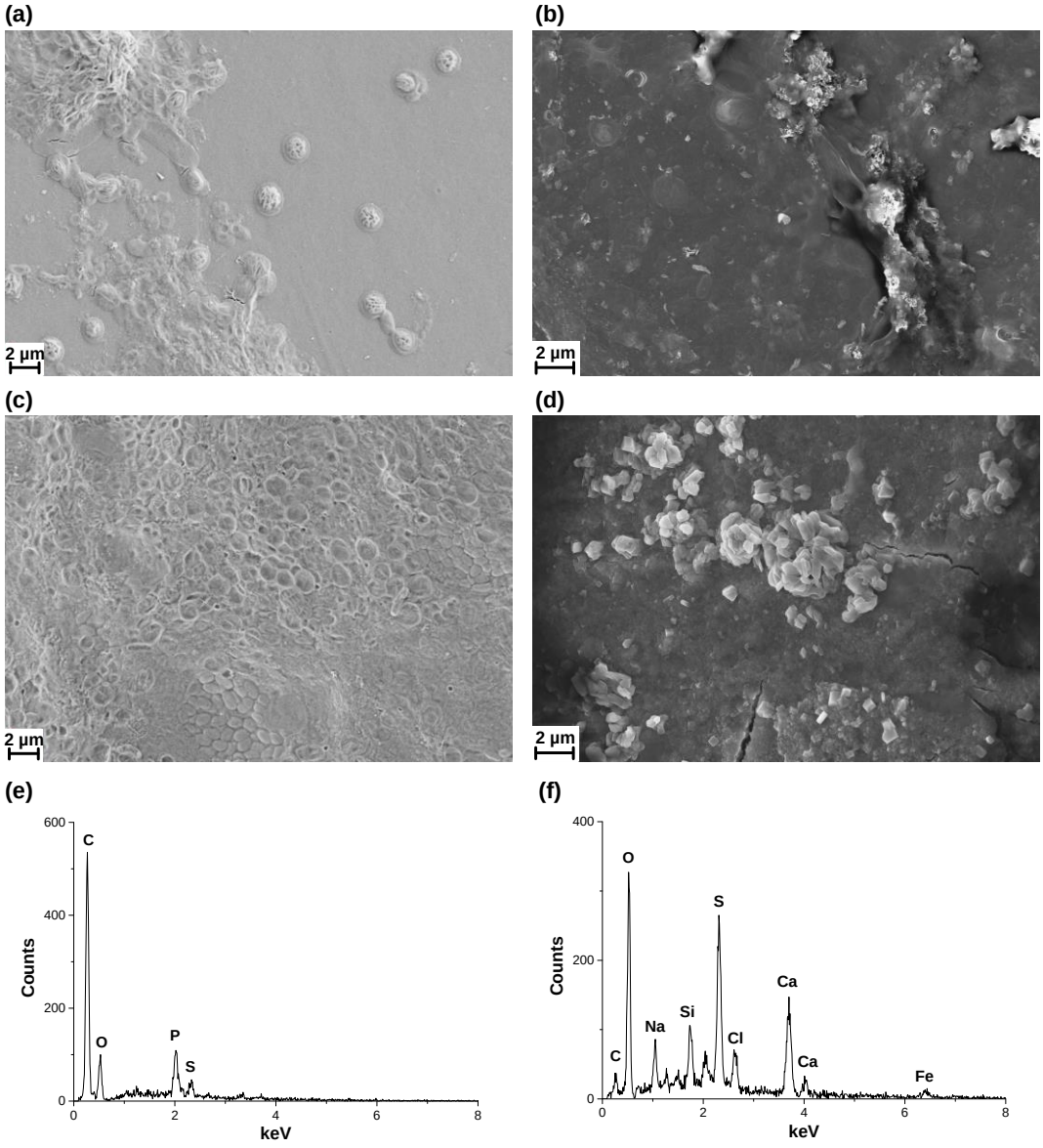

Figure 7.3: SEM images and EDX results comparing membrane fouled by swimming pool water A and B. (a) NTR-7470pHT at pool A, (b) NTR-7470pHT at pool B, (c) SB90 at pool A, (d) SB90 at pool B, (e) SB90 at pool A and (f) SB90 at pool B.

Table 7.2: Contact angle on cleaned and fouled membrane surface.

	NTR-7470pHT	SB90
Clean membrane	60 ± 4	65 ± 2
Fouled membrane, pool water A	60 ± 4	80 ± 6
Fouled membrane, pool water B	63 ± 6	22 ± 6

Results of contact angle measurements (Table 7.2) showed that the hydrophobicity of NTR-7470pHT didn't change clearly during filtration, probably because the surface fouling layer didn't completely

cover the membrane surface. The influences of fouling on the surface hydrophobicity were significant for SB90, because foulants formed cake layers on the dense SB90. SB90 became more hydrophobic when fouled with pool water A but much more hydrophilic when fouled with pool water B. Possible explanations can be that the high NOM content in pool water A accumulated to form a hydrophobic layer, while inorganic precipitants such as aluminium and iron hydroxides increased the hydrophilicity. This might explain why severe accumulation of Fe deposit on SB90 didn't result in further flux decline.

7.1.5 Fouling development

In order to follow the fouling development, during the experiments at the swimming pool B membrane samples were taken out for characterization after about 70 h, 230 h, and 405 h filtration time (duplicates). Results were ordered and associated with permeate volume over membrane area (m^3/m^2). Photos (Figure 7.4) of fouled membranes presented brown deposits, indicating iron precipitates. On NTR-7470pHT was a very thin fouling layer with brown deposit at the corners where was in contact with the feed spacer. SB90 showed more obvious increase of the fouling deposits. At the end the membrane was fully covered by brown layer.

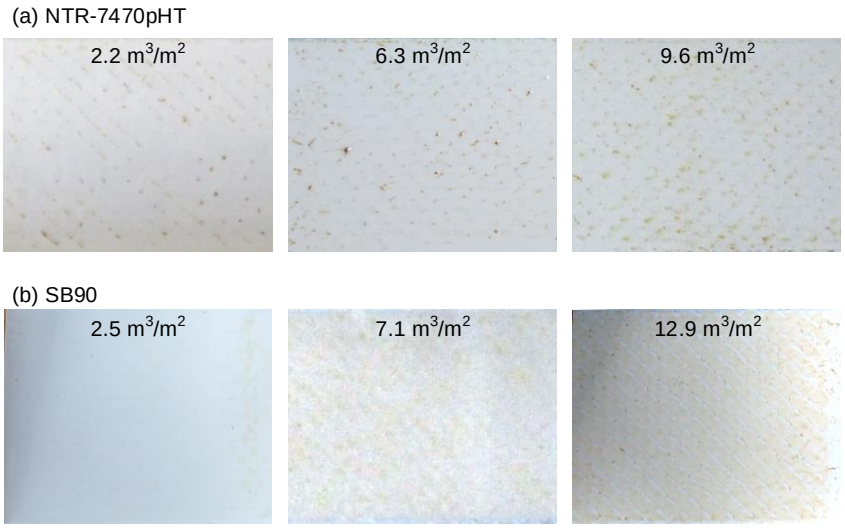

Figure 7.4: Photos of fouling development during experiment at the swimming pool B. Numbers on the top of the pictures represent the specific permeate volume in m^3/m^2.

Specific mass of key foulant constituents over membrane area was correlated with the fouling development and shown in Figure 7.5. In figure (a) organic fouling of NTR-7470pHT reached the maximal level after a permeate volume of 2.2 m^3/m^2 within 3 days and stabilized without further development, indicating the adsorption mechanism of organic foulants and the major factor for permeability decline. Further slight flux decline was probably attributed to Al and Fe accumulation. Figure (b) primarily demonstrated the vigorous accumulation of Fe on SB90, which corresponds to what was observed in the photos above. More severe Fe deposit on SB90 compared to NTR-7470pHT

might be attributed to the higher salt rejection of SB90. However, the increased Fe deposit didn't lead to further flux decline of SB90.

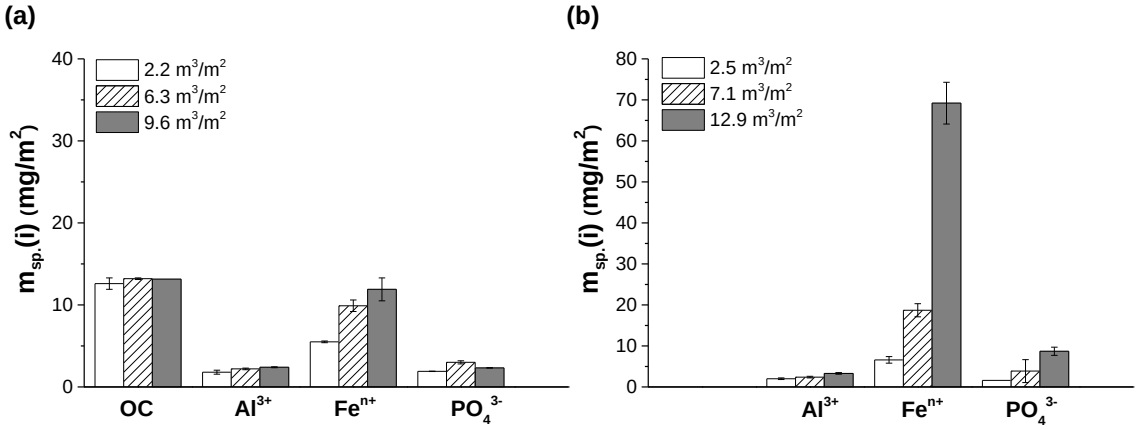

Figure 7.5: Specific mass ($m_{sp.}$) of key constituents in fouling deposits at the swimming pool B and the development with permeate volume: (a) NTR-7470pHT, (b)SB90.

7.2 Autopsy study of the pilot plant with chlorine resistant NF membrane

A front module (SB90) from the pilot plant, which was for 17 months in operation (approx. 2 years with two 4-month summer pauses), was autopsied. SB90 is chlorine resistant (1 mg/L) so free chlorine was not quenched in the feed (0.2 mg/L) during operation. The key parameters of feed properties are described in Chapter 6, Table 6.1.

7.2.1 Permeability profiles

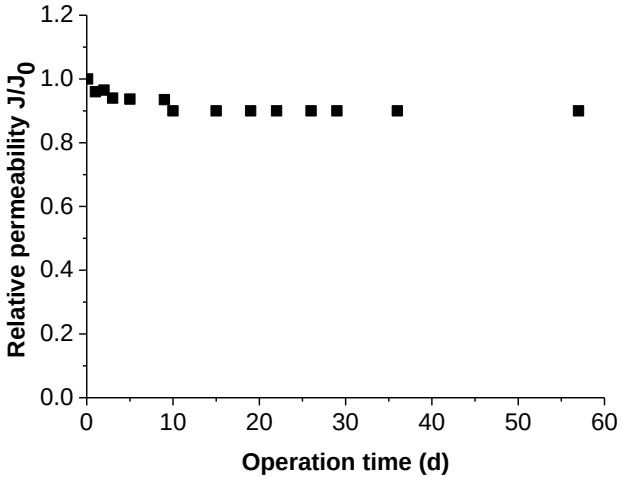

Figure 7.6: Relative permeability J/J_0 of the pilot NF plant using chlorine-resistant membrane SB90 over operation time for the first 60 days.

The chlorine-resistant membranes generally exhibited low permeability, accounting only 20–30% of which for TFC polyamide NF membranes. Material and production process has much higher influence than MWCO on permeability. At the beginning the averaged permeability of three SB90-4040 modules in the pilot-plant was 1.9 L/(h·m^2·bar). Relative permeability J/J_0 of the pilot NF plant using

SB90 for the first 60 days operation (Figure 7.6) showed a quick decline of permeability in the first three days followed by a stabilized profile, which can be expected from adsorption of organic substances. The relative permeability remained around 90% for the first two months and was not followed up during further operation period.

7.2.2 Constituents of fouling deposit and the distribution

Dry mass (dried at 110 °C) of fouling deposits in the three zones along the flow direction were 0.8, 0.8 and 0.6 g/m^2 respectively, with a high standard deviation of 0.5 g/m^2. On one side the high deviation indicated the heterogeneously distributed fouling deposits regarding small membrane areas. On the other side the little difference among three zones indicated a relatively even distribution along the flow direction in the membrane module.

Table 7.3: Constituents of fouling deposit on SB90 from the pilot plant experiments at the swimming pool A. $m_{sp.}$ is specific mass of each constituents over membrane area. Results are presented as mean value ± standard deviation calculated from triplicate analysis.

Parameter	Feed (n = 14) (mg/L)	$m_{sp.}$(i) (mg/m^2)			$m_{sp.}$(i) over feed concentration (mg/m^2)/(mg/L)
		Front	Middle	End	Range of three zones
Al^{3+}	0.017	0.5 ± 0.2	0.5 ± 0.1	0.4 ± 0.1	23–31
Ba^{2+}	0.109	0.9 ± 0.5	0.7 ± 0.2	0.3 ± 0.1	3–9
Ca^{2+}	103	48 ± 18	42 ± 11	45 ± 16	0.4–0.5
Fe^{n+}	0.012	0.12 ± 0.03	0.13 ± 0.01	0.20 ± 0.09	7–12
Na^{+}	21.6	2.1 ± 0.3	2.4 ± 0.4	2.3 ± 0.4	0.1
Cl^{-}	75	6.2 ± 0.2	6.6 ± 0.6	7.9 ± 0.8	0.1
P*	< 0.1	1.2 ± 0.6	1.0 ± 0.1	1.1 ± 0.3	> 10
PO_4^{3-}	0.2	1.7 ± 0.2	1.1 ± 0.2	1.4 ± 0.7	6–7
SO_4^{2-}	202	18.5 ± 0.7	20.2 ± 1.7	23.1 ± 4.9	0.1

* Phosphorous was measured as element P.

Table 7.3 summarizes the constituents of fouling deposit on SB90. Specific mass ($m_{sp.}$) over membrane area in three zones and the accumulation ratio ($m_{sp.}$ over concentration of each constituent in feed) for the total range of three zones were calculated. The same as the dry mass, along the flow direction no significant trend was observed. Easy soluble Na and Cl^- were set as reference element and the ratio higher than them (0.1 (mg/m^2)/(mg/L)) indicates the enrichment. As expected there was no SO_4^{2-} scaling, which has a ratio of 0.1. While the specific mass of Al, Fe and P in fouling deposits were low compared to other constituents, the enrichment ratio were the highest among inorganic constituents because concentration in feed were very low. A little Ba^{2+} also seemed to precipitate. It has to be noticed that the enrichment of total P is higher than of P from phosphate, probably coming from phospholipid in the retained bacteria on the membrane or the accumulated antiscalant.

Table 7.4: Comparison of organic carbon in different positions of SB90.

	Organic carbon (mg/m^2)		
	Front	Middle	End
Scrapped fouling deposit	388 ± 54	446 ± 69	661 ± 135
Spacer	380 ± 53	424 ± 66	463 ± 24
Sum	768	870	1124

Organic carbon in samples of scrapped fouling deposit and spacer were compared in Table 7.4. As mentioned previously, fouling layer on SB90 couldn't be extracted directly together with the membrane because the cellulose acetate material hydrolyzes during alkaline extraction. Therefore only fouling deposits scrapped off the membrane and in the spacer were extracted and analyzed. However, it's to be noticed that due to the smooth membrane surface there was almost no fouling layer left visible on the membrane after scrapping. Compared to total dry mass and elemental constituents in Table 7.3, in general, organic matters dominated in the fouling deposits. Extracted fouling deposit which was scrapped off from the membrane gave an organic carbon content of 388−661 mg/m^2 in three zones. Since the DOC in feed was 2.2 mg/L, organic carbon had an accumulation ratio of 176–300 (mg/m^2)/(mg/L). Almost half of the foulants were attached to the feed spacer. Organic foulants scrapped off the membrane and attached to the feed spacer showed no significant trend from inlet to outlet. Although the mean values out of triplicate measurements and the sum of two positions showed there might be an increase of the organic content from inlet to module outlet, the high standard deviations makes a difficult evaluation of the fouling development inside the module. The dry mass remained similar and the organic constituents increased from inlet to outlet, indicating that the proportion of organic fouling deposit probably became higher in the end zone, because particles or colloids such as aluminium hydroxides deposit preferably near the inlet, making the organic proportion lower.

7.2.3 CLSM analysis

Representative CLSM images from at least five measurements for each zone (front and middle) were shown in Figure 7.7. Large quantities of bacteria were observed especially in the front zone, which could come from the pretreatment. CLSM analysis showed that in general the fouling was heterogeneously distributed.

Most bacterial cells were associated with EPS glycoconjugates, sometimes could be nicely seen by the overlay of two constituents with yellow color. Filaments of bacteria were prevalent. Filamentous fungi with around 2 µm diameter and up to 200 µm length were as well observed. EPS formed heterogeneous layer out of small clusters up to 7 µm in diameter. There were also a few filamentous structures of EPS present, probably was EPS which surrounded the filaments of bacteria, which is inferred based on the same size.

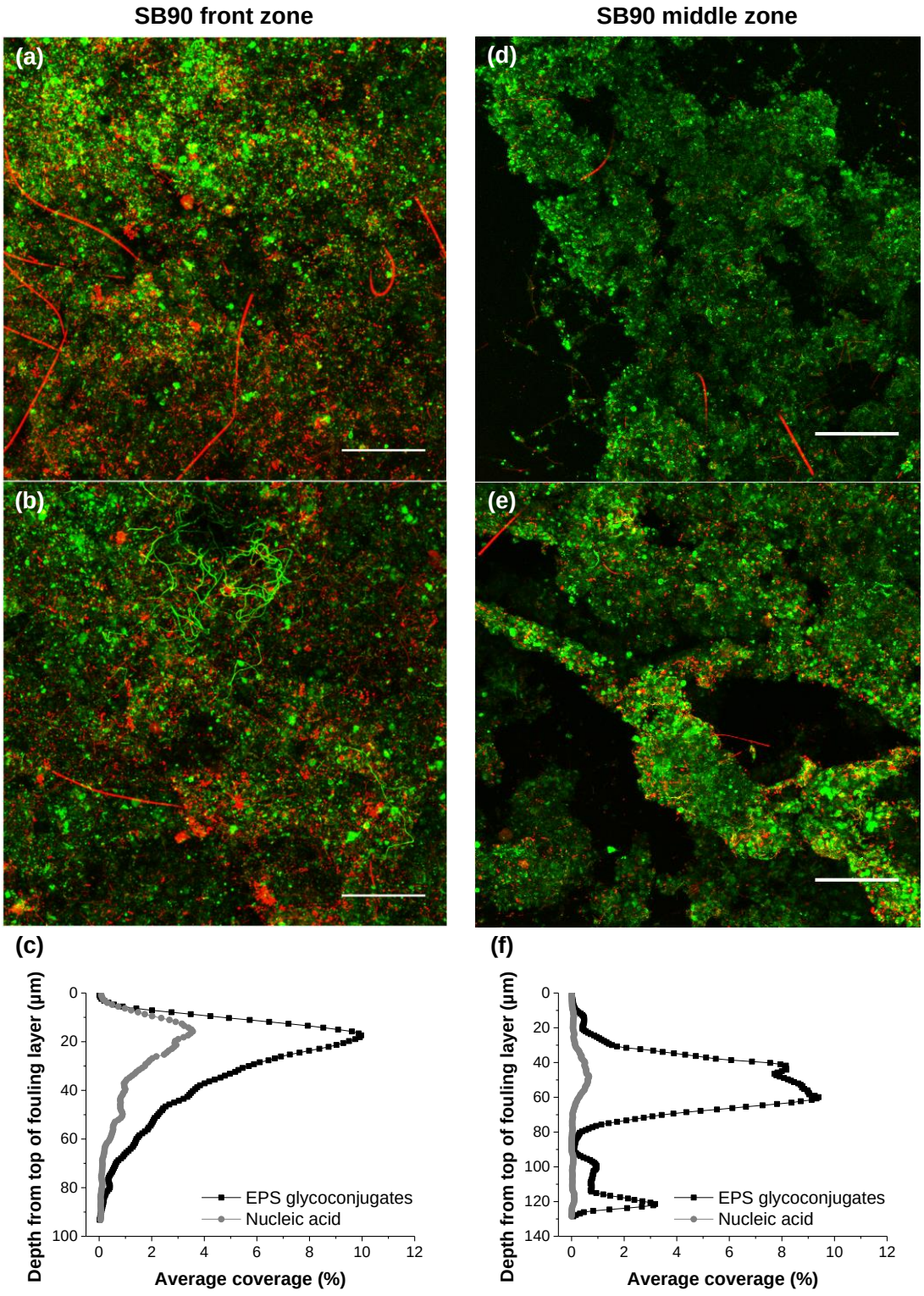

Figure 7.7: CLSM images of fouled SB90 after 17 months operation at the swimming pool A. (a) and (b): front zone; (d) and (e): middle zone; (c) and (f): quantification of average coverage. EPS glycoconjugates (green) and nucleic acid (red) were stained to present EPS and bacteria. The field of view was 266 × 266 µm^2. The scale bars correspond to 50 µm. Feed water was UF-pretreated backwash wastewater of UF membrane (free chlorine 0.2 mg/L).

By quantification of pixels it showed that the amount of EPS didn't change significantly along the flow direction. In contrast, the amount of bacteria became much less in the middle zone than in the

front zone. Different growth rate/stage of bacteria may lead to different EPS:cell ratio (Staudt et al., 2004). Nevertheless, it has to be noted that not specifically EPS in biofilm but all glycoconjugates in organic matters inclusive polysaccharides were stained (Neu et al., 2001). Therefore it can be assumed that also polysaccharides, which are prone to foul the membrane as organic fouling, were present in the fouling layer. Higher attachment of bacteria in the front zone in the spiral wound module can be attributed to higher drag force in the inlet, which decreases along the filtration channel (Heffernan et al., 2014). The profiles of surface coverage of EPS and bacteria along the biofilm depth corresponded with each other in the front zone, which indicated an active biofilm. In contrast, in the middle zone half of the selected spots showed much weaker correlation between EPS and bacteria profiles. The mismatching profiles indicate minor growth of bacteria compared to that in the front zone, where biofouling mainly occurred.

In swimming pool water most bacteria were supposed to be killed by chlorine. However, the CLSM images showed clear evidence of biofilm, at least in the front zone. Feed water of the pilot plant contained lower free chlorine (0.2 mg/L) than the pool water. This concentration level was not able to prevent the membrane from biofouling. The regulatory range of free chlorine in swimming pool water is 0.3–0.6 mg/L in Germany. Nevertheless, the presence of living bacteria in chlorine-containing water has been reported (Amagliani et al., 2012, Uhl et al., 2005). Therefore, even though chlorine resistant membrane is applied without quenching chlorine in feed water, biofouling seems to be inevitable in swimming pool water treatment. This can be attributed to the intrinsic properties of pool water such as various dissolved organic matters including easy biodegradable substances and the high water temperature.

7.2.4 Surface characterization

SEM images of fouled SB90 in the three zones along the flow direction are shown in Figure 7.8. The images underline the presence of fouling layer on the three zones of whole module. But some areas which are covered by little or very thin fouling layer were also observed. The amorphous fouling layer was heterogeneously distributed, which explained the high deviation of extraction results from small pieces of membrane samples. It presented a characteristic organic fouling structure. At those parts with thick fouling layer C and O were dominant, both belonging to the organic fouling layer and the membrane material. Ca was also found in the fouling layer but little inorganic structures could be observed on the membrane or in the fouling layer, which indicates that Ca came from the dried feed water. Some colloid-like structures in combination of organics (end zone) was observed. At those mixed structures of colloids and organics, barium, iron, aluminium and silicon were found by EDX, which corresponds to the analysis of constituents with ICP-OES. In Figure (a) some oval particles with a diameter of around 10 µm are shown, which were also observed often all over the module. They were found totally or partly embedded in the fouling layer. Based on the uniform and regular shape, they are suspected to be anthropogenic input. EDX results indicated that they mainly composed of P,

C, Ca and O. The contribution of anthropogenic input such as personal care products to the fouling layer is also possible. Although bacteria were observed with CLSM, they were hardly recognized with SEM. Probably because the volume of EPS was much higher than that of bacteria so compared to organic foulants bacteria themselves were not the major community. And the majority of bacteria were embedded within a biofilm matrix, which cannot be easily seen with surface observation using SEM.

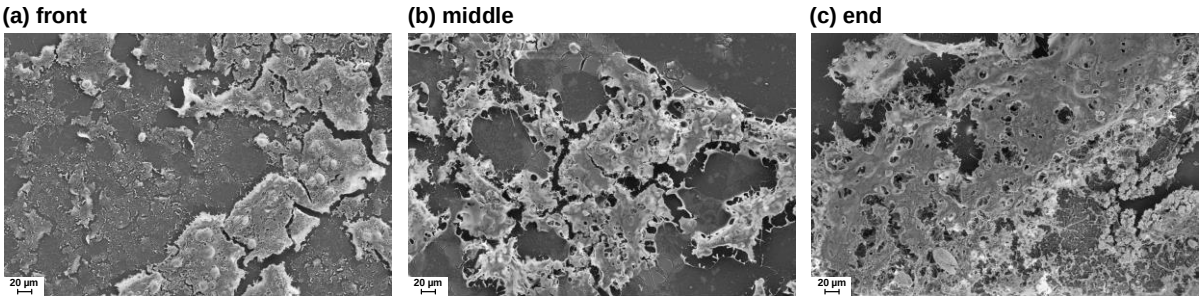

Figure 7.8: SEM images of fouled SB90 in the zones (a) front, (b) middle and (c) end along the flow direction.

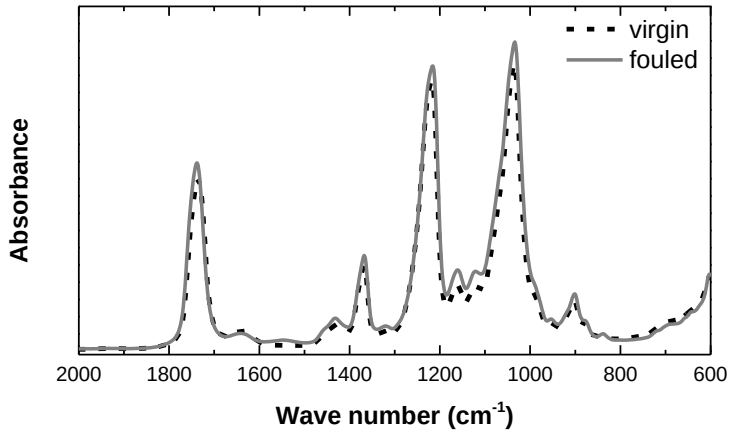

Figure 7.9: ATR-FTIR spectra of virgin and fouled SB90 in pilot plant.

Infrared spectroscopy was measured to determine the functional groups of possible foulants. In comparison to the spectra of the virgin membrane as a reference (Figure 7.9), no significant change can be distinguished when comparing the featured peaks. It seems the amount of fouling layer was too little to overcome the signals from the original membrane.

Table 7.5: Zeta potential and contact angle of fouled SB90 in three zones compared to new SB90.

	Zeta-potential (mV)	Contact angle (°)
Front	-17 ± 3	71 ± 5
Middle	-18 ± 3	63 ± 4
End	-18 ± 3	63 ± 6
New membrane	-11 ± 3	59 ± 4

Zeta potential and contact angle were measured (Table 7.5). Zeta potential here was measured with the original feed water from the swimming pool. Fouled membrane generally presented only slightly more negative charge than new membrane, probably due to the deposition of negative humic substances which came originally from the tap water. Membrane became more hydrophobic after fouling due to the deposition of hydrophobic organic foulants. The front zone seemed to be slightly more hydrophobic than the rear zones.

7.3 Autopsy study of a full-scale NF plant

A front module and a rear module (NF90) from the full-scale plant, which was for 8 months in operation, were autopsied. NF90 is not chlorine resistant (< 0.1 mg/L) so free chlorine was quenched in the feed during operation. The key parameters of feed properties are described in Chapter 6, Table 6.2.

7.3.1 Permeability profiles

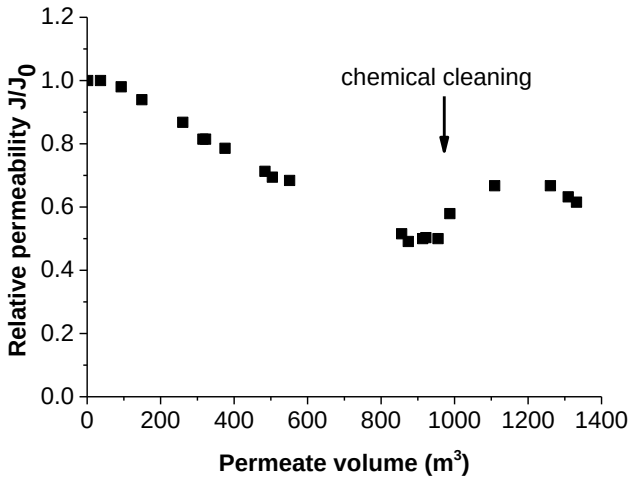

Figure 7.10: Relative permeability J/J_0 of the full-scale nanofiltration plant over produced permeate volume during 8 months operation time.

As expected, NF90 has much higher permeability than SB90. At the beginning the averaged permeability of ten NF90-4040 modules in the full-scale plant was 6.6 L/(h·m^2·bar). Relative permeability J/J_0 during the eight months operation was calculated over the produced permeate volume during 8 months (Figure 7.10). Permeability of the membrane modules continued to decline during operation, which was nearly in a linear correlation with the produced permeate volume. After 6 months the permeability has lost 50%. Chemical cleaning using alkaline surfactants (pH = 12) was carried out, which only brought the relative permeability back to about 67%. The low efficiency of chemical cleaning indicated that the fouling deposit was difficult to remove.

7.3.2 Constituents of fouling deposit and the distribution

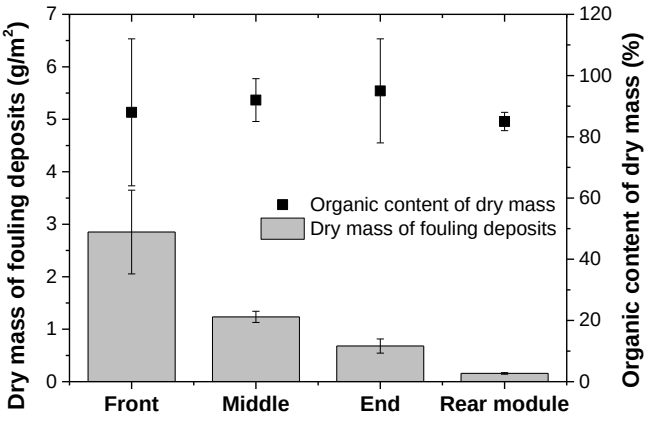

Figure 7.11: Dry mass of fouling deposits and the organic content of dry mass of fouled NF90 in three zones of the first module and in the rear module.

As shown in Figure 7.11, dry mass which means the scrapped fouling deposits after drying at 110 °C ranged from 0.7 to 2.9 g/m^2 in different zones of the first module. Dry mass decreased significantly in the flow direction, which were only 0.16 g/m^2 in the rear module. Compared to the fresh deposits, water content was 90–93%. Mass loss after ignition at 550 °C revealed that the fouling deposits were predominantly organics, accounting for more than 80% of the dry mass. The proportion of organic content remained similar in different zones and the rear stage.

Elemental analysis was carried out for the scrapped fouling deposits from a large area (≈ 0.5 m^2), which showed the fouling deposits contained a large amount of C accounting for 42.7% ± 2.3%, with H for 6.5% ± 0.5%, N for 7.5% ± 0.2%, and S for 2.4% ± 2.5%. The same kind of analysis was carried out for fouling in seawater desalination that had a composition of 30% in C, 5% in H, 4% in N, 1% in S and 0.7% in P, where the deposits were linked to biofilm (Mondamert et al., 2009). Another study with surface water for NOM fouling in bench-scale experiments resulted in a composition of 22% in C, 4% in H, 1% in N and 73% in O, S and ashes, loss on ignition 63% (Gorenflo, 2003). The fouling deposits in this study contain higher content of C compared to these studies. As the fouling deposits composed mostly of organics, the main source of C should be organic fouling or biofouling.

Table 7.6 summarizes the constituents of fouling deposit on NF90. The specific mass of most constituents decreased along the flow direction. In the rear module the specific mass of constituents was approximately one tenth of it in the front module. That can be explained by the decreasing trend of fouling deposits along the flow direction, which corresponds to the dry mass measurements. The same as previously, Na^+ and Cl^- were set as the reference for the accumulation ratio. The deposits contain a significant amount of aluminium which is probably a residual of the coagulant in the pretreatment. Mondamert et al. (2009) also reported that after pretreatment flocculants iron was still found in membrane fouling. The relatively higher concentration of P in feed water than in the pool water is attributed to the phosphonate content in the antiscalant. P had the highest accumulation ratio

but the majority couldn't be measured as PO_4^{3-}, which may be organically combined. Interestingly, easily soluble element K^+ was enriched. Biofouling may be the explanation because K^+ and P are both essential nutrients for microorganisms. The constituents Na^+, Cl^- and SO_4^{2-} which were not accumulated also showed decreasing trend, because they were adsorbed not only in the membrane matrix but also in the fouling layer which decreased significantly along the flow direction.

Table 7.6: Constituents of fouling layer on full-scale plant NF90.

Parameter	Feed (n = 16) (mg/L)	$m_{sp.}$(i) (mg/m^2)			$m_{sp.}$(i) over feed concentration (mg/m^2)/(mg/L)
	Mean ± SD	Front	Middle	End	Range of three zones
Al^{3+}	0.023	0.5 ± 0.1	0.5 ± 0.3	0.4 ± 0.2	17−22
Ba^{2+}	0.101	0.15 ± 0.02	0.14 ± 0.02	0.12 ± 0.03	1.2−1.5
Ca^{2+}	97	88 ± 25	72 ± 6	54 ± 9	0.6−0.9
Fe^{n+}	< 0.01	0.06 ± 0.01	0.05 ± 0.01	0.06 ± 0.03	> 5
K^+	3.1	12.7 ± 0.3	9.6 ± 0.8	7.0 ± 0.4	2−4
Na^+	24	3.1 ± 0.2	2.9 ± 0.3	2.0 ± 0.2	0.1
Cl^-	52	7.6 ± 0.4	7.5 ± 0.1	4.9 ± 0.5	0.1
P*	0.20	12.5 ± 1.7	10.6 ± 2.0	7.0 ± 3.7	35−63
PO_4^{3-}	3.0	5.4 ± 0.7	5.5 ± 0.7	6.9 ± 0.5	2
SO_4^{2-}	207	18.0 ± 0.5	16.3 ± 1.1	13.7 ± 2.5	0.1

* Phosphorous was measured as element P.

Table 7.7: Comparison of organic carbon in different positions of NF90.

	Organic carbon (mg/m^2)			
	Front	Middle	End	Rear module
Fouled membrane	248 ± 40	155 ± 20	126 ± 16	43 ± 2
Scrapped fouling deposit	160 ± 48	108 ± 56	83 ± 48	19 ± 1
Scrapped membrane	204 ± 60	111 ± 20	75 ± 26	36 ± 2
Spacer	132 ± 30	41 ± 19	33 ± 20	6 ± 1
Sum	744	415	317	104

Organic carbon in different positions of NF90 samples was compared in Table 7.7. As expected from the previous analysis, a general decreasing trend is presented. Fouling deposits are separated into different parts in different positions due to autopsy analysis. The largest part remained on the membrane. In contrast to SB90, foulants attached to the feed spacer were a small part and large amount of deposits remained on the scrapped membrane. Nonporous high pressure membranes such as in NF and RO undergo surface fouling only. However, highly rough surface of NF90 provided more barriers for fouling deposition which makes a complete scrapping of fouling deposits very difficult.

7.3.3 CLSM analysis

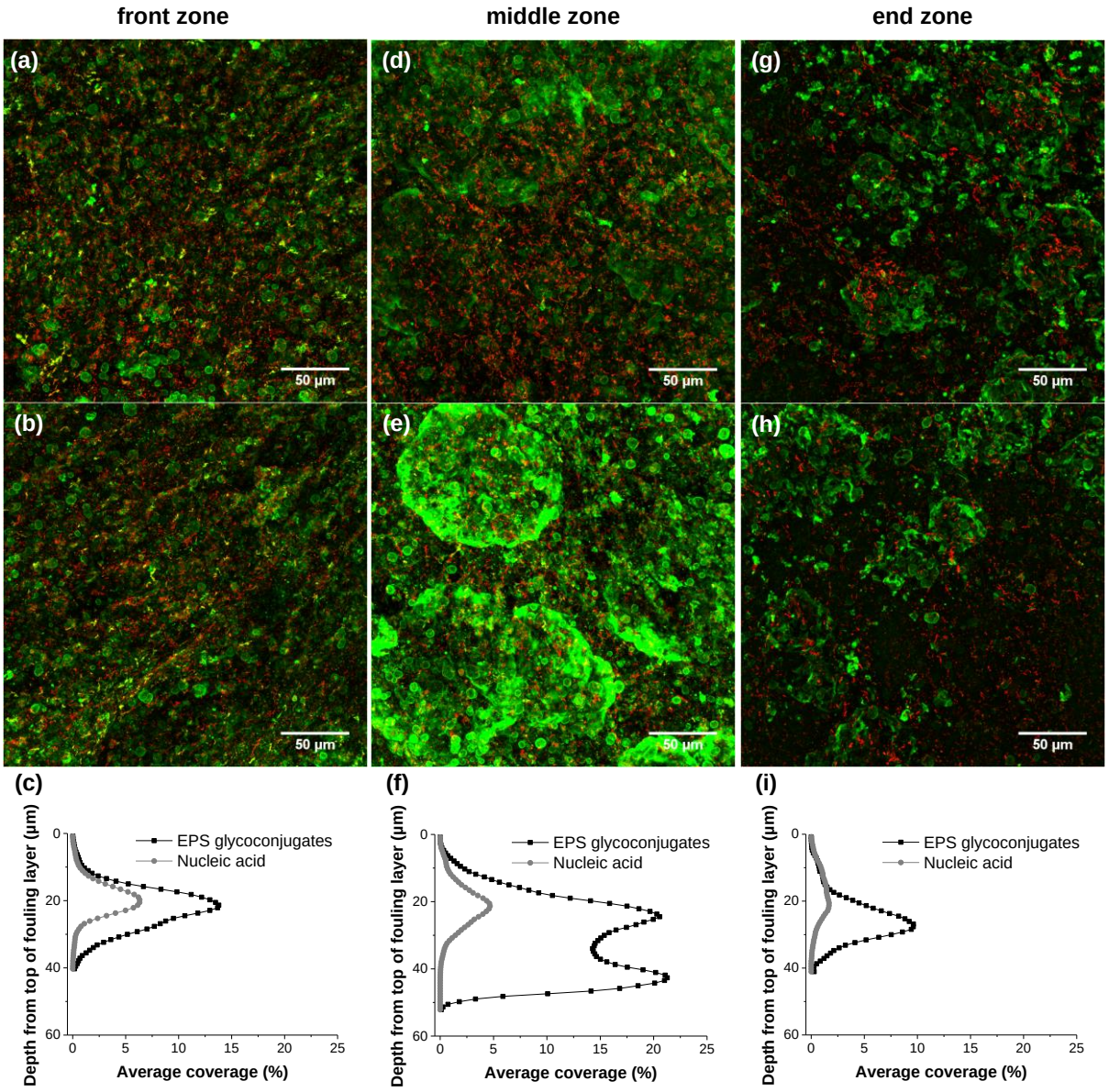

Figure 7.12: CLSM images of fouled NF90 after 8 months operation in the full-scale plant at the swimming pool A. (a) and (b): front zone; (d) and (e): middle zone; (g) and (h): end zone; (c), (f) and (i): quantification of average coverage. EPS glycoconjugates (green) and nucleic acid (red) were stained to present EPS and bacteria. The field of view was 266 × 266 µm^2. The scale bars correspond to 50 µm. Feed water was UF-pretreated swimming pool water and free chlorine was quenched.

Large quantities of bacteria and EPS were observed on NF90 using CLSM (Figure 7.12), although the pretreatment UF with 0.02 µm was supposed to remove all bacteria. A possibility is that the new membrane modules and the NF plant are commonly not sterilized before the operation, which could provide the initial source of bacteria. Besides, the impurity in the antiscalants or bisulfite could also be the initial source of bacteria. Although live or dead cells were not distinguished, the abundance of bacteria and structure demonstrated the presence of biofouling. Generally bacteria and EPS were evenly distributed within each zone across the fouling layer. Bacteria were mostly with rod or cocci morphology. Quantification of the average coverage showed that EPS was much more abundant than

microorganism according to the intensity variations with the distance of biofouling layer. Some single cells were found, but most occurred in clusters. Large amount of EPS was found as spherical form of 5–10 µm, especially in the front zone, probably from small protists (2–20 µm) or other organisms in higher order than bacteria. From the middle to the end zone some aggregated EPS clumps of around 50–100 µm were observed. In the end zone the amount of bacteria became less.

7.3.4 Surface characterization

Representative SEM images of fouled NF90 are presented (Figure 7.13). Front zone was fouled most intensely that the consistent fouling layer completely covered the rough membrane surface. Fouling decreased along the flow direction in the membrane module, which is shown by the less consistent fouling layer became small pieces. In the amorphous fouling layer a few precipitate grains in size between 50 and 100 nm observed in the deposits were identified as dominantly C and O in a mixture of Si, Ca, P, and Al. It seemed these inorganic foulants were likely to form nano-scale colloidal particles.

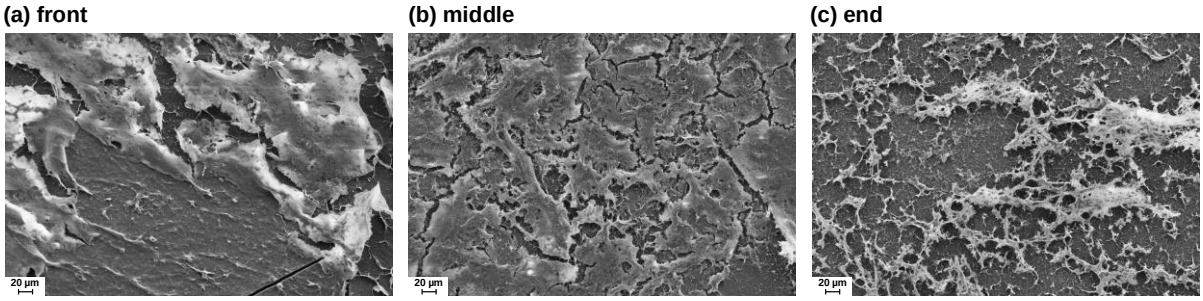

Figure 7.13: SEM images of fouled NF90 (front, middle and end).

Zeta potential here was measured with the original feed water (Table 7.8). Comparing to the zeta potential of new membrane measured in 10M KCl w2hich was -47.5 mV (Table 3.2), the zeta potential became less negative in pool water, probably because the presence of Ca^{2+} in pool water interacted with the negatively charged membrane and made the surface charge less negative. After fouling by pool water, no significant effect on the zeta potential was observed. In the first module, fouling increased the membrane hydrophobicity slightly. No significant trend along the flow direction in was observed. The first module was more hydrophobic than the rear module, which was almost the same as the new membrane because of the less fouling.

Table 7.8: Zeta-potential and contact angle of NF90

	Zeta-potential (mV)	Contact angle (°)
Front	-22 ± 1/-24 ± 2	67 ± 5
Middle	-21 ± 1	64 ± 4
End	- 21 ± 1	69 ± 4
Rear module	not determined	58 ± 2
New membrane	-19 ± 1	58 ± 3

ATR-FTIR spectra of the fouled membrane in the three zones were nearly the same. **S**pectra of the virgin and fouled (front zone) membranes are compared in Figure 7.14. Significant changes were observed after fouling. The amide I (1663 cm^{-1}) and aromatic amide (1609 cm^{-1}), main features from polyamide membrane was shield by a broader band in 1600–1700 cm^{-1} with the highest peak at 1635 cm^{-1}, which is mainly associated with C=O stretching of peptide linkages. The amide II (N–H bending, 1543 cm^{-1}) peak was still present. The broad polysaccharide bands in the region 950–1110 cm^{-1} were assigned to C–O–C and C–O–P stretching of carbohydrate-like substances or polyphosphates (Sari and Chellam, 2013, Sweity et al., 2015), which weakened the Ar–SO_2–Ar signals at 1107 cm^{-1} from the virgin membrane. The broad bands may include signals at 1048 cm^{-1}, revealing the C–O bonds associated with polysaccharides (Her et al., 2007). Strong signals in 600–900 cm^{-1} can be representative of aromatic compounds, which can also possibly arise from aromatic ring vibrations of various nucleotides and were considered as strong bacterial fingerprint region which suggested the biological origin of fouling (Howland, 1996). The prevalence of Ar–SO_2–Ar signals at 1240 cm^{-1}, individual C–C stretching (aromatic ring, 1585, 1487 and 1169 cm^{-1}) and the asymmetric O=S=O vibrations at around 1325 cm^{-1} for polysulfone layer underneath were weakened or shielded. The results indicate that proteins, polysaccharides and aliphatic and aromatic compounds were the major membrane foulants, possibly derived from organic or microbial matters.

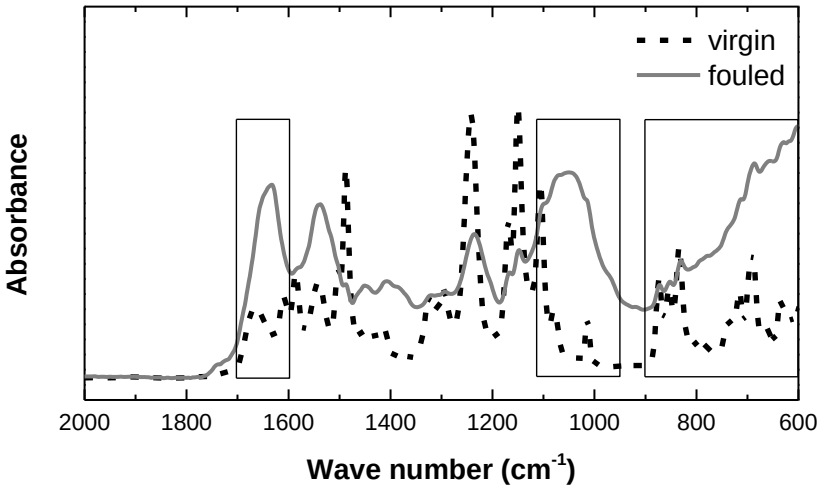

Figure 7.14: ATR-FTIR spectra of virgin and fouled NF90 in the full-scale plant at the swimming pool A. The band in 1600–1700 cm^{-1} with the highest peak at 1635 cm^{-1} is mainly associated with C=O stretching of peptide linkages. The broad polysaccharide bands in the region 950–1110 cm^{-1} were assigned to C–O–C and C–O–P stretching of carbohydrate-like substances or polyphosphates. Strong signals in 600–900 cm^{-1} can be representative of aromatic compounds, which can also possibly arise from aromatic ring vibrations of various nucleotides and were considered as strong bacterial fingerprint region which suggested the biological origin of fouling.

7.4 Discussion

SB90 (pilot plant) and NF90 (full-scale plant) faced very similar feed properties except the free chlorine and phosphorous content which was contributed by different antiscalants used. Fouling of

both membranes showed predominantly high organic content. Biofouling was evident in both plants with or without chlorine quenching. Inorganic fouling was significantly suppressed by antiscalant compared to the bench-scale experiments in which the recovery was even much lower.

Although the amount of fouling deposits on SB90 was not enough for elemental analysis, a higher proportion of organics for SB90 than for NF90 (> 80%) was expected from the less dry mass and more organic carbon contents. In autopsy studies in desalination water content accounted for 85–94% of fouling deposits and organic content accounted for 44–90% of dry foulants (Baker and Dudley, 1998, Farooque et al., 2009). Organic content in RO fouling by wastewater secondary effluent ranged from 44% to 87% (Kim et al., 2008, Raffin et al., 2012, Tang et al., 2014). The proportion of organic and inorganic content depends largely on the feed water properties.

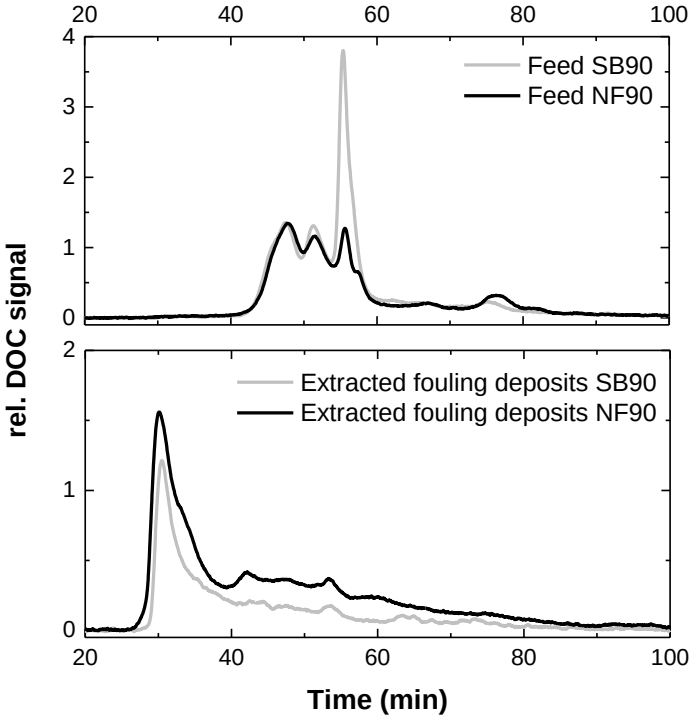

Figure 7.15: SEC-OCD results of feed water and extracted fouling deposits of SB90 (pilot plant) and NF90 (full-scale plant).

SEC-OCD chromatograms of two feed waters and dissolved fouling deposits on both membranes showed little difference (Figure 7.15). The high MW fraction was the major fraction, which is commonly defined as biopolymer fraction (t = 32 min) which includes compounds such as polysaccharides and protein (Huber et al., 2011). Although this biopolymer fraction can be hardly detected in feed water, it composed the major foulant for both membranes as the result of biofouling. These two tight NF membranes reject biopolymer and humic substances nearly completely. But a predominant accumulation was observed only for biopolymer, which indicates not only the preferential accumulation of biopolymer as foulants but also the biofouling origin of these biopolymers. The humic fraction (t = 40–50 min) was relatively only a minor composition. The last

fractions (t > 50 min) which contain low MW and hydrophobic molecules were not accumulated significantly. Two small peaks at t = 42 and 53 min were clearly seen on NF90 but not significantly on SB90.

Biofouling in SB90 and NF90 modules showed different characteristics. The average coverage of nucleic acids demonstrated more bacteria on NF90 than on SB90. EPS in 5–10 µm spherical forms were only observed on NF90. Organisms seemed to belong to higher order than bacteria and big EPS clumps were only observed on NF90 while filamentous structures were only observed on SB90. Bacteria clusters, filaments of bacteria and prevalent linked structures of bacteria and EPS on SB90 suggest the active biofilms which were producing EPS. The higher accumulation of K in NF90 also indicates that the biofilms on two membranes have different characteristics.

Almost all TFC membranes have much high surface roughness than CA membrane (Elimelech et al., 1997). Fouling by model biopolymers was found more sever on membrane with rougher surface (Li et al., 2007). However, (Baek et al., 2011) demonstrated that surface properties of RO membranes such as hydrophobicity, surface charge and roughness have no significant effects on biofouling. In comparison to surface roughness, feed properties such as chlorine concentration and assailants revealed higher influence. Under chlorine condition biofouling still existed on SB90. The ratio EPS:cells was even higher than on NF90. Probably because under the stress of chlorine bacteria tend to produce more EPS based on a protection mechanism against negative environment (Baker and Dudley, 1998). But after 17 months of operation the fouling dry mass on SB90 was less than on NF90. The low concentration of chlorine might have the control effect on biofilm. Another possible reason can be the different antiscalants applied. Chemicals introduced into the treatment process, such as impure acids or phosphate-based scale inhibitors, may also exacerbate biofouling. Antiscalants have already been reported to enhance biofouling (Sweity et al., 2013, Vrouwenvelder et al., 2000, Vrouwenvelder et al., 2010, Weinrich et al., 2013). Typically antiscalants consist of polycarboxylates, polyacrylates, polyphosphates and polyphosphonates. It's difficult to know the chemical composition of commercial antiscalants. Antiscalants often contain two or more phosphonate groups which are called polyphosphates, with the MW ranging from 1000 to 3500 g/mol. Phosphonates and phosphonic acids are organophosphorus compounds containing $C{-}PO(OH)_2$ or $C{-}PO(OR)_2$ groups (where R is alkyl or aryl). Phosphate containing chemicals provide an essential nutrient supply (Weinrich et al., 2013). In general, antiscalant degradation and assimilation by bacteria has not been clearly elucidated. Recently a comprehensive study showed polyacrylates and polyphosphonates containing antiscalant can enhance biofouling during RO filtration treating low organic content brackish water (Sweity et al., 2015). Polyacrylates alter the membrane surface properties and increase the bacterial adhesion, while polyphosphonates increase biofilm growth by providing the cells with phosphorous. Sweity et al. (2015) also indicated that polyacrylates causes more severe biofouling. The antiscalant used for NF90 contains both polyacrylates and polyphosphonates, while neutralized carboxylic and phosphonic acids

were present for SB90, which might be the reason for the more severe biofouling on NF90 than on SB90, as also expected by Sweity et al. (2015).

Scaling such as sulfate salts could be well suppressed by antiscalant. Inorganic constituents were measured in insignificant amount compared to the organic content. Among inorganic constituents, Al showed the highest accumulation ratio, probably as tiny colloids which were observed and associated using SEM and EDX. Phosphonate-based antiscalants have been reported to be ineffective to suppress the precipitation of aluminum silicates, where phosphorus from antiscalants can react with aluminium to form precipitates (Gabelich et al., 2005). Another study indicated that strong interactions between anionic humates and phosphates is possible in the presence of metal ions such as Al^{3+} that act as cationic ‘‘anchors (Riggle and von Wandruszka, 2005). Another autopsy study in brackish water treatment with low hydrogen carbonates concentration and 12 mg/L TOC showed amorphous matrix organic–Al–P complexes (Tran et al., 2007). Fe accumulated on both membranes. There is yet no specific pretreatment against Fe. Nevertheless, these inorganic accumulations are insignificant in comparison to a scaling problem.

The accumulation ratio of Ca^{2+} is similar for both membranes and in different zones. The ratio between OC and Ca^{2+} kept similar on different zones. In the presence of OM, Ca^{2+} plays an important role in organic conditioning and subsequent biofouling in NF (Zhao et al., 2015). It can be suggested that Ca^{2+} can be adsorbed with pool water as ion in the membrane polymer matrix and fouling layer or accumulated as a complex with organic substances, which was also suggested by Saravia et al. (2013). Besides, Ca can be accumulated also in biofilm (Mañas et al., 2011), which was shown by biologically induced precipitation of phosphorus as hydroxyl-apatite ($Ca_5(PO_4)_3(OH)$) in the core of granular sludge. Ca^{2+}, and to a lesser extent Mg^{2+}, accumulate within the biofilm matrix and act as cross-linking agents in EPS production within the biofilm (Applegate and Bryers, 1991). EPS formation rate in the biofilm was unaffected by calcium concentration (Turakhia and Characklis, 1989). The partner of Ca^{2+} precipitation here was not SO_4^{2-} or CO_3^{2-}. The only possible anion found accumulated was PO_4^{3-}. But the amount of Ca^{2+} was much higher than PO_4^{3-}. More importantly, on NF90 along the flow direction Ca showed clearly decreasing trend, while PO_4^{3-} increased. Therefore, biofilm and organic fouling complex should be responsible for Ca^{2+} accumulation.

After 17 months of operation, fouling deposits on SB90 relatively evenly distributed along the flow direction, while fouling on NF90 after 8 months of operation showed the decreasing trend along the flow direction. The rear module of NF90 had minor fouling which could be further used. However, based on the development from rapid to long-term biofouling, with longer time period this decreasing trend on NF90 tend to be less and a more evenly distribution is expected.

7.5 Summary

Fouling behavior of NF membranes was studied for the first time in long term and in large scale for swimming pool water treatment. A cellulose acetate membrane SB90 in a pilot plant and a polyamide membrane NF90 in a full-scale plant were respectively applied with highly similar feed waters. Autopsy studies showed that the decline of membrane permeability was mainly due to accumulation of organics and biofilms on the membrane. The foulants identified were mainly biopolymers including protein- and polysaccharide-like substances. A concentration of 0.2 mg/L chlorine in feed water of the pilot plant could not avoid biofouling but might influence the biofilm formation, which was shown by different morphology and composition of biofilm on two membranes. Antiscalant with polyacrylates and polyphosphonates might enhance biofouling and different antiscalants may have different extents of enhancement. Inorganic fouling played a minor role in this study. Al was found the most accumulated, probably from the flocculation pretreatment. The applied accumulation ratio of constituents in $(mg/m^2)/(mg/L)$ as the mass over membrane area and concentration in feed served as a valid and appropriate approach for evaluation of the key fouling constituents.

In summary, NF membrane fouling by swimming pool water, which has low hydrogen carbonate, high temperature and high DOC of NOM and anthropogenic input, has low scaling potential but is dominated by biofouling in combination of organic fouling. The results enable to choose the appropriate cleaning method for fouling under swimming pool water condition.

8 Conclusions and outlook

This dissertation aimed to investigate the application potential of NF for swimming pool water treatment. For a better understanding of the formation of DBP and therefore an appropriate treatment, pool water quality was continuously intensively studied for several months and a simple method for calculating THM concentration in real pool water system was established. The successful simulation supported the observed positive correlation between DOC and THM with a time delay of 2 days, which indicated a possible minimization of DBP by quick removal of the precursors using NF. For the first time NF was integrated in a real swimming pool water system as a branch current for the mainstream treatment. Long-term operation showed that NF reduced DBP and the precursors in pool water. As an indispensable aspect, fouling behavior of NF membranes in swimming pool water treatment was thoroughly investigated through bench-scale experiments in different water qualities and autopsy studies after realistic long-term operation. Results showed in swimming pool water NF membrane was dominated by biofouling in combination with organic fouling.

8.1 THM in swimming pool water

In a public indoor swimming pool water was sampled daily for three months to analyze the water quality with focus on organic load and DBP formation. The formation of THM in pool water showed a clear positive correlation to DOC with a time delay of two days. This time delay should depend on the pool water treatment process. The major part of THM formation takes two days in the case of conventional swimming pool treatment process which cannot remove DOC. DOC proved to be a suitable parameter for precursor to predict THM production, while the number of visitors is not reliable to estimate the organic load brought into water and to predict THM formation due to different behaviors of visitors. For the first time a simple simulation based on mass balance for predicting the THM concentration in indoor swimming pool water was developed. In the simulation, production of THM from reaction of DOC and chlorine, loss into air and elimination by pool water treatment were considered. The simulated results were generally in good agreement with measurements in reality and in good compliance with published characteristics. Thereby, one step towards the prediction of THM in swimming pool water is provided. The unknown variance of DOC characteristics and activities of visitors contributed to the deviation between measurement and simulation. The method can be used to estimate THM concentration under real indoor swimming pool water conditions with a reduced amount of data required, and practically be useful in conducting health-related risk assessment concerning exposure to DBP and in estimating infrastructure needs for upgrading treatment facilities. The production of THM from DOC is slow compared to a typical turnover rate of swimming pool water. Therefore, a quick removal of organic precursors through pool water treatment could be an effective way to minimize the THM production.

8.2 Minimization of DBP in swimming pool water

Carefully designed laboratory experiments using dead-end filtration were carried out to study the THM rejection by three NF membranes of different materials. Each experiment took six days for a comprehensive evaluation of the rejection properties including the effects of adsorption and fouling on rejection. NF has actually limited rejection of THM (max. 30–50%) despite the contradictory results reported in literature. Large extent of THM adsorption to membrane leads to severe overestimation of rejection in short term experiments. Adsorption has significant influence on rejection mechanism, facilitating the mass transport of THM through NF membrane. Membrane material plays a substantial role in the intrinsic adsorption capacity and consequently has the impact on rejection. Occupation extent of the available adsorption capacity in the membrane plays a significant role due to the fact that adsorption facilitates the transport of molecules through the membrane and thus decreases membrane rejection. Competitive adsorption among THM was observed. NOM in feed solution and organic fouling layer had little effects on THM rejection. Organic fouling lowered the adsorption of less adsorptive THM due to blocking of the membrane surface.

Given the fact that the direct THM rejection by NF is low, application of NF in swimming pool water treatment contributed merely to the elimination of DOC and AOX, leading to a high elimination of the DBP precursors. For the first time NF was integrated in a real swimming pool water system in a pilot-plant for the backwash wastewater treatment and in a full-scale plant as a branch current for the mainstream treatment. Chlorine-resistant NF membrane of cellulose acetate (SB90) fulfilled sufficient rejection performance for 17 months under pool water condition with 0.2 mg/L free chlorine present in feed water. By quenching chlorine in advance the polyamide (non-chlorine resistance) NF90 membrane endured excellent rejection performance in 8 months operation. Compared to the original treatment process PAC+UF, integration of a branch current NF treatment for 1.3% of the mainstream could reduce the general level of DBP and the precursors (30% in AOX- and 18% in DOC-reduction) as well as the DBP reactivity (35% in THMFP/DOC- and AOXFP/DOC-reduction) in swimming pool water. Results implied the feasibility of minimizing DBP formation by quick removal of DBP precursors from the pool water. Long-term onsite experiments at a real swimming pool demonstrated a realistic option of an efficient treatment, which provided a better pool water quality with only marginally increased fresh water consumption compared to the original treatment PAC+UF.

8.3 Fouling of NF membrane in swimming pool water treatment

Fouling is an essential aspect when considering the realistic application especially in the long run. Swimming pool water has low bicarbonate concentration, high temperature and high DOC of NOM and anthropogenic input. And there is almost no information available about fouling formation under these conditions. Fouling behavior of NF membranes in swimming pool water treatment was thoroughly investigated onsite through bench-scale experiments in different water qualities and autopsy studies after realistic long-term operation. A polyamide membrane and a cellulose acetate

membrane were applied with similar feed waters with chlorine quenched or not. Autopsy studies showed that the decline of membrane permeability was mainly due to accumulation of organics and biofilms on the membrane. The foulants identified were mainly biopolymers including protein- and polysaccharide-like substances. A concentration of 0.2 mg/L chlorine in feed water could not avoid biofouling but might influence the biofilm morphology and composition. Antiscalant with polyacrylates and polyphosphonates might enhance biofouling. Among the little inorganic foulants, Al was found the most accumulated, probably from the flocculation pretreatment. The applied accumulation ratio of constituents in $(mg/m^2)/(mg/L)$ as the mass over membrane area and concentration in feed served as a valid and appropriate approach for evaluation of the key fouling constituents. In summary, NF membrane in swimming pool water treatment has low scaling potential but is dominated by biofouling in combination of organic fouling. The results enable to choose the appropriate cleaning and pre-treatment method for fouling under swimming pool water condition.

8.4 Outlook

Although DBP have been of research interest for decades and considerable work has been done, there are still areas remained to be further investigated. Modelling of DBP has been primarily in drinking water. Complex mathematical models for DBP which give an accurate prediction in swimming pool water can be of great interest.

Despite that the general level of DBP was reduced by integrating NF in swimming pool water treatment, minimization of THM was not significant. Probably higher share of NF branch current is worth further investigation. NF is not able to remove the organic molecules in water completely and it is not clear how the small organic molecules remained in permeate react further with chlorine in the swimming pool water system. Additional information about the DBP reactivity/formation of different organic matters may lead to specific treatment which can be more effective reducing the THM concentrations in swimming pool water.

As more DBP have been identified with developing analytical methods, the study could be expanded out of the few focused DBP such as THM and HAA. In swimming pool water the presence of pharmaceuticals such as N,N-diethyl-m-toluamide (DEET) and caffeine was observed (Weng et al., 2014), which indicated the pharmaceuticals not completely metabolized in human can excreted via urine. Due to the persistence it's hardly degraded by treatment and will accumulate in the nearly fully recirculated system. Such accumulation of pharmaceuticals was nearly not studied to date. Although the concentrations of pharmaceuticals are low and no significant effects on visitors are expected, more information of the potential risks is needed. Furthermore, by integration of NF treatment the accumulation of pharmaceuticals can be minimized.

Due to the biofouling problem the continuous chlorination/dechlorination method is becoming less popular. Chlorine-resistant membrane enables a cleaning with chlorine and so that an easier and more

efficient treatment of water with biofouling propensity. Although this work showed 0.2 mg/L free chlorine couldn’t prevent biofouling, directly treating pool water with higher chlorine concentration using chlorine resistant membrane can be interesting. However, the most critical point of chlorine resistant membranes is the high pressure demand and low permeability. If the fouling problem can be under control using chlorine resistant membrane in higher chlorine concentration, the treatment costs of membrane cleaning and energy demand should be compared for a more cost-effective solution.

Appendix

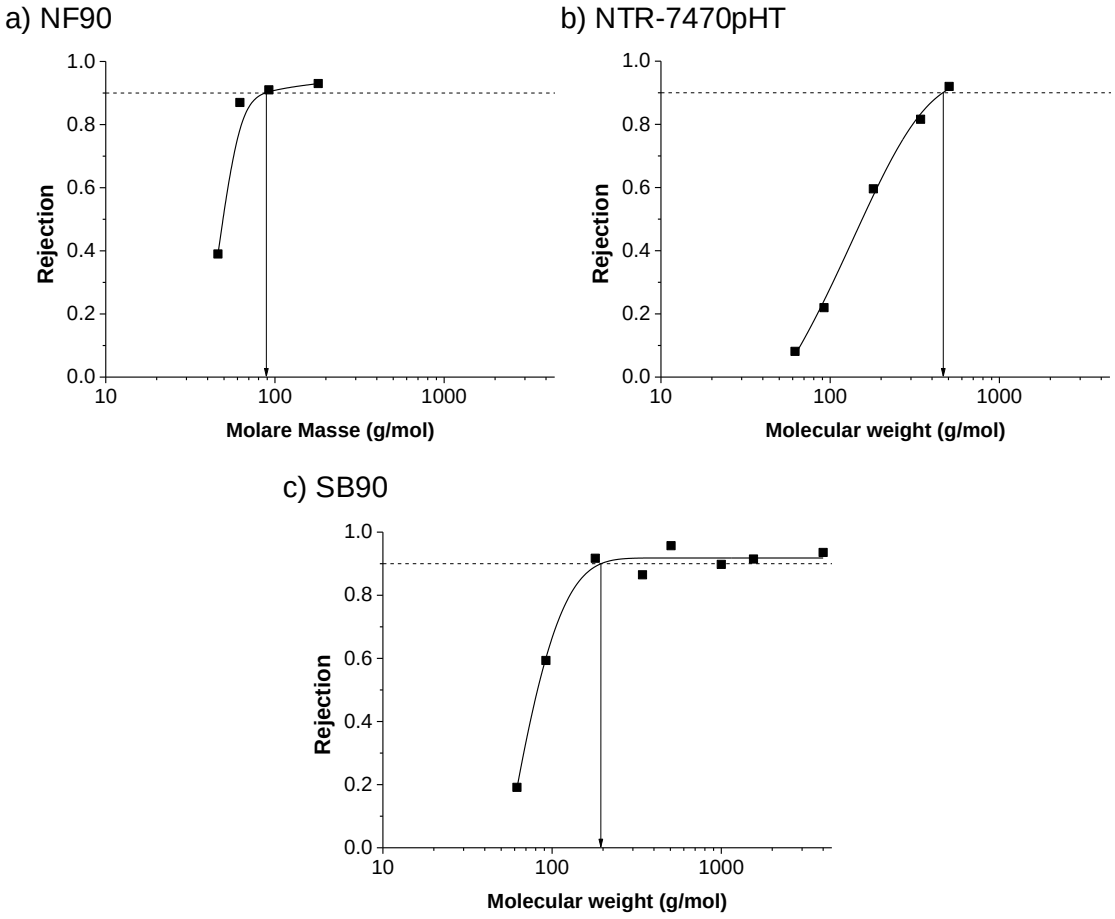

Figure A1: Determination of the MWCO for three nanofiltration membranes applied. a) NF90, b) NTR-7470pHT und c) SB90. Test condition: 25°C, cross-flow filtration at 8 bar, $V_{crossflow}$ = 0.22 m/s, neutral organic compounds such as sugars and polyethylene glycols in demineralized water.

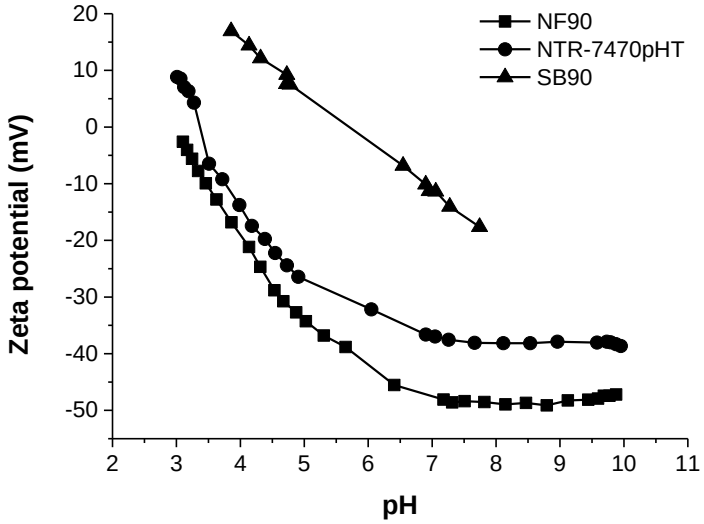

Figure A2: Zeta-potential results of three nanofiltration membranes applied (NF90, NTR-7470pHT and SB90).

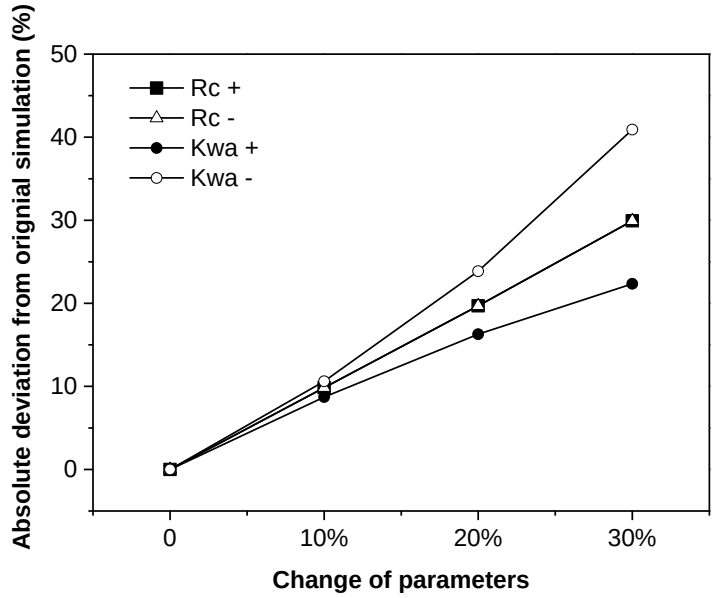

Figure A3: Sensitivity analysis of the key parameters R_C and K_{wa} for the simulation.

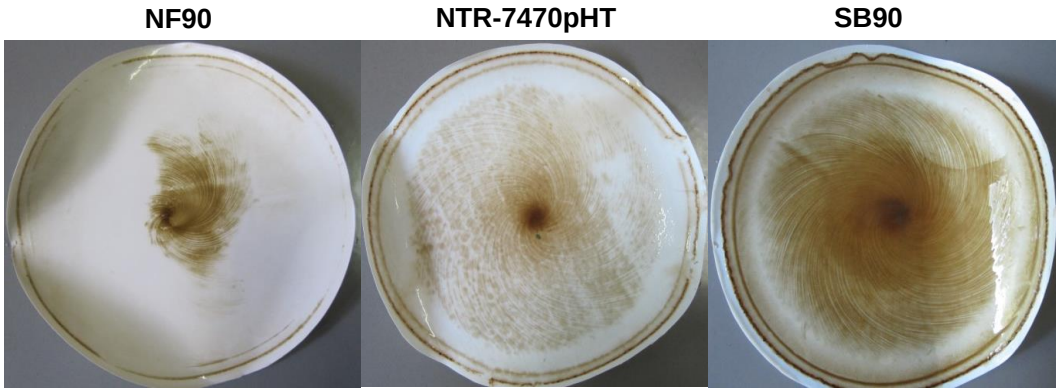

Figure A4: NF membranes fouled by NOM rich lake water.

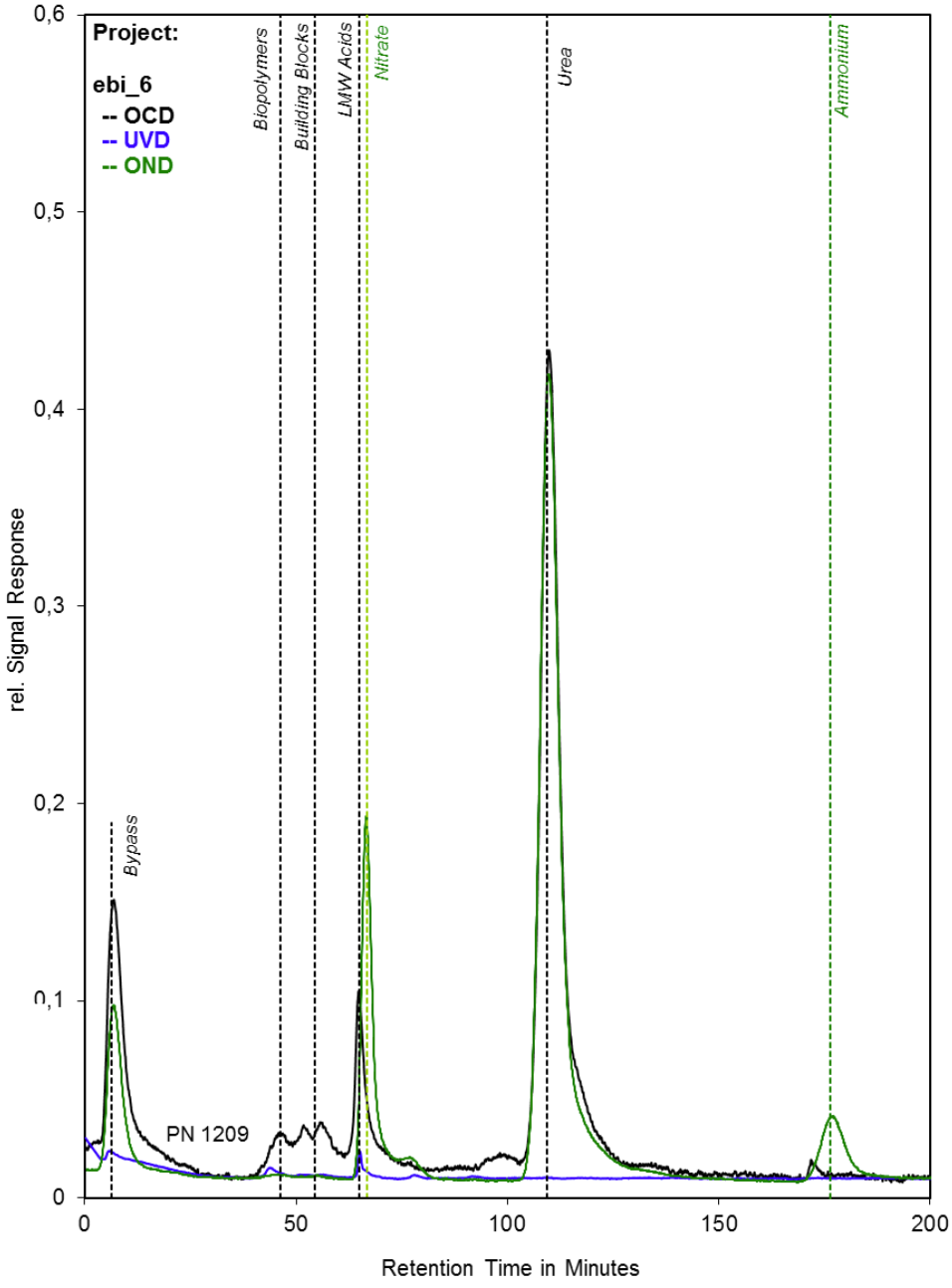

Figure A5: SEC-OCD chromatograms with organic nitrogen detection of permeate NF in the full-scale plant for swimming pool water A (DOC 0.4 mg/L).

Nomenclature

A	water surface area of swimming pool
AOX	absorbable organically bound halogens adsorbable on activated carbon
AOXFP	maximum formation potential of AOX
DBP	disinfection by-product(s)
DBPFP	disinfection by-product formation potential
DOC	dissolved organic carbon
DOM	dissolved organic matter
FP	formation potential
FT-ICR MS	Fourier transform ion cyclotron mass spectroscopy
HAA	haloacetic acids
H_C	Henry's law constant
k	removal coefficient of THM
k_a	air-phase mass transfer coefficient
k_w	water-phase mass transfer coefficient
K_a	overall mass transfer coefficient in the air phase
K_w	overall mass transfer coefficient in the liquid phase
K_{wa}	overall water-air mass transfer coefficient
m	mass
MW	molecular weight
MWCO	molecular weight cut-off
NF	nanofiltration
NOM	natural organic matter
Q_{FW}	filling water inflow
Q_{TM}	volumetric flow rate of pool water treatment
R_C	specific production ratio of THM from DOC
RO	Reverse Osmosis
t	time
TFC	thin-film composite
THM	trihalomethanes
THMFP	maximum formation potential of THM
UF	ultrafiltration
V_{Pool}	total water volume in the swimming pool
X_{THM}	THM removal ratio during one passage of the pool water treatment process
ρ_{DOC}	DOC concentration in swimming pool water
ρ_{THM}	THM concentration in swimming pool water

References

296/2010, B.R. (2010) Pool Regulation, Victoria, British Columbia, Canada.

Abdullah, A. and Hussona, S.E.-d. (2013) Predictive model for disinfection by-product in Alexandria drinking water, northern west of Egypt. Environmental Science and Pollution Research 20(10), 7152-7166.

Agenson, K.O., Oh, J.-I. and Urase, T. (2003) Retention of a wide variety of organic pollutants by different nanofiltration/reverse osmosis membranes: controlling parameters of process. Journal of Membrane Science 225(1–2), 91-103.

Agenson, K.O. and Urase, T. (2007) Change in membrane performance due to organic fouling in nanofiltration (NF)/reverse osmosis (RO) applications. Separation and Purification Technology 55(2), 147-156.

Al-Amoudi, A. and Lovitt, R.W. (2007) Fouling strategies and the cleaning system of NF membranes and factors affecting cleaning efficiency. Journal of Membrane Science 303(1-2), 4-28.

Al-Amoudi, A.S. (2010) Factors affecting natural organic matter (NOM) and scaling fouling in NF membranes: A review. Desalination 259(1-3), 1-10.

Al-Amoudi, A.S. and Farooque, A.M. (2005) Performance restoration and autopsy of NF membranes used in seawater pretreatment. Desalination 178(1–3), 261-271.

Alturki, A.A., Tadkaew, N., McDonald, J.A., Khan, S.J., Price, W.E. and Nghiem, L.D. (2010) Combining MBR and NF/RO membrane filtration for the removal of trace organics in indirect potable water reuse applications. Journal of Membrane Science 365(1-2), 206-215.

Amagliani, G., Parlani, M.L., Brandi, G., Sebastianelli, G., Stocchi, V. and Schiavano, G.F. (2012) Molecular detection of Pseudomonas aeruginosa in recreational water. International Journal of Environmental Health Research 22(1), 60-70.

Applegate, D.H. and Bryers, J.D. (1991) Effects of carbon and oxygen limitations and calcium concentrations on biofilm removal processes. Biotechnology and Bioengineering 37(1), 17-25.

Arnal, J.M., García-Fayos, B. and Sancho, M. (2011) Expanding Issues in Desalination. Ning, R.Y. (ed), INTECH Open Access Publisher.

Arsuaga, J.M., López-Muñoz, M.J. and Sotto, A. (2010) Correlation between retention and adsorption of phenolic compounds in nanofiltration membranes. Desalination 250(2), 829-832.

Ates, N., Yilmaz, L., Kitis, M. and Yetis, U. (2009) Removal of disinfection by-product precursors by UF and NF membranes in low-SUVA waters. Journal of Membrane Science 328(1–2), 104-112.

Baek, Y., Yu, J., Kim, S.-H., Lee, S. and Yoon, J. (2011) Effect of surface properties of reverse osmosis membranes on biofouling occurrence under filtration conditions. Journal of Membrane Science 382(1–2), 91-99.

Baker, J.S. and Dudley, L.Y. (1998) Biofouling in membrane systems — A review. Desalination 118(1–3), 81-89.

Barbot, E. and Moulin, P. (2008) Swimming pool water treatment by ultrafiltration–adsorption process. Journal of Membrane Science 314(1–2), 50-57.

Barrett, S.E., Krasner, S.W. and Amy, G.L. (2000) Natural Organic Matter and Disinfection By-Products, pp. 2-14, American Chemical Society.

Bellona, C., Drewes, J.E., Xu, P. and Amy, G. (2004) Factors affecting the rejection of organic solutes during NF/RO treatment--a literature review. Water Research 38(12), 2795-2809.

Bessonneau, V., Derbez, M., Clément, M. and Thomas, O. (2011) Determinants of chlorination by-products in indoor swimming pools. International Journal of Hygiene and Environmental Health 215(1), 76-85.

Beyer, F., Rietman, B.M., Zwijnenburg, A., van den Brink, P., Vrouwenvelder, J.S., Jarzembowska, M., Laurinonyte, J., Stams, A.J.M. and Plugge, C.M. (2014) Long-term performance and fouling analysis of full-scale direct nanofiltration (NF) installations treating anoxic groundwater. Journal of Membrane Science 468, 339-348.

Black and Veatch, C. (2010) White's Handbook of Chlorination and Alternative Disinfectants, pp. 1-67, John Wiley & Sons, Inc.

Bond, T., Goslan, E.H., Parsons, S.A. and Jefferson, B. (2010) Disinfection by-product formation of natural organic matter surrogates and treatment by coagulation, MIEX® and nanofiltration. Water Research 44(5), 1645-1653.

Bond, T., Goslan, E.H., Parsons, S.A. and Jefferson, B. (2012) A critical review of trihalomethane and haloacetic acid formation from natural organic matter surrogates. Environmental Technology Reviews 1(1), 93-113.

Borgmann-Strahsen, R. (2003) Comparative assessment of different biocides in swimming pool water. International Biodeterioration & Biodegradation 51(4), 291-297.

Boussu, K., Vandecasteele, C. and Van der Bruggen, B. (2008) Relation between membrane characteristics and performance in nanofiltration. Journal of Membrane Science 310(1–2), 51-65.

Braeken, L., Boussu, K., Van der Bruggen, B. and Vandecasteele, C. (2005a) Modeling of the Adsorption of Organic Compounds on Polymeric Nanofiltration Membranes in Solutions Containing Two Compounds. ChemPhysChem 6(8), 1606-1612.

Braeken, L., Ramaekers, R., Zhang, Y., Maes, G., Bruggen, B.V.d. and Vandecasteele, C. (2005b) Influence of hydrophobicity on retention in nanofiltration of aqueous solutions containing organic compounds. Journal of Membrane Science 252(1–2), 195-203.

Braghetta, A. and DiGiano, F.A. (1998) NOM Accumulation at NF Membrane Surface: Impact of Chemistry and Shear. Journal of Environmental Engineering 124(11), 1087.

Bureau, C. (2009) Statistical Abstract of the United States, 2010, U.S. Census Bureau.

Chen, M.-J., Lin, C.-H., Duh, J.-M., Chou, W.-S. and Hsu, H.-T. (2011) Development of a multi-pathway probabilistic health risk assessment model for swimmers exposed to chloroform in indoor swimming pools. Journal of Hazardous Materials 185(2–3), 1037-1044.

Cho, J., Amy, G., Pellegrino, J. and Yoon, Y. (1998) Characterization of clean and natural organic matter (NOM) fouled NF and UF membranes, and foulants characterization. Desalination 118(1–3), 101-108.

Chon, K. and Cho, J. (2016) Fouling behavior of dissolved organic matter in nanofiltration membranes from a pilot-scale drinking water treatment plant: An autopsy study. Chemical Engineering Journal 295, 268-277.

Chon, K., Cho, J. and Shon, H.K. (2013) Fouling characteristics of a membrane bioreactor and nanofiltration hybrid system for municipal wastewater reclamation. Bioresource Technology 130(0), 239-247.

Chowdhury, S., Alhooshani, K. and Karanfil, T. (2014) Disinfection byproducts in swimming pool: Occurrences, implications and future needs. Water Research 53(0), 68-109.

Chowdhury, S., Champagne, P. and McLellan, P.J. (2009) Models for predicting disinfection byproduct (DBP) formation in drinking waters: A chronological review. Science of The Total Environment 407(14), 4189-4206.

Chu, H. and Nieuwenhuijsen, M.J. (2002) Distribution and determinants of trihalomethane concentrations in indoor swimming pools. Occupational and Environmental Medicine 59(4), 243-247.

Communities, E. (2007) Drinking Water (NO. 2) Regulations 2007, Implement of Directive 98/83/EC of 3 November 1998 on the quality of water intended for human consumption. Agency, E.P. and Group, W.S.T. (eds), The Stationery Office, Dublin.

Contreras, A.E., Kim, A. and Li, Q. (2009) Combined fouling of nanofiltration membranes: Mechanisms and effect of organic matter. Journal of Membrane Science 327(1–2), 87-95.

Cortés-Francisco, N., Harir, M., Lucio, M., Ribera, G., Martínez-Lladó, X., Rovira, M., Schmitt-Kopplin, P., Hertkorn, N. and Caixach, J. (2014) High-field FT-ICR mass spectrometry and NMR spectroscopy to characterize DOM removal through a nanofiltration pilot plant. Water Research 67, 154-165.

Creber, S.A., Pintelon, T.R.R., Graf von der Schulenburg, D.A.W., Vrouwenvelder, J.S., van Loosdrecht, M.C.M. and Johns, M.L. (2010) Magnetic resonance imaging and 3D simulation studies of biofilm accumulation and cleaning on reverse osmosis membranes. Food and Bioproducts Processing 88(4), 401-408.

Cyna, B., Chagneau, G., Bablon, G. and Tanghe, N. (2002) Two years of nanofiltration at the Méry-sur-Oise plant, France. Desalination 147(1–3), 69-75.

de la Rubia, Á., Rodríguez, M., León, V.M. and Prats, D. (2008) Removal of natural organic matter and THM formation potential by ultra- and nanofiltration of surface water. Water Research 42(3), 714-722.

De Laat, J., Feng, W., Freyfer, D.A. and Dossier-Berne, F. (2011) Concentration levels of urea in swimming pool water and reactivity of chlorine with urea. Water Res 45(Copyright (C) 2011 U.S. National Library of Medicine.), 1139-1146.

de Ridder, D.J. (2012) Adsorption of organic micropollutants onto activated carbon and zeolites. Dissertation, Technische Universiteit Delft, the Netherlands.

DIN (2005) DIN EN ISO 9562 - Water quality - Determination of adsorbable organically bound halogens (AOX) (ISO 9562:2004); German version EN ISO 9562:2004, p. 32, Beuth Verlag GmbH.

DIN (2007) DIN 38407-30 - German standard methods for the examination of water, waste water and sludge – Jointly determinable substances (group F) – Part 30: Determination of trihalogenmethanes in bathing water and pool water with headspace-gas chromatography (F 30), p. 32, Beuth Verlag GmbH.

DIN (2012a) DIN 19643-1 - Treatment of water of swimming pools and baths – Part 1: General requirements. e.V., N.W.N.i.D.D.I.f.N. (ed), Beuth Verlag GmbH, Berlin.

DIN (2012b) DIN 19643-4 - Treatment of water of swimming pools and baths – Part 4: Combinations of process with ultrafiltration. e.V., N.W.N.i.D.D.I.f.N. (ed), Beuth Verlag GmbH, Berlin.

Do, V.T., Tang, C.Y., Reinhard, M. and Leckie, J.O. (2012) Effects of hypochlorous acid exposure on the rejection of salt, polyethylene glycols, boron and arsenic(V) by nanofiltration and reverse osmosis membranes. Water Research 46(16), 5217-5223.

Doederer, K., Farré, M.J., Pidou, M., Weinberg, H.S. and Gernjak, W. (2014) Rejection of disinfection by-products by RO and NF membranes: Influence of solute properties and operational parameters. Journal of Membrane Science 467(0), 195-205.

Dreszer, C., Wexler, A.D., Drusová, S., Overdijk, T., Zwijnenburg, A., Flemming, H.C., Kruithof, J.C. and Vrouwenvelder, J.S. (2014) In-situ biofilm characterization in membrane systems using Optical Coherence Tomography: Formation, structure, detachment and impact of flux change. Water Research 67(0), 243-254.

DVGW (1997) Arbeitsblatt W 295 - Deatermination of potentials of THM-formation of drinking water, water of swimming pools and baths. e.V., D.D.V.d.G.-u.W. (ed), Wirtschafts- und Verlagsgesellschaft Gas und Wasser GmbH, Bonn.

Dyck, R., Sadiq, R., Rodriguez, M.J., Simard, S. and Tardif, R. (2011) Trihalomethane exposures in indoor swimming pools: A level III fugacity model. Water Research 45(16), 5084-5098.

Elimelech, M., Xiaohua, Z., Childress, A.E. and Seungkwan, H. (1997) Role of membrane surface morphology in colloidal fouling of cellulose acetate and composite aromatic polyamide reverse osmosis membranes. Journal of Membrane Science 127(1), 101-109.

EPA (2002) Stage 1 Disinfectants and Disinfection Byproducts Rule: Laboratory Quick Reference Guide. (4606), O.o.W. (ed).

Erdinger, L.D. and Kühn, K.D. (2004) Removal of halogenation products in chlorinated water, especially drinking or swimming pool water, by addition of bromide ion source followed by irradiation, Google Patents.

Farooque, A.M., Green, T.N., Mohammed, N.K. and Al-Muali, F.A. (2009) Autopsy of NF membranes after 5 years of operation at the Ummlujj SWRO plant. Desalination and Water Treatment 3(1-3), 83-90.

Gabelich, C.J., Frankin, J.C., Gerringer, F.W., Ishida, K.P. and Suffet, I.H. (2005) Enhanced oxidation of polyamide membranes using monochloramine and ferrous iron. Journal of Membrane Science 258(1–2), 64-70.

Glauner, T. (2007) Treatment of swimming pool water - Formation and detection of disinfection by-products and their elimination with membrane and oxidation processes. Translated from "Aufbereitung von Schwimmbeckenwasser - Bildung und Nachweis von Desinfektionsnebenprodukten und ihre Minimierung mit Membran- und Oxidationsverfahren". Veröffentlichungen des Lehrstuhles für Wasserchemie und der DVGW-Forschungsstelle am Engler-Bunte-Institut des Karlsruher Institutes für Technologie 47.

Glauner, T., Frimmel, F.H. and Zwiener, C. (2004) Schwimmbadwasser – wie gut muss es sein und was kann man technisch tun. GWF-Wasser/Abwasser 145(10), 706-713

Glauner, T., Kunz, F., Zwiener, C. and Frimmel, F.H. (2005a) Elimination of Swimming Pool Water Disinfection By-products with Advanced Oxidation Processes (AOPs). Acta hydrochimica et hydrobiologica 33(6), 585-594.

Glauner, T., Waldmann, P., Frimmel, F.H. and Zwiener, C. (2005b) Swimming pool water--fractionation and genotoxicological characterization of organic constituents. Water Research 39(18), 4494-4502.

Golfinopoulos, S.K. and Arhonditsis, G.B. (2002) Quantitative assessment of trihalomethane formation using simulations of reaction kinetics. Water Research 36(11), 2856-2868.

Gorenflo, A. (2003) Rückhalt und Fouling von natürlichen organischen Substanzen bei der Nano- und Ultrafiltration. Veröffentlichungen des Lehrstuhls für Wasserchemie und der DVGW-Forschungsstelle am Engler-Bunte-Institut der Universität Karlsruhe 38.

Gorenflo, A., Eker, S. and Frimmel, F.H. (2001) Surface and pore fouling of flat sheet nanofiltration and ultrafiltration membranes by NOM, pp. 145-154, Tel Aviv, Israel.

Gorenflo, A., Velázquez-Padrón, D. and Frimmel, F.H. (2002) Nanofiltration of a German ground water of high hardness and NOM content: Performance and costs. Desalination 151, 253-265

Graf von der Schulenburg, D.A., Vrouwenvelder, J.S., Creber, S.A., van Loosdrecht, M.C.M. and Johns, M.L. (2008) Nuclear magnetic resonance microscopy studies of membrane biofouling. Journal of Membrane Science 323(1), 37-44.

Guo, Z. and Roache, N.F. (2003) Overall Mass Transfer Coefficient for Pollutant Emissions from Small Water Pools under Simulated Indoor Environmental Conditions. Annals of Occupational Hygiene 47(4), 279-286.

Gwon, E.-m., Yu, M.-j., Oh, H.-k. and Ylee, Y.-h. (2003) Fouling characteristics of NF and RO operated for removal of dissolved matter from groundwater. Water Research 37(12), 2989-2997.

Habimana, O., Semião, A.J.C. and Casey, E. (2014) Upon Impact: The Fate of Adhering Pseudomonas fluorescens Cells during Nanofiltration. Environmental Science & Technology.

Hajibabania, S., Verliefde, A., McDonald, J.A., Khan, S.J. and Le-Clech, P. (2011) Fate of trace organic compounds during treatment by nanofiltration. Journal of Membrane Science 373(1–2), 130-139.

Hambsch, B., Schmiedel, U., Werner, P. and Frimmel, F.H. (1993) Investigations on the Biodegradability of Chlorinated Fulvic Acids Untersuchungen zur mikrobiellen Verwertbarkeit gechlorter Fulvinsäuren. Acta hydrochimica et hydrobiologica 21(3), 167-173.

Hansen, K.M., Willach, S., Antoniou, M.G., Mosbaek, H., Albrechtsen, H.J. and Andersen, H.R. (2012) Effect of pH on the formation of disinfection byproducts in swimming pool water--is less THM better? Water Res 46(19), 6399-6409.

Heffernan, R., Habimana, O., Semião, A.J.C., Cao, H., Safari, A. and Casey, E. (2014) A physical impact of organic fouling layers on bacterial adhesion during nanofiltration. Water Research 67(0), 118-128.

Her, N., Amy, G., Plottu-Pecheux, A. and Yoon, Y. (2007) Identification of nanofiltration membrane foulants. Water Research 41(17), 3936-3947.

Herzberg, M., Kang, S. and Elimelech, M. (2009) Role of Extracellular Polymeric Substances (EPS) in Biofouling of Reverse Osmosis Membranes. Environmental Science & Technology 43(12), 4393-4398.

Hong, S. and Elimelech, M. (1997) Chemical and physical aspects of natural organic matter (NOM) fouling of nanofiltration membranes. Journal of Membrane Science 132(2), 159-181.

Howland, J.L. (1996) Infrared spectroscopy of biomolecules, Headington Hill Hall, New York.

Hsu, H.T., Chen, M.J., Lin, C.H., Chou, W.S. and Chen, J.H. (2009) Chloroform in indoor swimming-pool air: Monitoring and modeling coupled with the effects of environmental conditions and occupant activities. Water Research 43(15), 3693-3704.

Hua, G., Kim, J. and Reckhow, D.A. (2014) Disinfection byproduct formation from lignin precursors. Water Research 63(0), 285-295.

Huang, X., Guillen, G.R. and Hoek, E.M.V. (2010) A new high-pressure optical membrane module for direct observation of seawater RO membrane fouling and cleaning. Journal of Membrane Science 364(1–2), 149-156.

Huber, S.A., Balz, A., Abert, M. and Pronk, W. (2011) Characterisation of aquatic humic and non-humic matter with size-exclusion chromatography – organic carbon detection – organic nitrogen detection (LC-OCD-OND). Water Research 45(2), 879-885.

Huber, S.A. and Frimmel, F.H. (1994) Direct gel chromatographic characterization and quantification of marine dissolved organic carbon using high-sensitivity DOC detection. Environmental Science & Technology 28(6), 1194-1197.

IfD-Allensbach (2016) Anzahl der Personen in Deutschland, die in der Freizeit Schwimmen gehen, nach Häufigkeit von 2012 bis 2015 (in Millionen). Statista - Das Statistik-Portal.

Jarusutthirak, C. and Amy, G. (2007) Understanding soluble microbial products (SMP) as a component of effluent organic matter (EfOM). Water Research 41(12), 2787-2793.

Judd, S.J. and Bullock, G. (2003) The fate of chlorine and organic materials in swimming pools. Chemosphere 51(9), 869-879.

Judd, S.J. and Jeffrey, J.A. (1995) Trihalomethane formation during swimming pool water disinfection using hypobromous and hypochlorous acids. Water Research 29(4), 1203-1206.

Kanan, A. and Karanfil, T. (2011) Formation of disinfection by-products in indoor swimming pool water: The contribution from filling water natural organic matter and swimmer body fluids. Water Research 45(2), 926-932.

Kang, G.-D., Gao, C.-J., Chen, W.-D., Jie, X.-M., Cao, Y.-M. and Yuan, Q. (2007) Study on hypochlorite degradation of aromatic polyamide reverse osmosis membrane. Journal of Membrane Science 300(1-2), 165-171.

Kasai, S., Takubo, Y., Nasu, M. and Kondo, M. (1990) Removal of Trihalomethanes and Chlorinated Organic Solvents in Water by Membranes. I. Separation by Reverse Osmosis Membranes. Eisei kagaku 36(3), 248-253.

Keuten, M.G.A., Peters, M.C.F.M., Daanen, H.A.M., de Kreuk, M.K., Rietveld, L.C. and van Dijk, J.C. (2014) Quantification of continual anthropogenic pollutants released in swimming pools. Water Research 53(0), 259-270.

Keuten, M.G.A., Schets, F.M., Schijven, J.F., Verberk, J.Q.J.C. and van Dijk, J.C. (2012) Definition and quantification of initial anthropogenic pollutant release in swimming pools. Water Research 46(11), 3682-3692.

Kim, H., Shim, J. and Lee, S. (2002) Formation of disinfection by-products in chlorinated swimming pool water. Chemosphere 46(1), 123-130.

Kim, J., DiGiano, F.A. and Reardon, R.D. (2008) Autopsy of high-pressure membranes to compare effectiveness of MF and UF pretreatment in water reclamation. Water Research 42(3), 697-706.

Kimura, K., Amy, G., Drewes, J. and Watanabe, Y. (2003a) Adsorption of hydrophobic compounds onto NF/RO membranes: an artifact leading to overestimation of rejection. Journal of Membrane Science 221(1–2), 89-101.

Kimura, K., Amy, G., Drewes, J.E., Heberer, T., Kim, T.-U. and Watanabe, Y. (2003b) Rejection of organic micropollutants (disinfection by-products, endocrine disrupting compounds, and pharmaceutically active compounds) by NF/RO membranes. Journal of Membrane Science 227(1-2), 113-121.

Kimura, K., Miyoshi, T., Naruse, T., Yamato, N., Ogyu, R. and Watanabe, Y. (2008) The difference in characteristics of foulants in submerged MBRs caused by the difference in the membrane flux. Desalination 231(1–3), 268-275.

Kiso, Y. (1986) Factors affecting adsorption of organic solutes on cellulose acetate in an aqueous solution system. Chromatographia 22(1), 55-58.

Klüpfel, A. (2012) Nanofiltration bei der Aufbereitung von Trink- und Schwimmbeckenwasser – Foulingmechanismen und Rückhalt anthropogener Kontaminanten. Veröffentlichungen des Lehrstuhles für Wasserchemie und der DVGW-Forschungsstelle am Engler-Bunte-Institut des Karlsruher Institutes für Technologie 56.

Klüpfel, A.M., Glauner, T., Zwiener, C. and Frimmel, F.H. (2011a) Nanofiltration for enhanced removal of disinfection by-product (DBP) precursors in swimming pool water–retention and water quality estimation. Water Science & Technology 63(8), 1716-1725.

Klüpfel, A.M., Glauner, T., Zwiener, C. and Frimmel, F.H. (2011b) Nanofiltration for enhanced removal of disinfection by-products (DBP) precursrs in swimming pool water-retention and water qualtiy estimation. Water Science and Technology 63(8), 1716-1725.

Koichi, N. and John, C. (2003) Handbook of Plastics Analysis. Lobo, H. and Bonilla, J.V. (eds), pp. 201-340, Marcel Dekker.

Koros, W.J., Ma, Y.H. and Shimidzu, T. (1996) Terminology for membranes and membrane processes. Pure and Applied Chemistry 68(7), 1479-1489.

Krasner, S.W., Weinberg, H.S., Richardson, S.D., Pastor, S.J., Chinn, R., Sclimenti, M.J., Onstad, G.D. and Thruston, A.D. (2006) Occurrence of a New Generation of Disinfection Byproducts†. Environmental Science & Technology 40(23), 7175-7185.

Kristensen, G.H., Klausen, M.M., Hansen, V.A. and Lauritsen, F.R. (2010) On-line monitoring of the dynamics of trihalomethane concentrations in a warm public swimming pool using an unsupervised

membrane inlet mass spectrometry system with off-site real-time surveillance. Rapid Communications in Mass Spectrometry 24(1), 30-34.

Kunacheva, C. and Stuckey, D.C. (2014) Analytical methods for soluble microbial products (SMP) and extracellular polymers (ECP) in wastewater treatment systems: A review. Water Research 61(0), 1-18.

Kwon, Y.-N., Shih, K., Tang, C. and Leckie, J.O. (2012) Adsorption of perfluorinated compounds on thin-film composite polyamide membranes. Journal of Applied Polymer Science 124(2), 1042-1049.

Lee, S., Choi, J.-S. and Lee, C.-H. (2009) Behaviors of dissolved organic matter in membrane desalination. Desalination 238(1–3), 109-116.

Lee, S. and Elimelech, M. (2006) Relating Organic Fouling of Reverse Osmosis Membranes to Intermolecular Adhesion Forces. Environmental Science & Technology 40(3), 980-987.

Lee, S., Kwon, B., Sun, M. and Cho, J. (2005) Characterizations of NOM included in NF and UF membrane permeates. Desalination 173(2), 131-142.

Leenheer, J.A. and Croué, J.-P. (2003) Peer Reviewed: Characterizing Aquatic Dissolved Organic Matter. Environmental Science & Technology 37(1), 18A-26A.

Levine, B.B., Madireddi, K., Lazarova, V., Stenstrom, M.K. and Suffet, M. (1999) Treatment of trace organic compounds by membrane processes: At the Lake Arrowhead water reuse pilot plant. Water Science and Technology 40(4–5), 293-301.

Li, Q. and Elimelech, M. (2006) Synergistic effects in combined fouling of a loose nanofiltration membrane by colloidal materials and natural organic matter. Journal of Membrane Science 278(1-2), 72-82.

Li, Q., Xu, Z. and Pinnau, I. (2007) Fouling of reverse osmosis membranes by biopolymers in wastewater secondary effluent: Role of membrane surface properties and initial permeate flux. Journal of Membrane Science 290(1–2), 173-181.

Liviac, D., Wagner, E.D., Mitch, W.A., Altonji, M.J. and Plewa, M.J. (2010) Genotoxicity of Water Concentrates from Recreational Pools after Various Disinfection Methods. Environmental Science & Technology 44(9), 3527-3532.

Lourencetti, C., Grimalt, J.O., Marco, E., Fernandez, P., Font-Ribera, L., Villanueva, C.M. and Kogevinas, M. (2012) Trihalomethanes in chlorine and bromine disinfected swimming pools: Air-water distributions and human exposure. Environment International 45(0), 59-67.

Lu, C., Chung, Y.-L. and Chang, K.-F. (2005) Adsorption of trihalomethanes from water with carbon nanotubes. Water Research 39(6), 1183-1189.

Luo, M. and Wang, Z. (2001) Complex fouling and cleaning-in-place of a reverse osmosis desalination system. Desalination 141(1), 15-22.

Mackay, D., Shiu, W.Y., Ma, K.-C. and Lee, S.C. (2006) Handbook of Physical-Chemical Properties and Environmental Fate for Organic Chemicals, Second Edition, pp. 921-1256, CRC Press.

Mahlangu, T.O., Hoek, E.M.V., Mamba, B.B. and Verliefde, A.R.D. (2014) Influence of organic, colloidal and combined fouling on NF rejection of NaCl and carbamazepine: Role of solute–foulant–membrane interactions and cake-enhanced concentration polarisation. Journal of Membrane Science 471(0), 35-46.

Mahlangu, T.O., Thwala, J.M., Mamba, B.B., D'Haese, A. and Verliefde, A.R.D. (2015) Factors governing combined fouling by organic and colloidal foulants in cross-flow nanofiltration. Journal of Membrane Science 491, 53-62.

Mañas, A., Biscans, B. and Spérandio, M. (2011) Biologically induced phosphorus precipitation in aerobic granular sludge process. Water Research 45(12), 3776-3786.

Mänttäri, M., Puro, L., Nuortila-Jokinen, J. and Nyström, M. (2000) Fouling effects of polysaccharides and humic acid in nanofiltration. Journal of Membrane Science 165(1), 1-17.

Mohammad, A.W., Teow, Y.H., Ang, W.L., Chung, Y.T., Oatley-Radcliffe, D.L. and Hilal, N. (2015) Nanofiltration membranes review: Recent advances and future prospects. Desalination 356(0), 226-254.

Mondamert, L., Labanowski, J., Berjeaud, J.M., Rapenne, S. and Croué, J.P. (2009) Autopsy of RO desalination membrane: Part 2. Chemical characterisation of the foulant. Desalination and Water Treatment 9(1-3), 73-81.

Mulder, M. (1996) Basic Principles of Membrane Technology, Kluwer Academic Publishers, The Netherlands.

Müller, S. and Uhl, W. (2011) Effects of high bathing loads on pool water treated by coagulation-ultrafiltration, Porto, Portugal.

Murphy, D. and de Pinho, M.N. (1995) An ATR-FTIR study of water in cellulose acetate membranes prepared by phase inversion. Journal of Membrane Science 106(3), 245-257.

Neu, T.R., Swerhone, G.D.W. and Lawrence, J.R. (2001) Assessment of lectin-binding analysis for in situ detection of glycoconjugates in biofilm systems. Microbiology 147(2), 299-313.

Nghiem, L.D. and Hawkes, S. (2007) Effects of membrane fouling on the nanofiltration of pharmaceutically active compounds (PhACs): Mechanisms and role of membrane pore size. Separation and Purification Technology 57(1), 176-184.

Nghiem, L.D. and Hawkes, S. (2009) Effects of membrane fouling on the nanofiltration of trace organic contaminants. Desalination 236(1–3), 273-281.

Nghiem, L.D., Schäfer, A.I. and Elimelech, M. (2004) Removal of Natural Hormones by Nanofiltration Membranes: Measurement, Modeling, and Mechanisms. Environmental Science & Technology 38(6), 1888-1896.

Nghiem, L.D., Vogel, D. and Khan, S. (2008) Characterising humic acid fouling of nanofiltration membranes using bisphenol A as a molecular indicator. Water Research 42(15), 4049-4058.

NSW, H.P. (2013) Public swimming pool and spa pool advisory document, Sydney.

Panyakapo, M., Soontornchai, S. and Paopuree, P. (2008) Cancer risk assessment from exposure to trihalomethanes in tap water and swimming pool water. Journal of Environmental Sciences 20(3), 372-378.

Pasquarella, C., Veronesi, L., Napoli, C., Castaldi, S., Pasquarella, M.L., Saccani, E., Colucci, M.E., Auxilia, F., Gallè, F., Di Onofrio, V., Tafuri, S., Signorelli, C. and Liguori, G. (2014) What about behaviours in swimming pools? Results of an Italian multicentre study. Microchemical Journal 112(0), 190-195.

Patterson, C., Anderson, A., Sinha, R., Muhammad, N. and Pearson, D. (2012) Nanofiltration Membranes for Removal of Color and Pathogens in Small Public Drinking Water Sources. Journal of Environmental Engineering 138(1), 48-57.

Pontié, M., Thekkedath, A., Kecili, K., Habarou, H., Suty, H. and Croué, J.P. (2007) Membrane autopsy as a sustainable management of fouling phenomena occurring in MF, UF and NF processes. Desalination 204(1-3), 155-169.

Potwora, R.J. (2006) Trihalomethane Removal with Activated Carbon, pp. 22-23, Kurt C. Peterson.

Raffin, M., Germain, E. and Judd, S. (2012) Assessment of fouling of an RO process dedicated to indirect potable reuse. Desalination and Water Treatment 40(1-3), 302-308.

Reinhard, M., Goodman, N.L., McCarty, P.L. and Argo, D.G. (1986) Removing Trace Organics by Reverse Osmosis Using Cellulose Acetate and Polyamide Membranes. Journal (American Water Works Association) 78(4), 163-174.

Richardson, S.D., DeMarini, D.M., Kogevinas, M., Fernandez, P., Marco, E., Lourencetti, C., Ballesté, C., Heederik, D., Meliefste, K., McKague, A.B., Marcos, R., Font-Ribera, L., Grimalt, J.O. and Villanueva, C.M. (2010) What's in the Pool? A Comprehensive Identification of Disinfection By-

products and Assessment of Mutagenicity of Chlorinated and Brominated Swimming Pool Water. Environmental Health Perspectives 118(11), 1523-1530.

Richardson, S.D., Plewa, M.J., Wagner, E.D., Schoeny, R. and DeMarini, D.M. (2007) Occurrence, genotoxicity, and carcinogenicity of regulated and emerging disinfection by-products in drinking water: A review and roadmap for research. Mutation Research/Reviews in Mutation Research 636(1–3), 178-242.

Riggle, J. and von Wandruszka, R. (2005) Binding of inorganic phosphate to dissolved metal humates. Talanta 66(2), 372-375.

Roccaro, P., Vagliasindi, F.G.A. and Korshin, G.V. (2014) Relationships between trihalomethanes, haloacetic acids, and haloacetonitriles formed by the chlorination of raw, treated, and fractionated surface waters. Journal of Water Supply: Research and Technology - AQUA 63(1), 21-30.

Rook, J.J. (1974) Formation of haloforms during chlorination of natural waters. Water Treat. Exam. 23, Pt. 2(Copyright (C) 2011 American Chemical Society (ACS). All Rights Reserved.), 234-243.

Rousseau, R.W. (1987) Handbook of Separation Process Technology, Wiley, New York.

Sablani, S.S., Goosen, M.F.A., Al-Belushi, R. and Wilf, M. (2001) Concentration polarization in ultrafiltration and reverse osmosis: a critical review. Desalination 141(3), 269-289.

Sadiq, R. and Rodriguez, M.J. (2004) Disinfection by-products (DBPs) in drinking water and predictive models for their occurrence: a review. Science of The Total Environment 321(1–3), 21-46.

Sadrnourmohamadi, M. and Gorczyca, B. (2015) Effects of ozone as a stand-alone and coagulation-aid treatment on the reduction of trihalomethanes precursors from high DOC and hardness water. Water Research 73, 171-180.

Sander, R. (1999) Compilation of Henry's Law Constants for Inorganic and Organic Species of Potential Importance in Environmental Chemistry, Air Chemistry Department, Max-Planck Institute of Chemistry, Mainz, Germany.

Saravia, F., Klüpfel, A., Zamora Richard, A. and Frimmel, F.H. (2013) Identification of nanofiltration fouling layer constituents. Desalination and Water Treatment, 1-8.

Saravia, F., Lankes, U., Gorenflo, A. and Frimmel, F.H. (2003) Untersuchung des Membranfoulings mit NMR-Spektroskopie. Melin, T. and Dohmann, M. (eds), Aachen.

Sari, M.A. and Chellam, S. (2013) Surface water nanofiltration incorporating (electro) coagulation-microfiltration pretreatment: Fouling control and membrane characterization. Journal of Membrane Science 437, 249-256.

Schäfer, A.I., Andritsos, N., Karabelas, A.J., Hoek, E.M.V., Schneider, R. and Nyström, M. (2004) Nanofiltration – Principles and Applications. Schäfer, A.I., T.D., W. and Fane, A.G. (eds), pp. 169-239, Elsevier.

Schäfer, A.I., Fane, A.G. and Waite, T.D. (2000) Fouling effects on rejection in the membrane filtration of natural waters. Desalination 131(1–3), 215-224.

Schaule, G., Rapenne, S., Strathmann, M., Grobe, S., Robert, C. and Jacquemet, V. (2009) Autopsy of RO desalination membranes: Part 1 microbial characterization of foulants. Desalination and Water Treatment 9(1-3), 66-72.

Schlesinger, R., Götzinger, G., Sixta, H., Friedl, A. and Harasek, M. (2006) Evaluation of alkali resistant nanofiltration membranes for the separation of hemicellulose from concentrated alkaline process liquors. Desalination 192(1-3), 303-314.

Schmalz, C., Frimmel, F.H. and Zwiener, C. (2011) Trichloramine in swimming pools - Formation and mass transfer. Water Research 45(8), 2681-2690.

Seidel, A. and Elimelech, M. (2002) Coupling between chemical and physical interactions in natural organic matter (NOM) fouling of nanofiltration membranes: implications for fouling control. Journal of Membrane Science 203(1–2), 245-255.

Semião, A.J.C., Habimana, O. and Casey, E. (2014) Bacterial adhesion onto nanofiltration and reverse osmosis membranes: Effect of permeate flux. Water Research 63(0), 296-305.

Sentana, I., Puche, R.D.S., Sentana, E. and Prats, D. (2011) Reduction of chlorination byproducts in surface water using ceramic nanofiltration membranes. Desalination 277(1-3), 147-155.

Sentana, I., Rodríguez, M., Sentana, E., M'Birek, C. and Prats, D. (2010) Reduction of disinfection by-products in natural waters using nanofiltration membranes. Desalination 250(2), 702-706.

Shirazi, S., Lin, C.-J. and Chen, D. (2010) Inorganic fouling of pressure-driven membrane processes — A critical review. Desalination 250(1), 236-248.

Siddiqui, M., Amy, G., Ryan, J. and Odem, W. (2000) Membranes for the control of natural organic matter from surface waters. Water Research 34(13), 3355-3370.

Simard, S., Tardif, R. and Rodriguez, M.J. (2013) Variability of chlorination by-product occurrence in water of indoor and outdoor swimming pools. Water Research 47(5), 1763-1772.

Staudt, C., Horn, H., Hempel, D.C. and Neu, T.R. (2004) Volumetric measurements of bacterial cells and extracellular polymeric substance glycoconjugates in biofilms. Biotechnology and Bioengineering 88(5), 585-592.

Steinle-Darling, E., Litwiller, E. and Reinhard, M. (2010) Effects of Sorption on the Rejection of Trace Organic Contaminants During Nanofiltration. Environmental Science & Technology 44(7), 2592-2598.

Sweity, A., Oren, Y., Ronen, Z. and Herzberg, M. (2013) The influence of antiscalants on biofouling of RO membranes in seawater desalination. Water Research 47(10), 3389-3398.

Sweity, A., Zere, T.R., David, I., Bason, S., Oren, Y., Ronen, Z. and Herzberg, M. (2015) Side effects of antiscalants on biofouling of reverse osmosis membranes in brackish water desalination. Journal of Membrane Science 481, 172-187.

Tan, Z. (2014) Air Pollution and Greenhouse Gases: From Basic Concepts to Engineering Applications for Air Emission Control, Springer Singapore.

Tang, C.Y., Chong, T.H. and Fane, A.G. (2011) Colloidal interactions and fouling of NF and RO membranes: A review. Advances in Colloid and Interface Science 164(1–2), 126-143.

Tang, C.Y., Kwon, Y.-N. and Leckie, J.O. (2007) Fouling of reverse osmosis and nanofiltration membranes by humic acid—Effects of solution composition and hydrodynamic conditions. Journal of Membrane Science 290(1–2), 86-94.

Tang, C.Y., Kwon, Y.-N. and Leckie, J.O. (2009) Effect of membrane chemistry and coating layer on physiochemical properties of thin film composite polyamide RO and NF membranes: I. FTIR and XPS characterization of polyamide and coating layer chemistry. Desalination 242(1–3), 149-167.

Tang, F., Hu, H.-Y., Sun, L.-J., Wu, Q.-Y., Jiang, Y.-M., Guan, Y.-T. and Huang, J.-J. (2014) Fouling of reverse osmosis membrane for municipal wastewater reclamation: Autopsy results from a full-scale plant. Desalination 349, 73-79.

Tay, J.-H., Liu, J. and Sun, D.D. (2003) Quantification of membrane fouling using thermogravimetric method. Journal of Membrane Science 217(1–2), 17-28.

Teixeira, M.R. and Rosa, M.J. (2006) The impact of the water background inorganic matrix on the natural organic matter removal by nanofiltration. Journal of Membrane Science 279(1-2), 513-520.

Touffet, A., Baron, J., Welte, B., Joyeux, M., Teychene, B. and Gallard, H. (2015) Impact of pretreatment conditions and chemical ageing on ultrafiltration membrane performances. Diagnostic of a coagulation/adsorption/filtration process. Journal of Membrane Science 489, 284-291.

Toussaint, H. and Truijens, M. (2005) Biomechanical aspects of peak performance in human swimming. Animal Biology 55(1), 17-40.

Tran, T., Bolto, B., Gray, S., Hoang, M. and Ostarcevic, E. (2007) An autopsy study of a fouled reverse osmosis membrane element used in a brackish water treatment plant. Water Research 41(17), 3915-3923.

TrinkwV (2016) Verordnung über die Qualität von Wasser für den menschlichen Gebrauch (Trinkwasserverordnung – TrinkwV 2001 in der Fassungder Bekanntmachung vom 10. September 2016 (BGBI. I S. 459)). Gesundheit, B.f., Bundesministerium für Verbraucherschutz, E.u.L.i.E., Technologie, B.f.W.u. and Bundesministerium für Umwelt, N.u.R. (eds).

Turakhia, M.H. and Characklis, W.G. (1989) Activity of Pseudomonas aeruginosa in biofilms: Effect of calcium. Biotechnology and Bioengineering 33(4), 406-414.

Uhl, W., Hartemann, C. and Kreckel, B. (2005) Bacterial Regrowth and Disinfection Byproduct Removal in Granular Activated Carbon Filters in Pool Water Treatment, Budapest, Hungary.

Uyak, V., Koyuncu, I., Oktem, I., Cakmakci, M. and Toroz, I. (2008) Removal of trihalomethanes from drinking water by nanofiltration membranes. Journal of Hazardous Materials 152(2), 789-794.

Van der Bruggen, B., Braeken, L. and Vandecasteele, C. (2002a) Evaluation of parameters describing flux decline in nanofiltration of aqueous solutions containing organic compounds. Desalination 147(1–3), 281-288.

Van der Bruggen, B., Braeken, L. and Vandecasteele, C. (2002b) Flux decline in nanofiltration due to adsorption of organic compounds. Separation and Purification Technology 29(1), 23-31.

Verliefde, A.R.D., Cornelissen, E.R., Heijman, S.G.J., Hoek, E.M.V., Amy, G.L., Bruggen, B.V.d. and van Dijk, J.C. (2009a) Influence of Solute−Membrane Affinity on Rejection of Uncharged Organic Solutes by Nanofiltration Membranes. Environmental Science & Technology 43(7), 2400-2406.

Verliefde, A.R.D., Cornelissen, E.R., Heijman, S.G.J., Petrinic, I., Luxbacher, T., Amy, G.L., Van der Bruggen, B. and van Dijk, J.C. (2009b) Influence of membrane fouling by (pretreated) surface water on rejection of pharmaceutically active compounds (PhACs) by nanofiltration membranes. Journal of Membrane Science 330(1–2), 90-103.

Verliefde, A.R.D., Cornelissen, E.R., Heijman, S.G.J., Verberk, J.Q.J.C., Amy, G.L., Van der Bruggen, B. and van Dijk, J.C. (2008) The role of electrostatic interactions on the rejection of organic solutes in aqueous solutions with nanofiltration. Journal of Membrane Science 322(1), 52-66.

Villanueva, C.M., Cantor, K.P., Grimalt, J.O., Malats, N., Silverman, D., Tardon, A., Garcia-Closas, R., Serra, C., Carrato, A., Castano-Vinyals, G., Marcos, R., Rothman, N., Real, F.X., Dosemeci, M. and Kogevinas, M. (2007) Bladder cancer and exposure to water disinfection by-products through ingestion, bathing, showering, and swimming in pools. Am J Epidemiol 165(Copyright (C) 2013 U.S. National Library of Medicine.), 148-156.

Vos, K.D., Burris, F.O. and Riley, R.L. (1966) Kinetic study of the hydrolysis of cellulose acetate in the pH range of 2–10. Journal of Applied Polymer Science 10(5), 825-832.

Vrouwenvelder, J.S., Manolarakis, S.A., Veenendaal, H.R. and van der Kooij, D. (2000) Membranes in Drinking and Industrial Water ProductionBiofouling potential of chemicals used for scale control in RO and NF membranes. Desalination 132(1), 1-10.

Vrouwenvelder, J.S., Picioreanu, C., Kruithof, J.C. and van Loosdrecht, M.C.M. (2010) Biofouling in spiral wound membrane systems: Three-dimensional CFD model based evaluation of experimental data. Journal of Membrane Science 346(1), 71-85.

Vrouwenvelder, J.S. and van der Kooij, D. (2001) Diagnosis, prediction and prevention of biofouling of NF and RO membranes. Desalination 139(1–3), 65-71.

Vrouwenvelder, J.S., van Paassen, J.A.M., Wessels, L.P., van Dam, A.F. and Bakker, S.M. (2006) The Membrane Fouling Simulator: A practical tool for fouling prediction and control. Journal of Membrane Science 281(1–2), 316-324.

Wang, X.-m., Li, B., Zhang, T. and Li, X.-y. (2015) Performance of nanofiltration membrane in rejecting trace organic compounds: Experiment and model prediction. Desalination 370, 7-16.

Wang, Y.N. and Tang, C.Y. (2011) Nanofiltration membrane fouling by oppositely charged macromolecules: Investigation on flux behavior, foulant mass deposition, and solute rejection. Environmental Science and Technology 45(20), 8941-8947.

Waniek, A., Bodzek, M. and Konieczny, K. (2002) Trihalomethane Removal from Water Using Membrane Processes. Polish Journal of Environmental Studies 11(2), 171-178.

Weinrich, L., Haas, C.N. and LeChevallier, M.W. (2013) Recent advances in measuring and modeling reverse osmosis membrane fouling in seawater desalination: a review. Journal of Water Reuse and Desalination 3(2), 85-101.

Weng, S.C., Sun, P.Z., Ben, W.W., Huang, C.H., Lee, L.T. and Blatchley, E.R. (2014) The Presence of Pharmaceuticals and Personal Care Products in Swimming Pools. Environmental Science & Technology Letters 1(12), 495-498.

West, S., Horn, H., Hijnen, W.A.M., Castillo, C. and Wagner, M. (2014) Confocal laser scanning microscopy as a tool to validate the efficiency of membrane cleaning procedures to remove biofilms. Separation and Purification Technology 122(0), 402-411.

West, S., Wagner, M., Engelke, C. and Horn, H. (2016) Optical coherence tomography for the in situ three-dimensional visualization and quantification of feed spacer channel fouling in reverse osmosis membrane modules. Journal of Membrane Science 498, 345-352.

WHO (2006) Guidelines for safe recreational water environments. Volume 2: Swimming pools and similar environments, World Health Organization, Geneva.

Xu, P., Bellona, C. and Drewes, J.E. (2010) Fouling of nanofiltration and reverse osmosis membranes during municipal wastewater reclamation: Membrane autopsy results from pilot-scale investigations. Journal of Membrane Science 353(1-2), 111-121.

Xu, P., Drewes, J.E., Bellona, C., Amy, G., Kim, T.U., Adam, M. and Heberer, T. (2005) Rejection of emerging organic micropollutants in nanofiltration-reverse osmosis membrane applications. Water Environment Research 77(1), 40-48.

Xu, P., Drewes, J.E., Kim, T.-U., Bellona, C. and Amy, G. (2006) Effect of membrane fouling on transport of organic contaminants in NF/RO membrane applications. Journal of Membrane Science 279(1-2), 165-175.

Yangali-Quintanilla, V., Sadmani, A., McConville, M., Kennedy, M. and Amy, G. (2009) Rejection of pharmaceutically active compounds and endocrine disrupting compounds by clean and fouled nanofiltration membranes. Water Research 43(9), 2349-2362.

Zhang, X.-l., Yang, H.-w., Wang, X.-m., Fu, J. and Xie, Y.F. (2013) Formation of disinfection by-products: Effect of temperature and kinetic modeling. Chemosphere 90(2), 634-639.

Zhang, X. and Minear, R.A. (2006) Removal of low-molecular weight DBPs and inorganic ions for characterization of high-molecular weight DBPs in drinking water. Water Research 40(5), 1043-1051.

Zhao, F., Xu, K., Ren, H., Ding, L., Geng, J. and Zhang, Y. (2015) Combined effects of organic matter and calcium on biofouling of nanofiltration membranes. Journal of Membrane Science 486, 177-188.

Zwiener, C., Richardson, S.D., De Marini, D.M., Grummt, T., Glauner, T. and Frimmel, F.H. (2007) Drowning in disinfection byproducts? Assessing swimming pool water. Environmental Science & Technology 41, 363-372.

Publications

Peer reviewed journals

Peng, D., Saravia, F., Abbt-Braun, G., Horn, H. (2016) Occurrence and simulation of trihalomethanes in swimming pool water: A simple prediction method based on DOC and mass balance. Water Research, 88, 634-642.

Peng, D., Saravia, F., Bock, K., Pelikan, M., Abbt-Braun, G., Horn, H. The rejection of trihalomethanes by nanofiltration membranes: influences of adsorption and NOM fouling. Submitted in 12.2016.

Conference contributions

Peng, D., Saravia, F., Pelikan, M., Abbt-Braun, G., Horn, H. (2015) Rejection of disinfection by-products by clean and fouled nanofiltration membranes. Poster, Euromembrane 2015, September 06-10, Aachen, Germany.

Peng, D., Saravia, F., Abbt-Braun, G., Horn, H. (2014) Application of Nanofiltration in swimming pool water treatment. Oral presentation, The 10th International Congress on Membranes and Membrane Progresses (ICOM2014), Suzhou, China.

Peng, D., Saravia, F., Abbt-Braun, G., Horn, H. (2014) Application of Nanofiltration in Swimming Pool Water Treatment to Minimize the Disinfection By-products. Poster, DBP 2014: Disinfection By-products in drinking water, Mülheim an der Ruhr, Germany.

Peng, D., Saravia, F., West, D., Abbt-Braun, G., Horn, H. (2014) Analyze of chlorine-resistance of Nanofiltration membranes. Poster, 15th Aachener Membran Kolloquium, Aachen, Germany.

Conference proceedings

Thompson, K.C., Gillespie, S. and Goslan, E.H. (2015) Disinfection By-products in Drinking Water, Royal Society of Chemistry. Chapter 21: **Peng, D.**, Saravia, F., Abbt-Braun, G., Horn, H. Application of Nanofiltration in Swimming Pool Water Treatment to Minimize the Disinfection By-products.

Chapter 4: Verification of the contribution from the co-authors

Title: Occurrence and simulation of trihalomethanes in swimming pool water: A simple prediction method based on DOC and mass balance

Journal: Water Research, (2016), 88: 634–642 (http://dx.doi.org/10.1016/j.watres.2015.10.061)

Authors: Di Peng, Florencia Saravia, Gudrun Abbt-Braun, Harald Horn

Position in the dissertation:

The content of this paper has been included in Chapter 4

Contribution of Di Peng (80%)

- conceived the concept
- design and conduction of the experiment
- analysis and discussion of the data/results
- development of the simulation
- wrote and corrected the manuscript

Contribution of Florencia Saravia (10%)

- design of the experiment
- discussion on the data/results
- correction of the manuscript

Contribution of Gudrun Abbt-Braun (5%)

- discussion on the data/results
- correction of the manuscript

Contribution of Harald Horn (5%)

- discussion on the data/results
- correction of the manuscript

Signature of the authors:

Author	*Electronic signature*
Di Peng	
Florencia Saravia	
Gudrun Abbt-Braun	
Harald Horn	

Permission from Elsevier:

Authors can include their articles in full or in part in a thesis or dissertation for non-commercial purposes.

Source: https://www.elsevier.com/about/company-information/policies/copyright/permissions

(Retrieved on Dec. 10th, 2016)

Schriftenreihe des Lehrstuhls für Wasserchemie und Wassertechnologie und der DVGW-Forschungsstelle am Engler-Bunte-Institut des Karlsruher Instituts für Technologie (KIT)

Band 35: Symposium on Refractory Organic Substances in the Environment – ROSE, 1997, 248 S., 12,80 €.

Band 36: Symposium on Refractory Organic Substances in the Environment – ROSE II, 2000, 265 S., 12,80 €.

Band 37: Thomas Brinkmann: Alkalischer und solarinduzierter Abbau von natürlicher organischer Materie, 2003, 212 S., 15,00 €.

Band 38: Andreas Gorenflo: Rückhalt und Fouling von natürlichen organischen Substanzen bei der Nano- und Ultrafiltration, 2003, 219 S., 18,00 €.

Band 39: Philip Hörsch: Einfluss der chemischen Oxidation auf das toxische Potenzial und das biologische Abbauverhalten von Industrieabwässern, 2004, 210 S., 20,00 €.

Band 40: Margit B. Müller: Bewertung von Anreicherungs- und Fraktionierungsverfahren für die strukturelle Charakterisierung der gelösten organischen Substanz in Gewässern, 2004, 185 S., 18,00 €.

Band 41: Fritz H. Frimmel, Gudrun Abbt-Braun: Praktikum Allgemeine Chemie und Chemie in wässrigen Lösungen – Qualitative und quantitative Bestimmungen, 2004, 158 S., 18,00 €.

Band 42: Tusnelda E. Doll: Photochemischer und photokatalytischer Abbau von Carbamazepin, Clofibrinsäure, Iomeprol und Iopromid, 2004, 158 S., 18,00 €.

Band 43: Ayşe B. Değer: Entfernung von organischen Schadstoffen aus Wasser mit Hilfe von Poly(ε-caprolacton), 2005, 205 S., 18,00 €.

Band 44: Fritz H. Frimmel, Gudrun Abbt-Braun: Wassertechnologisches und wasserchemisches Praktikum, 2005, 201 S., 20,00 €.

Band 45-I, 45-II: Fritz H. Frimmel, Gudrun Abbt-Braun (Eds.): Humic Substances – Linking Structure to Functions. Proceedings of the 13th Meeting of the International Humic Substances Society, July 30 to August 4, 2006, Universität Karlsruhe, 2006, 492 S. (45-I), 623 S. (45-II), 50,00 €.

Band 46: Fritz H. Frimmel, Gudrun Abbt-Braun: Praktikum Allgemeine Chemie und Chemie in wässrigen Lösungen – Qualitative und quantitative Bestimmungen II, 2. verbesserte und ergänzte Neuauflage 2007, 139 S., 20,00 €.

Band 47: Thomas Glauner: Aufbereitung von Schwimmbeckenwasser – Bildung und Nachweis von Desinfektionsnebenprodukten und ihre Minimierung mit Membran- und Oxidationsverfahren, 2007, 233 S., 20,00 €.

Band 48: George Metreveli: Kolloidale Wechselwirkungen und kolloidgetragener Transport von Metall(oid)en in porösen Medien, 2008, 215 S., 20,00 €.

Band 49: Florencia Saravia: Entfernung von organischen Spurenstoffen und Untersuchung von Foulingprozessen in getauchten Membranen und Hybridverfahren, 2009, 213 S., 20,00 €.

Band 50: Markus Delay: Dynamische versus statische Elutionsversuche – Ein Beitrag zur Beurteilung der Wiederverwertbarkeit von Abfallmaterialien, 2010, 206 S., 20,00 €.

Band 51: Luis A. Tercero Espinoza: Heterogeneous photocatalysis with titanium dioxide suspensions containing bromide and dissolved organic matter, 2010, 172 S., 20,00 €.

Band 52: Ulrich-M. Metzger: Extrazelluläre polymere Substanzen aus Biofilmen – Aufklärung von Strukturen und ihr Einfluss auf die Foulingbildung in Membranbioreaktoren, 2011, 211 S., 20,00 €.

Band 53: Fritz H. Frimmel, Gudrun Abbt-Braun: Praktikum Allgemeine Chemie und Chemie in wässrigen Lösungen – Qualitative und quantitative Bestimmungen, 3. überarbeitete Neuauflage 2011, 139 S., 20,00 €.

Band 54: Markus Ziegmann: Beurteilung von Cyanobakterienblüten und Untersuchung geeigneter Verfahrenskombinationen zur Elimination cyanobakterieller Zellen und Toxine, 2011, 191 S., 20,00 €.

Band 55: Fritz H. Frimmel, Gudrun Abbt-Braun: Praktikum Allgemeine Chemie und Chemie in wässrigen Lösungen – Qualitative und quantitative Bestimmungen, 4. ergänzte Neuauflage 2012, 137 S., 20,00 €.

Band 56: Angela Klüpfel: Nanofiltration bei der Aufbereitung von Trink- und Schwimm-beckenwasser – Foulingmechanismen und Rückhalt anthropogener Kontaminanten, 2012, 259 S., 20,00 €.

Band 57: Christina Schmalz: Bildung, Phasentransfer und Toxizität halogenierter Desinfektionsnebenprodukte im Aufbereitungszyklus von Schwimmbeckenwasser – Schwerpunkt stickstoffhaltige Verbindungen, 2012, 195 S., 20,00 €.

Band 58: Fritz H. Frimmel, Gudrun Abbt-Braun, Harald Horn: Praktikum Allgemeine Chemie und Chemie in wässrigen Lösungen – Qualitative und quantitative Bestimmungen, 5. ergänzte Neuauflage 2013, 120 S., 20,00 €.

Band 59: Heiko Schwegmann: Wechselwirkungen zwischen anorganischen Nanopartikeln und Mikroorganismen – Nutzungs- und Gefährdungspotentiale, 2013, 149 S., 20,00 €.

Band 60: Fritz H. Frimmel, Gudrun Abbt-Braun, Harald Horn: Praktikum Allgemeine Chemie und Chemie in wässrigen Lösungen – Qualitative und quantitative Bestimmungen, 6. Überarbeitete Neuauflage 2014, 129 S., 20,00 €.

Band 61: Carsten Jobelius: Anaerobe Metabolite organischer Schadstoffe im Grundwasser - Analytik, Bildung und Nutzung als Indikatoren, 2014, 247 S., 20,00 €.

Band 62: Eva M. Gilbert: Partielle Nitritation / Anammox bei niedrigen Temperaturen, 2014, 115 S., 20,00 €.

Band 63: Aleksandr O. Kondrakov: Heterogeneous photocatalysis and sensitized photolysis for enhanced degradation of bisphenol A and its analogues, 2015, 155 S., 20,00 €.

Band 64: Meijie Ren: TiO_2: application in photocatalysis for the degradation of organic pollutants and aggregation behavior in aquatic systems, 2015, 121 S., 20,00 €.

Band 65: Fritz H. Frimmel, Gudrun Abbt-Braun, Harald Horn: Praktikum Allgemeine Chemie und Chemie in wässrigen Lösungen – Qualitative und quantitative Bestimmungen, 7. überarbeitete Neuauflage 2016, 126 S., 20,00 €.

Band 66: Chunyan Li: Using optical coherence tomography to quantify biofilm structure and mass transfer in combination with mathematical modeling, 2016, 121 S., 20,00 €.

Band 67: Maria Pia Herrling: Nanoparticles in biofilm systems – assessment of their interactions by magnetic susceptibility balance and magnetic resonance imaging, 2016, 132 S., 20,00 €.

Band 68: Elham Fatoorehchi: Sludge disintegration techniques – assessment of their impacts on solubilization of organic carbon and methane production, 2016, 116 S., 20,00 €.

Band 69: Norman Hack: Refraktäre organische Substanzen im Kapillarsaum: ihre Dynamik, Gradienten und Reaktionen, 2016, 152 S., 20,00 €.

Band 70: Di Peng: Disinfection by-products and the application potential of nanofiltration in swimming pool water treatment, 2016, 112 S., 20,00 €.

Preise verstehen sich zzgl. der gesetzlichen Mehrwertsteuer und Versandkosten.

Bestellungen über:

Lehrstuhl für Wasserchemie und Wassertechnologie und DVGW-Forschungsstelle

am Engler-Bunte-Institut des Karlsruher Instituts für Technologie (KIT)

Engler-Bunte-Ring 9

D-76131 Karlsruhe

Tel.: +49-(0)721-608-42581

Fax: +49-(0)721-608-46497

E-mail: ebi-sekretariat-wasserchemie@kit.edu